

Summer 1987

The Geochemistry of Selenium and Sulfur in a Coastal Salt Marsh

David Jay Velinsky
Old Dominion University

Follow this and additional works at: https://digitalcommons.odu.edu/oeas_etds



Part of the [Biogeochemistry Commons](#), and the [Oceanography Commons](#)

Recommended Citation

Velinsky, David J.. "The Geochemistry of Selenium and Sulfur in a Coastal Salt Marsh" (1987). Doctor of Philosophy (PhD), Dissertation, Ocean & Earth Sciences, Old Dominion University, DOI: 10.25777/z5cp-zc86

https://digitalcommons.odu.edu/oeas_etds/157

This Dissertation is brought to you for free and open access by the Ocean & Earth Sciences at ODU Digital Commons. It has been accepted for inclusion in OES Theses and Dissertations by an authorized administrator of ODU Digital Commons. For more information, please contact digitalcommons@odu.edu.

THE GEOCHEMISTRY OF SELENIUM AND SULFUR
IN A COASTAL SALT MARSH

by

David Jay Velinsky
B.S. June 1977, Florida Institute of Technology

A Dissertation Submitted to the Faculty of
Old Dominion University in Partial Fulfillment of the
Requirements for the Degree of

DOCTOR OF PHILOSOPHY

OCEANOGRAPHY

OLD DOMINION UNIVERSITY
AUGUST, 1987

Approved by:

~~Dr. Gregory A. Cutter~~ (Director)

~~Dr. David J. Burdige~~

~~Dr. Thomas M. Church~~

~~Dr. William M. Dunstan~~

~~Dr. George T.F. Wong~~

Copyright by David Jay Velinsky 1987
All Rights Reserved

This dissertation is dedicated in memory of my father:
Irving H. Velinsky

ACKNOWLEDGEMENTS

I would like to express my sincere appreciation to Dr. Gregory A. Cutter, for his financial support, guidance, inspiration and "kicks in the butt" throughout this study. Greg was a real life saver when the chips were down. The expertise, critical suggestions and support provided by my thesis committee, Dr. David Burdige, Dr. Thomas Church, Dr. William Dunstan, and Dr. George Wong were invaluable.

A special thanks goes to Dr. Terry Wade whose initial support and guidance provided me with a goal that I have finally reached.

I would like to thank Dr. Tom Church for use of his facilities at University of Delaware and Joseph Scudlark for sweating it out in the field, laboratory and at the Rose 'n Crown. Joe sacrificed many hours for this study and it surely benefited from his help. Thanks to Dr. George Luther III for providing me with various ancillary data needed for this research. Chris Krahforst and Jeff Busa provided valuable field assistance and Bob Kluckhohn for his greigite analyses.

I am grateful to Dr. David Burdige for his assistance in helping me with data interpretation, diagenetic modeling, ancillary information and writing the "great" paper of 1983.

I would like to thank Lynda A. Cutter for her help in the laboratory and proofreading various parts of this dissertation.

Over the past 7 long years, I have benefited from my association with many students at ODU. Through all the ups and downs they have all provided support and encouragement that made my stay at ODU bearable and most often fun. I am especially indebted to Tom Oatts for his laboratory help and friendship while at ODU. I would also like to thank my other colleagues in the initial Chemical Oceanography Group, Jim Todd, Kazufumi Takayanagi, Charlie Farmer and Robb Brown for their laboratory and field assistance in the various projects I undertook. Their intellectual stimulation and friendship made chemical oceanography interesting and exciting. To Mario Paula, Kimberley G. Davis, E.A. Stern, Chris Krahforst, Darrin Mann, and many others for help along the way. Marcia Berman provided unimaginable physical and mental feats that, even today, cannot and should not be fully described. A special thanks to Maria Lourdes Casino San Diego McGlone whose help, moral support and friendship will undoubtedly last a lifetime.

My surfing buddies, Dave Timpy, Rusty Butt and Alan Friedlander helped in keeping my sanity and priorities straight at times of frustration and self destruction.

Thanks to Ken, Sarah and Jason Petroske for making my life a little nicer and providing me a home while in Norfolk.

Finally, I a special thanks to my mother whose support, both moral and financial, was deeply appreciated. "If only you were a real doctor!".

I am grateful to the Department of Oceanography, ODU for various financial support throughout my graduate career.

TABLE OF CONTENTS

	Page
DEDICATION.....	ii
ACKNOWLEDGEMENTS	iii
TABLE OF CONTENTS	vi
LIST OF TABLES	ix
LIST OF FIGURES	xi
CHAPTER 1: GENERAL INTRODUCTION	1
Scientific Background	9
Chemistry of Selenium in the Environment. 9	
Selenium in Oceanic Waters	13
Selenium in Geologic Material	16
Study Area	30
CHAPTER 2: THE DETERMINATION OF SELENIUM AND SULFUR SPECIATION IN MARINE SEDIMENTS	35
Introduction	35
Sampling Methods	35
Water Sample Analyses	37
Experimental	37
Discussion	45
Sediment Analyses	47
Experimental	47
Discussion	60
CHAPTER 3: SULFUR GEOCHEMISTRY IN THE GREAT MARSH ..	74
Introduction	74

TABLE OF CONTENTS (continued)

	PAGE
Results and Discussion	77
Total carbon, nitrogen, and sulfur	77
Iron Monosulfides	81
Greigite	85
Elemental Sulfur	87
Pyrite	88
A Quantitative Assessment of Pyritization	95
Conclusions	100
 CHAPTER 4: SELENIUM GEOCHEMISTRY IN THE GREAT MARSH.	 102
Introduction	102
Results and Discussions	102
Dissolved Selenium in Pore and Creek Waters	109
Chemical Forms of Sedimentary Selenium ..	114
Input of Selenium to the Marsh	130
Internal Cycling of Selenium in Marsh Sediments	136
Export of Selenium from the Marsh	139
Summary and Conclusions	156
 CHAPTER 5: COMPARATIVE GEOCHEMISTRIES OF SELENIUM AND SULFUR	 159
Introduction	159
Discussion	159
Comparative Chemistries of Selenium and Sulfur	159

TABLE OF CONTENTS (continued)

	PAGE
Geochemical Behavior of Selenium and Sulfur in Marine Sediments	167
Conclusions	174
CHAPTER 6: SUMMARY AND CONCLUSIONS	177
REFERENCES	181

LIST OF TABLES

TABLE	PAGE
1.1	Free energy change for some bacterial reactions..... 4
1.2a	Selected physical properties for selenium and sulfur compounds..... 10
1.2b	Reduction potentials for some analogous selenium and sulfur compounds..... 11
1.3	Solubility products of some metal selenides... 14
1.4	Concentrations of selenium in selected rock types..... 18
1.5	Various selenium minerals..... 20
1.6	Selenium concentrations in minerals of diagenetic origins..... 22
2.1	List of parameters measured for this study.... 38
2.2	Recovery of elemental selenium using sodium sulfite..... 63
2.3	Recovery of elemental selenium from marsh sediment using a sodium sulfite leach and nitric-perchloric digest..... 65
2.4	Sodium sulfite leach results of marsh sediment at pH 7 and 9..... 67
2.5	Carbon, nitrogen, and sulfur recoveries after sodium sulfite leach..... 69
3.1	Concentrations of sedimentary sulfur species, organic carbon, total nitrogen, total sulfur, and iron oxides from the Great Marsh..... 78
4.1	Seasonal marsh redox cycle..... 104
4.2	Pore water ancillary data in the Great Marsh.. 106
4.3	Pore water selenium data in the Great Marsh... 110
4.4	Creek water total dissolved selenium data..... 113

LIST OF TABLES (continued)

TABLE		PAGE
4.5	Concentrations of sedimentary selenium species in the Great Marsh.....	115
4.6	Chromium reducible selenium data normalized to total selenium in the Great Marsh.....	128
4.7	Diagenetic model results.....	144
4.8	Solid phase selenium:sulfur (atomic) data in the Great Marsh.....	153
4.9	Sulfur gas fluxes from various marshes.....	155
4.10	Summary of Model Results.....	157
5.1	Physical and chemical properties of selenium and sulfur.....	160
5.2	Total sedimentary selenium concentrations from different environments.....	168

LIST OF FIGURES

FIGURE		PAGE
1.1	Schematic distribution of oxidants and their products in the pore waters of marine sediments.....	3
1.2	E_H -pH of the predominant selenium species in the aqueous environment.....	12
1.3	Vertical depth profiles of total dissolved selenium, selenite, selenate, organic selenide and nutrients from Vertex II site....	15
1.4	Diagram of the proposed marine biogeochemical cycle of selenium in the oceans.....	17
1.5	E_H -pH diagram of selenium-sulfur-iron species in earth surface aqueous environments.	23
1.6	Distribution of selenium, iron, pyrite, and manganese in the surface sediments from Japan to Hawaii.....	28
1.7	Location map of study site Great Marsh, Lewes, Delaware.....	31
2.1	Flow chart for sample processing and analyses.	39
2.2	Apparatus for dissolved selenium speciation...	40
2.3	Stripper/6-way valve system used for chromium reducible selenium.....	49
2.4	Typical chromatogram showing the separation of hydrogen selenide and sulfide.....	57
2.5	Typical calibration curve for chromium reducible selenium.....	59
2.6	Recovery of chromium reducible selenium with time.....	71
3.1	Carbon:nitrogen ratios (atomic) in sediments from the Great Marsh.....	80
3.2	Depth distribution of total sulfur in the Great Marsh.....	82

LIST OF FIGURES (continued)

FIGURE	PAGE
3.3 Depth distribution of iron monosulfide in the Great Marsh.....	84
3.4 Depth distribution of greigite in the Great Marsh.....	86
3.5 Depth distribution of elemental sulfur in the Great Marsh.....	89
3.6 Depth distribution of pyrite in the Great Marsh.....	91
3.7 Depth distribution of all inorganic sulfur species for the April 4, 1985 core from the Great Marsh.....	94
4.1 Schematic of selenium's geochemical cycle in a salt marsh.....	108
4.2 Depth distribution of total pore water selenium in the Great Marsh.....	111
4.3 Depth distribution of total sedimentary selenium in the Great Marsh.....	117
4.4 Depth distribution of sedimentary (selenite+selenate) normalized to total sedimentary selenium in the Great Marsh.....	118
4.5 Depth distribution of elemental selenium normalized to total selenium in the Great Marsh.....	119
4.6 Composite depth distribution of elemental selenium in the Great Marsh.....	120
4.7 Depth distribution of organic selenium normalized to total selenium in the Great Marsh.....	121
4.8 Composite depth distribution of total sedimentary selenium in the Great Marsh.....	142
4.9 Selenium as a function of time during the flux chamber experiment.....	148

LIST OF FIGURES (continued)

FIGURE		PAGE
5.1	E_H -pH diagram for the aqueous sulfur system.....	163
5.2	Composite depth distribution of selenium: sulfur ratio (molar) in the Great Marsh.....	170

ABSTRACT

THE GEOCHEMISTRY OF SELENIUM AND SULFUR IN A COASTAL SALT MARSH

David Jay Velinsky
Old Dominion University
Director: Dr. Gregory A. Cutter

Salt marshes are unique sedimentary environments that can be utilized to investigate redox processes over relatively short time periods (months) and depth intervals (cm). Investigation of the various chemical forms of selenium and sulfur in sediments and pore waters can provide information about various oxidation/reduction processes. Five cores were obtained from the Great Marsh (DE), from April 1985 to June 1986. The sampling times were chosen to coincide with the seasonal redox cycle known to occur within the marsh system. Sediments were analyzed for various selenium and sulfur phases utilizing specific chemical leaches.

Iron monosulfides and elemental sulfur both display large seasonal changes in concentration and distribution with depth, indicating a coupling with redox conditions. In contrast, the depth distribution of greigite did not show appreciable changes with season. Pyrite underwent large concentration changes in the upper 15 cm of sediment during

spring, but remained relatively constant with respect to concentration and distribution below this zone. Using a mass balance approach for the upper marsh sediment (0-15 cm), sulfur needed for the observed rapid pyritization is found to be derived from elemental sulfur, iron monosulfide, and sulfate reduction. In the deeper sediments (15-30 cm), diagenetic modeling confirms that greigite is an intermediate in pyrite formation.

The depth distribution of total sedimentary selenium shows minor variations with season. Concentrations are generally higher in the surface layers and then decrease with depth. Elemental selenium exhibits a trend with depth similar to total selenium. Chromium reducible selenium was generally undetectable in most cores and shows little seasonality. In contrast, sedimentary (selenite+selenate) shows marked seasonality. In spring, sedimentary (selenite+selenate) is less than 10% of the total sedimentary selenium throughout the profile. However in summer, a broad maximum (30% of the total selenium) occurs just above the redoxcline. Below the redoxcline sedimentary (selenite+selenate) accounts for less than 10% of the total sedimentary selenium. Pore water selenium exhibits a seasonal trend, concurrent with the cyclic changes in sedimentary (selenite+selenate). Diagenetic modeling shows that the loss of total sedimentary selenium is controlled by the decrease in elemental selenium. Mass balance modeling indicates that the major export of selenium from the marsh

sediment is either gaseous emissions of selenium or the flux of Spartina alterniflora litter from the marsh system. The export of gaseous selenium from the marsh is a potentially important source of selenium to the atmosphere.

Chapter 1

GENERAL INTRODUCTION

The biogeochemistry of salt marsh ecosystems is an important area for investigation by chemical oceanographers. Marshes are an initial boundary between the ocean and continents, and are usually the first area to be affected by man's activities in the estuarine environment. These activities (e.g., industrial discharge) can cause abnormally high concentrations of trace elements to be deposited in estuarine systems, including salt marshes (Windom, 1975; Breteler et al., 1981). Processes within the sediments, affected in part by changes in redox conditions, can then redistribute trace elements between pore waters and various sedimentary solid phases (Giblin et al., 1983; 1986). This redistribution can make marshes act either as sources or sinks of trace elements to the estuarine/coastal environment (Nixon, 1979; Church et al., 1983; Giblin et al., 1983; Bollinger and Moore, 1984; Tramontano, et al., 1985).

In temperate latitudes, salt marsh sediments are exposed to varying conditions related to tidal movements and periodic exposure to the atmosphere. The salinity, temperature, E_H , and pH of marsh sediments can show temporal variations on the time scales of hours to months. These variations, due to their periodicity, allow processes in the marsh to cycle over similar time periods (i.e., seasonal changes in the oxidizing and reducing conditions within the

sediment). In this respect, salt marsh sediments may provide ideal natural laboratories for examining the behavior of trace elements during the early diagenesis of marine sediments. In particular, processes such as dissolution and precipitation of certain mineral phases (e.g., iron oxides and pyrite; Lord and Church, 1983; King et al., 1985) can be studied over clearly resolved depth ranges (0 to 40 cm) and relatively short time scales (months). Moreover, sampling logistics are straightforward and relatively inexpensive. The information obtained from studying marsh sediments can then be used as a basis for the investigation of similar processes in coastal and oceanic sediments where temporal are longer and logistics are far more complicated.

The types of processes affecting trace metals within salt marsh sediments are determined by the energy (electron) flow within the sediment. High energy substrates (e.g., proteins, carbohydrates, lipids) are produced in the surface layers (0 to 10 cm) of the marsh via photosynthesis and undergo biogeochemical degradation and burial with increasing depth. Degradation of organic matter proceeds using a series of electron acceptors beginning with oxygen (Figure 1.1). The sequence in which these electron acceptors are utilized indicates that they are consumed by bacteria in the order of decreasing energy per mole of organic carbon oxidized (Berner, 1980; Stumm and Morgan, 1981). Table 1.1 lists the idealized sequence of electron acceptors, some products in aerobic and anaerobic respiration, and the free

Figure 1.1. Schematic distribution of oxidants and their products in the pore waters of marine sediments.

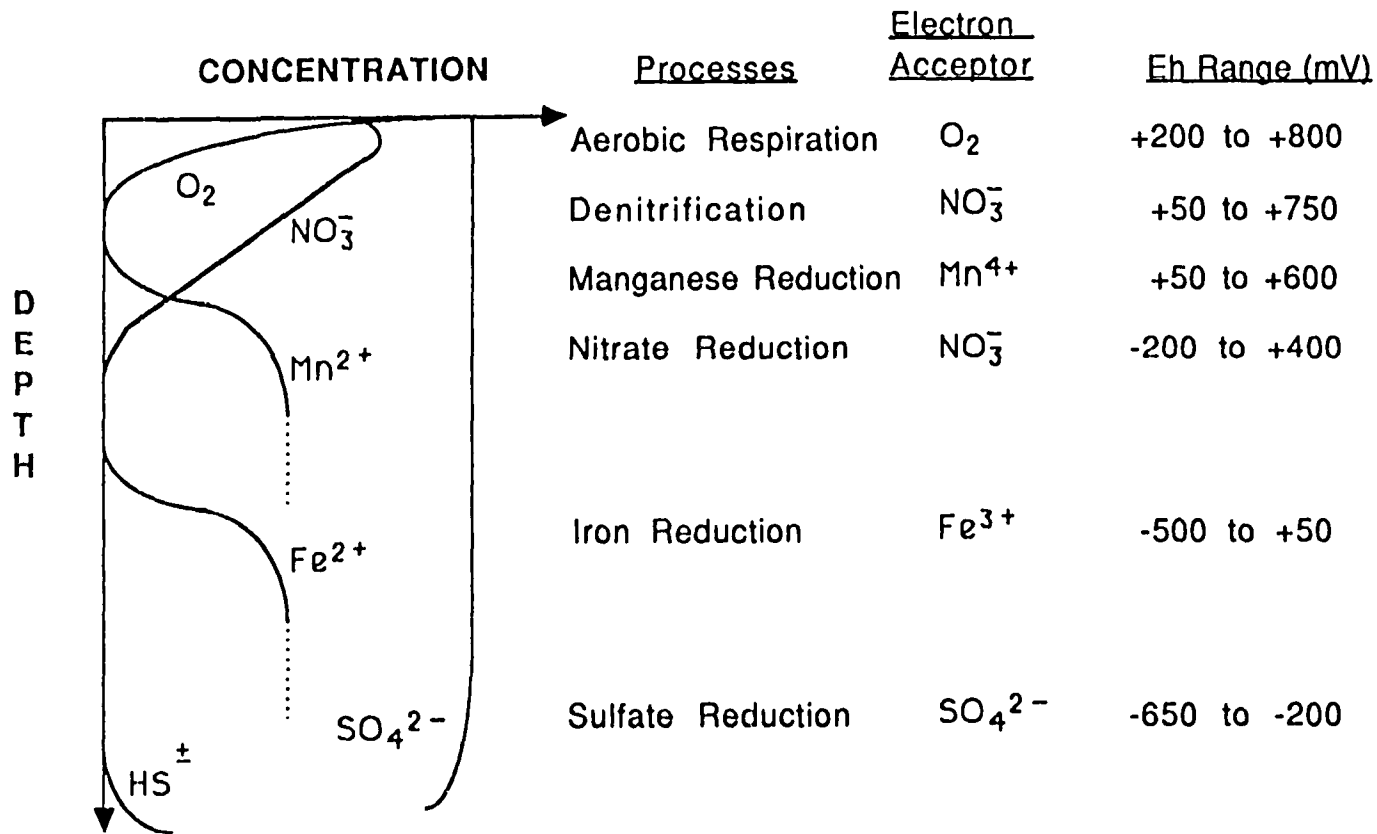


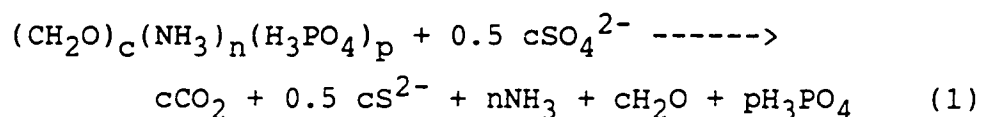
Table 1.1

Standard State Free Energy Changes for some Bacterial Reactions
(from Berner, 1980)

Reaction ^a	G (kJ/ mol CH ₂ O)
$\text{CH}_2\text{O} + \text{O}_2 \text{ ---> } \text{CO}_2 + \text{H}_2\text{O}$	-475
$5\text{CH}_2\text{O} + 4\text{HNO}_3^- \text{ ---> } 2\text{N}_2 + 4\text{HCO}_3^- + \text{CO}_2 + 3\text{H}_2\text{O}$	-448
$\text{CH}_2\text{O} + 3\text{CO}_2 + \text{H}_2\text{O} + 2\text{MnO}_2 \text{ ---> } 2\text{Mn}^{+2} + 4\text{HCO}_3^-$	-349
$\text{CH}_2\text{O} + 7\text{CO}_2 + 4\text{Fe}(\text{OH})_3 \text{ ---> } 4\text{Fe}^{+2} + 8\text{HCO}_3^- + 3\text{H}_2\text{O}$	-114
$2\text{CH}_2\text{O} + \text{SO}_4^{-2} \text{ ---> } \text{H}_2\text{S} + 2\text{HCO}_3^-$	-77
$2\text{CH}_2\text{O} \text{ ---> } \text{CH}_4 + \text{CO}_2$	-58

^a Data for CH₂O and MnO₂, are for sucrose and birnessite, respectively.

energy change for these microbial reactions. This redox sequence follows the model first proposed by Richards et al. (1965), and further developed by various researchers (e.g., Berner, 1974; Sholkovitz, 1973; Martens et al., 1978; Froelich et al., 1979; Reeburgh, 1983). In the marine environment, sulfate is the predominant electron acceptor in anoxic marine sediments, with oxidation of organic matter through bacterial dissimilatory sulfate reduction playing a pivotal role in the biogeochemistry of salt marsh sediments. From previous pore water studies (Richards, 1965; Berner, 1974; Martens et al., 1978; and others), the stoichiometry of sulfate reduction has been proposed to be:



where the subscripts c, n, and p are the C:N:P ratio of decomposing organic matter, usually 106:16:1.

Sulfate reduction is geochemically important since its products can influence the transformation of certain solid phases occurring within marine sediments. The role of the products of reaction (1), for example sulfide and phosphate, in controlling trace metal solubility and mobility is only partially understood (Suess, 1979; Aller, 1980; Giblin and Howarth, 1984). For example, metal sulfides have very low solubilities and their precipitation in the sediments would be expected to limit the mobility of dissolved metals (e.g., iron and manganese) in the pore waters of anoxic sediments.

However, the existence of organic ligands within the pore waters, and the resulting metal-organic complexes, can lead to dissolved metal concentrations being higher than those predicted by thermodynamic and solubility calculations (Elderfield et al., 1979; Presley and Trefry, 1980). Sulfide produced during bacterial sulfate reduction can also be transported out of reducing layers of the sediments and its oxidation by chemoautotrophic (sulfur oxidizing) bacteria can provide further chemical energy to the marsh system (Howarth and Teal, 1980; Howarth et al., 1983; Howarth, 1984).

In marine sediments, iron is probably the most studied of all the metals (e.g., Aller, 1980; Lord, 1980; Boulegue et al., 1982; Gibling and Howarth, 1984). Ferric oxides are present near the sediment surface, but with increasing depth these oxides are reduced predominantly by HS^- or other possible reductants (Stone and Morgan, 1987). As a result, pore water concentrations of soluble ferrous iron increase dramatically with depth (Aller, 1980; Lord, 1980; Gibling and Howarth, 1984). The ferrous iron then diffuses either upwards, where it is reoxidized, or downwards to be precipitated with sulfide as FeS and eventually pyrite (Gibling and Howarth, 1984). In marine sediments, pyrite is the major sink for iron and sulfur over geologically long time periods (Goldhaber and Kaplan, 1974). Pyrite formation may also affect other trace elements, and in particular, selenium (Leutwein, 1972).

While there have been many studies of selenium in the water column (e.g., Measures et al., 1983; 1984; Cutter and Bruland, 1984; Takayanagi and Wong, 1985) there has been little research on the geochemistry of selenium in marine sediments. Selenium can exist in a variety of oxidation states (-II,0,IV,VI) with both organic and inorganic forms, and therefore its sedimentary geochemistry may be very complex. Since the different oxidation states of selenium show markedly different solubilities and affinities for solid phases, changes from one oxidation state to another may affect the potential mobility of selenium in marine sediments. The types of reactions that affect selenium in sediments can be biotically and abiotically controlled, involve conversions between particulate and dissolved phases, and include redox reactions which change the oxidation state of selenium. Examples of such processes include: 1) scavenging of selenite (Se (IV)) by Fe/Mn oxides; 2) release or degradation of organic selenide (Se (-II)) during the diagenesis of organic matter; 3) precipitation of selenium as achavalite (FeSe), ferroselite (FeSe₂), or elemental selenium (Se(0)), and 4) incorporation of selenium into/with other phases such as pyrite or elemental sulfur.

It is the purpose of this dissertation to examine the processes which affect the distribution and speciation of selenium in salt marsh sediments. Since selenium and sulfur are Group VI elements, a concurrent study of the various

sulfur phases (FeS , Fe_3S_4 , S^0 , FeS_2) was also undertaken to elucidate any similarities in the diagenetic pathways of these two elements. These data can also be used to calculate the rates of interconversion for the various selenium and sulfur species in marsh sediments of.

Specific questions addressed in this dissertation related to the sedimentary cycling of selenium include:

- 1) Is there a relationship and/or similarity between the various selenium, sulfur and iron phases during the early diagenesis of salt marsh sediments?
- 2) Are the mineral phases, ferroselite, achavalite, and elemental selenium, formed during the diagenesis of selenium?
- 3) Are marsh sediments sources or sinks of selenium with respect to adjacent estuarine waters?
- 4) Can the changes in the distribution of selenium and sulfur in salt marsh sediments be quantified using diagenetic models?

To answer these questions the remainder of this dissertation will be divided into five self-contained chapters which are:

Chapter 2: The Determination of Selenium and Sulfur Speciation in Marine Sediments.

Chapter 3: Sulfur Geochemistry in the Great Marsh.

Chapter 4: Selenium Geochemistry in the Great Marsh.

Chapter 5: Comparative Geochemistries of Selenium and Sulfur.

To set the stage for this research, a brief review of selenium geochemistry will first be presented. Included in this section are thermodynamic data on the speciation and solid phases of selenium and sulfur. Following this

background section a detailed description of the study area will be presented.

SCIENTIFIC BACKGROUND

Chemistry of Selenium in the Environment

Selenium (atomic number: 34; atomic mass: 78.962) is a Group VI element, which also includes oxygen, sulfur, tellurium, and polonium. Selenium exists in four formal oxidation states; selenide (-II), elemental (0), selenite (IV), and selenate (VI). Certain chemical properties of selenium are summarized in Tables 1.2a and b; data for sulfur are also included for comparison. Selenium is less electronegative than sulfur, and a stronger oxidant. Elemental selenium is found in both metallic (gray hexagonal) and non-metallic (red and black crystalline) forms. Under natural conditions, the non-metallic forms are metastable with respect to the metallic form (Geering et al., 1968).

The equilibrium speciation of selenium in oxygenated natural waters can be calculated using available thermodynamic data (Sillen, 1961; Latimer, 1952). In seawater with a pH of 8.1 and a E_H of 0.7, the selenite to selenate ratio is calculated to be 10^{-12} (Sillen, 1961). Therefore, in selenate should be the only detectable species of selenium in oxygenated ocean waters.

An E_H versus pH diagram for selenium in the aqueous environment is shown in Figure 1.2. In anoxic waters (e.g.,

Table 1.2a

Selected Physical Properties of Selenium and
Sulfur Compounds (from Lakin, 1973)

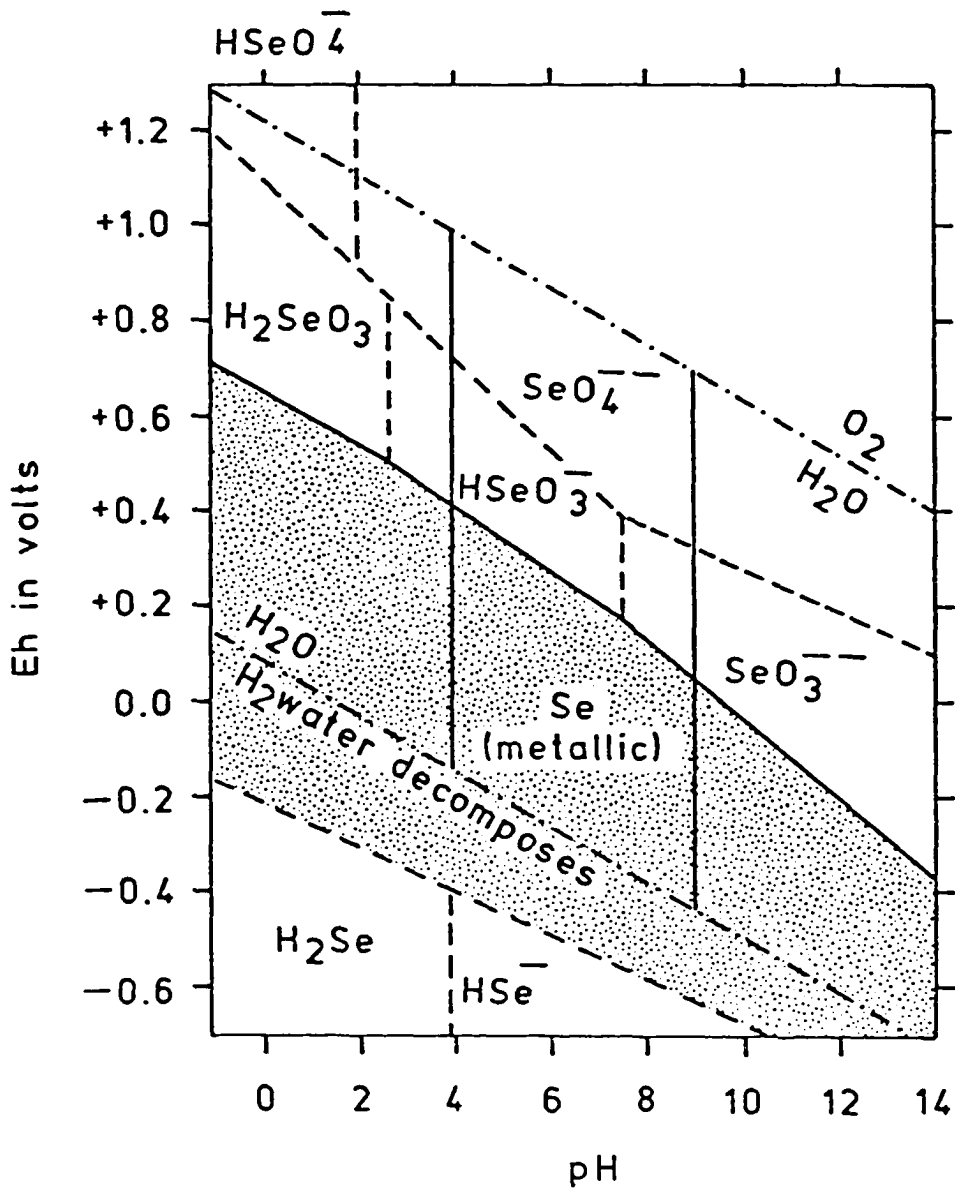
Chemical Form	Melting Point (°C)	Boiling Point (°C)
S ⁰	112-119	445
Se ⁰	170-217	681-688
H ₂ S	-85	-60
H ₂ Se	-66	-41
SO ₂	-76	-10
SeO ₂	340	Sublime 315

Table 1.2b

Reduction Potentials for some Analogous Selenium and Sulfur Compounds

<u>Reaction</u>	<u>Potential (V)</u>
$\text{Se} + 2\text{H}^+ + 2\text{e}^- \text{ ----> } \text{H}_2\text{Se}$	-0.360
$\text{S} + 2\text{H}^+ + 2\text{e}^- \text{ ----> } \text{H}_2\text{S}$	0.141
$\text{H}_2\text{SeO}_3 + 4\text{H}^+ + 4\text{e}^- \text{ ----> } \text{Se} + 3\text{H}_2\text{O}$	0.740
$\text{H}_2\text{SO}_3 + 4\text{H}^+ + 4\text{e}^- \text{ ----> } \text{S} + 3\text{H}_2\text{O}$	0.450
$\text{SeO}_4^{2-} + 4\text{H}^+ + 2\text{e}^- \text{ ----> } \text{H}_2\text{SeO}_3 + \text{H}_2\text{O}$	1.15
$\text{SO}_4^{2-} + 4\text{H}^+ + 2\text{e}^- \text{ ----> } \text{H}_2\text{SO}_3 + \text{H}_2\text{O}$	0.20

Figure 1.2. Stability field of selenium at 25°C, 1 atm, and [Se] = 10⁻⁶M (from Coleman and Delevaux, 1957).



$E_H < -0.2$) hydrogen selenide is not thermodynamically stable since HSe^- has a lower potential than the H^+/H_2 couple (Garrels and Christ, 1965; Faust and Aly, 1981). According to thermodynamic calculations, elemental selenium is stable over a wide range of E_H and pH values (Figure 1.2). Metal selenides have also been shown to exist in sediments due to their low solubilities (Sindeeva, 1964; Faust and Aly, 1981). Table 1.3 lists values for the log of the solubility product of some metal selenides. Based on the data in Figure 1.2 and Table 1.3, the precipitation of elemental selenium or metal selenides can be important factors affecting the concentration and distribution of selenium in waters and sediments (Howard, 1977; Cutter, 1982).

Thermodynamic diagrams, as in Figure 1.2, may be useful in predicting the dominant oxidation state of selenium under given conditions. Such equilibrium calculations have practical limitations since they do not take into account kinetic effects and biological mediation of certain redox reactions (Stumm and Morgan, 1981). It is well documented that biological processes greatly affect the redox chemistry of a number of elements including selenium (e.g., Cutter and Bruland, 1984).

Selenium in Oceanic Waters

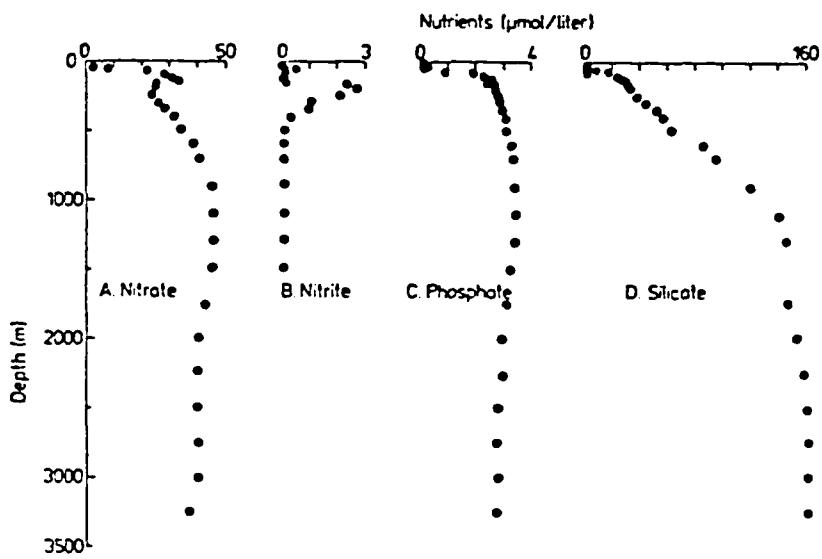
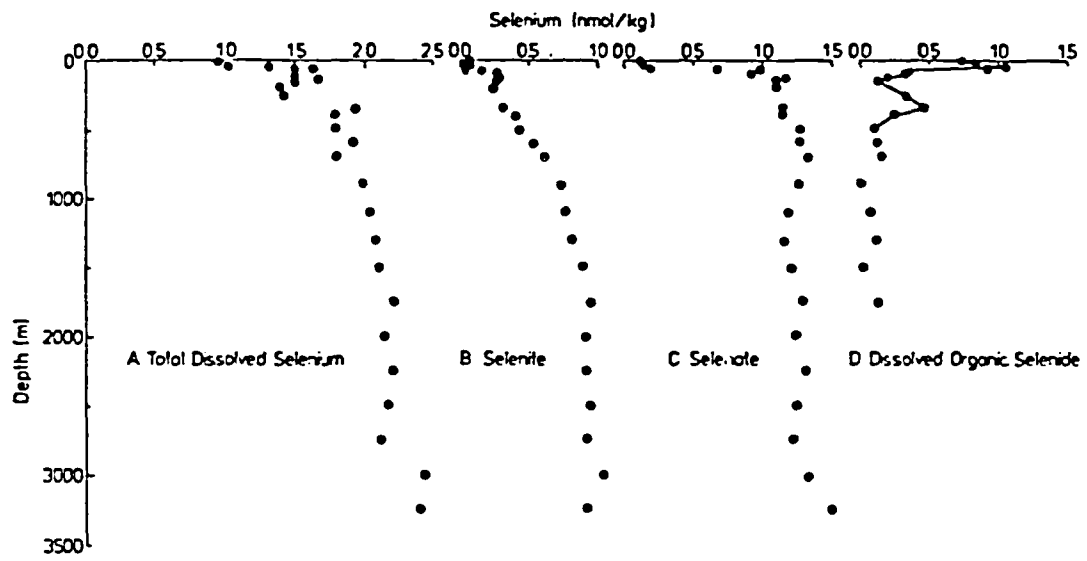
Selenium species display nutrient-like distributions in seawater (Measures et al. 1983, 1984; Cutter and Bruland, 1984; Figure 1.3). Correspondingly, marine organisms have

Table 1.3

Solubility of some Metal Selenides
(from Faust and Aly, 1981)

Metal	Log K_{sp}
Mn (+II)	-11.5
Fe (+II)	-26.0
Cu (+I)	-60.8
Cu (+II)	-48.1
Zn (+II)	-29.4
Cd (+II)	-35.2
Hg (+II)	-64.5
Pb (+II)	-42.1

Figure 1.3. Vertical depth profiles of total dissolved selenium, selenite, selenate, organic selenide and nutrients from Vertex II site, 18°N, 108°W (from Cutter and Bruland, 1984).



been shown to affect the speciation and distribution of selenium (Wrench, 1978; Wrench and Measures, 1982; Foda et al., 1983; Cutter and Bruland, 1984). Cutter and Bruland (1984) proposed an oceanic cycle for selenium (Figure 1.4). This cycle includes the selective uptake of inorganic selenite, reductive incorporation (i.e., selenide formation) into the tissue of phytoplankton, particulate transport via detritus, and a multi-step regeneration. Regeneration first involves the transformation of particulate organic selenide to dissolved organic selenide. Dissolved organic selenide is then oxidized to selenite, which in turn is oxidized to selenate. The persistence of thermodynamically unstable selenite in seawater indicates that there is kinetic stabilization of selenite (i.e., the rate of selenite oxidation to selenate must be slow). Overall, the oceanic cycle of selenium is dynamic and intimately tied to biological processes that affect its concentration, speciation, and distribution (Wrench and Measures, 1982; Cutter and Bruland, 1984). Direct analysis of selenium speciation in sediments can allow mechanistic details of selenium biogeochemistry to be observed, an approach which has been successfully exploited in the water column studies cited above.

Selenium in Geologic Materials

Selenium is widely distributed in the earth's crust (Table 1.4), and is usually not present at concentrations above 500 ug Se/g (Shamberger, 1983). The primary sources of

Figure 1.4. A diagram of the proposed marine biogeochemical cycle of selenium. Underlining reflects the relative concentrations of selenium species in surface and deep seawater. The preferential uptake of selenite in surface waters is indicated by a larger dissolved-to-particulate arrow (from Cutter and Bruland, 1984).

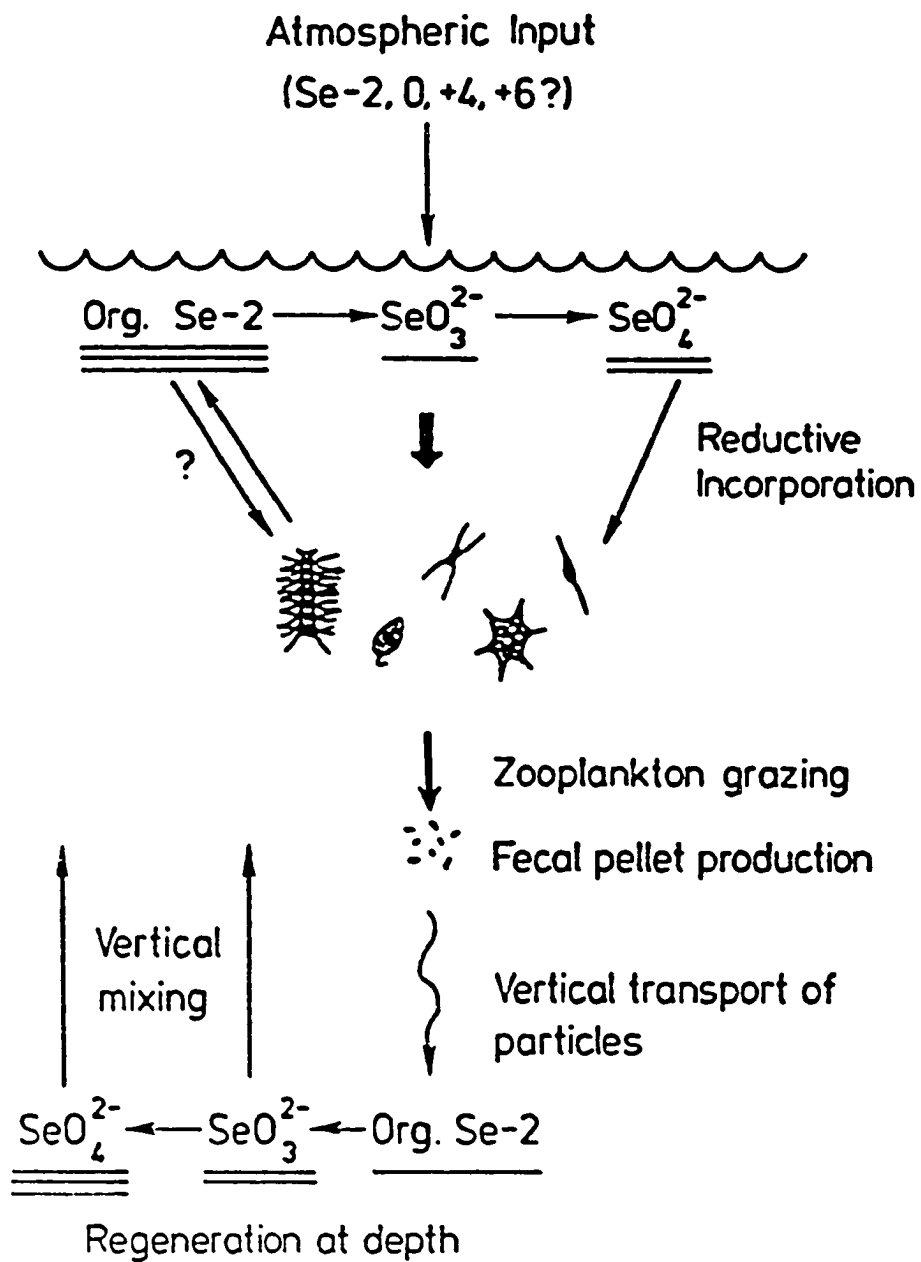


Table 1.4

Selenium in the Earth's Crust
(from Leutwein, 1972).

<u>Rock Type</u>	<u>Total Se (ug Se/g)</u>
Igneous	0.05
Shales	0.60
Sandstones	0.05
Carbonates	0.08

selenium to the earth's crust are volcanic emanations and metallic sulfides associated with igneous activity (Lakin, 1973). Goldschmidt (1958) estimated the abundance of selenium in igneous rock to be 0.09 ug Se/g. This value was calculated by using the measured selenium/sulfur ratio in sulfides (1.67×10^{-4} , by weight) and a sulfur concentration of 520 ug S/g. Turekian and Wedepohl (1961) revised the concentration of igneous sulfur downward to 300 ug S/g, thereby lowering the calculated selenium concentration in igneous rock to 0.05 ug Se/g. Shales have about an order of magnitude higher selenium concentration than other rock types (Leutwein, 1972). Tourtelot (1964) and Webb et al. (1966) showed that the concentration of selenium in marine and non-marine shales is significantly higher than that estimated from crustal abundances. A correlation between selenium and organic carbon in shales has been shown by Tourtelot (1962) and Vine et al. (1969).

Berzelius, in 1818, discovered the first selenium minerals, berzelianite (Cu_2Se) and eucairite (AgCuSe). Selenium forms minerals with elements of higher atomic numbers (e.g. Pb, Hg, Cu, Fe), and selenium compounds with light metals do not exist (Sindeeva, 1964). In nature, selenium has little lithophilic tendency and silicates of selenium are not known (Wedepohl, 1972). Various selenium minerals are listed in Table 1.5.

There exist a great number of selenium-bearing or -substituted minerals. The range of selenium concentrations

Table 1.5

Various Selenium Minerals
(from Leutwein, 1972).

I) Selenides and intermetallic compounds:	
Naumannite	Ag_2Se
Aguilarte	Ag_4SSe
Crookesite	$(\text{Cu}, \text{Tl}, \text{Ag})_2\text{Se}$
Clausthalite	PbSe
Tiemannite	HgSe
Onofrite	$\text{Hg}(\text{Se})$
Wurtzite	CdSe
Klockmannite	CuSe
Stilleite	ZnSe
Trogtalite	CoSe_2
Freboldite	CoSe
Blockite	NiSe_2
II) Sulfosalts:	
Weibullite	$\text{PbBi}_2(\text{S}, \text{Se})_4$
Platynite	$\text{PbBi}_2(\text{Se}, \text{S})_3$
III) Oxides	
Selenolite	SeO_2
IV) Selenates and selenites:	
Kerstenite	$\text{PbSeO}_4 \cdot 2\text{H}_2\text{O}$
Chalcomenite	$\text{CuSeO}_3 \cdot 2\text{H}_2\text{O}$
Ahlfeldite	$\text{NiSeO}_3 \cdot 2\text{H}_2\text{O}$

in minerals of diagenetic origin are given in Table 1.6 (Leutwein, 1972; Sindeeva, 1964). Because of the chemical similarities between selenium and sulfur, sulfides and native sulfur deposits often contain selenium in significant amounts (Faust and Aly, 1981; Leutwein, 1972). Further discussions on the mineralogy of selenium compounds can be found in Sindeeva (1964) and Wedepohl (1972).

The sedimentary geochemistry of selenium in marine environments has not been studied extensively. Based on the previous discussion, the speciation (i.e. oxidation state), phase association (i.e., carbonate, oxides, organic, and residual phases), and concentration of selenium in sediments will most likely be controlled by physical-chemical factors that are related to pH, E_H , and mineral solubilities. Most of the published data for marine sediments (Geering et al., 1968; Granger, 1966; Wiersma and Lee, 1971; Howard, 1977; Sokolova and Pilipchuk, 1973; Tamari, 1978) report only total selenium concentrations; speciation and phase association data are largely overlooked. Therefore, a starting point in this discussion is the theoretically (thermodynamic) predicted distribution of the various selenium oxidation states and compounds.

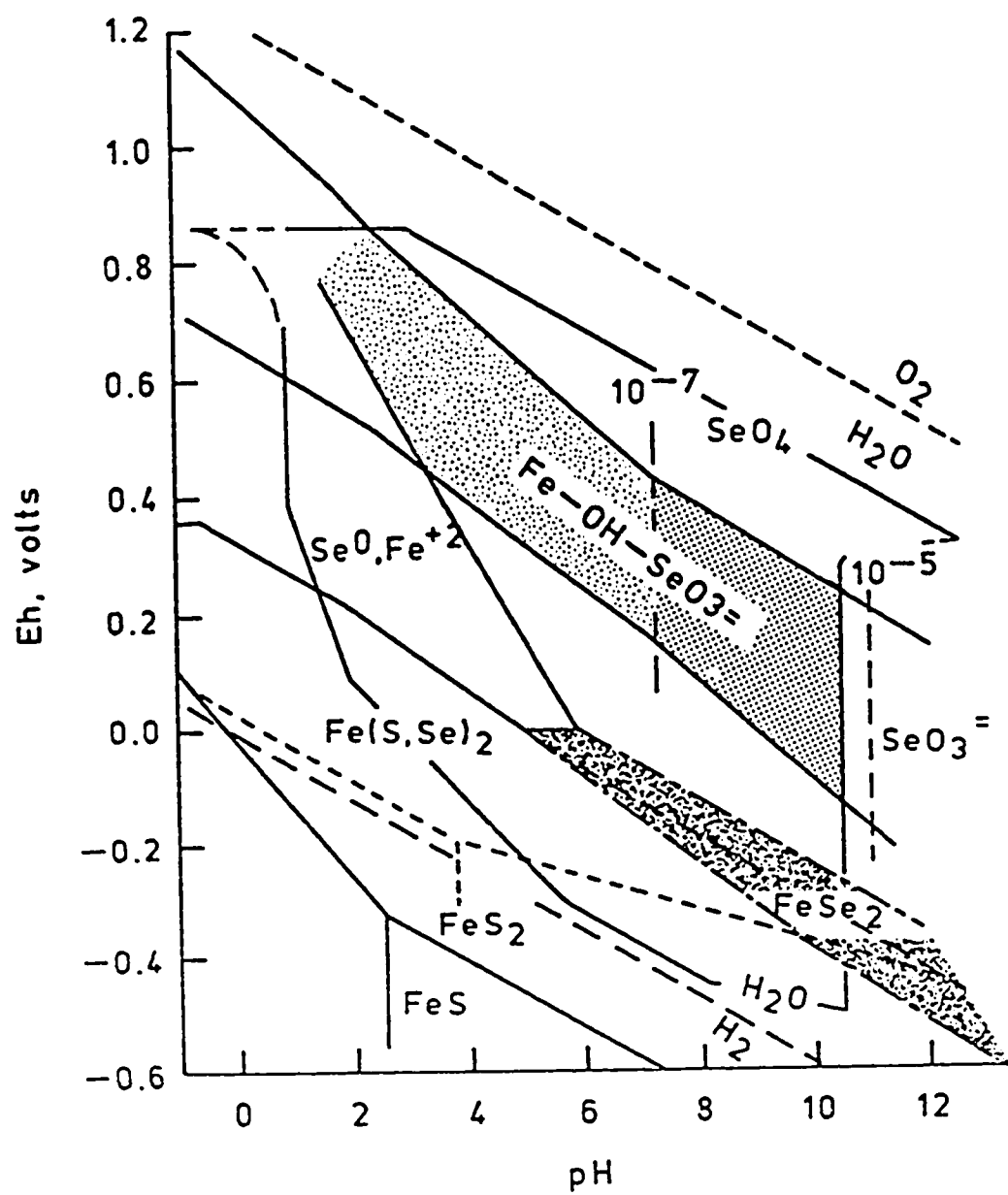
At equilibrium the oxidation states of selenium in sediments can be represented in an E_H /pH diagram (Figure 1.5). This figure is based on the calculations of Howard (1977) which incorporate the possible interactions of a Fe-S-Se system at equilibrium. It must be stated again that

Table 1.6

Selenium concentrations in minerals of diagenetic origin
(from Leutwein, 1972).

Mineral	% Se	Mineral	ug Se/g
Galena	0-20	Pentlandite	27-67
Molybdenite	0-0.1	Millerite	5-10
Volcanic Sulfur	0-5.2	Sphalerite	1-120
Linneite	0-4.7	Pyrrhotite	1-60
Chalcopyrite	0-0.1	Arsenopyrite	1-144
Pyrite	0-3	Marcasite	3-80
Cinnabar	0-0.4		
Bismuthinite	0.02-0.8		

Figure 1.5. E_H -pH diagram of predominant Se species in earth surface aqueous environments with $\text{Fe(II)} = 10^{-3}\text{M}$, total sulfur = 10^{-1}M and total selenium = 10^{-5}M (from Howard, 1977).



using such thermodynamic calculations to describe natural systems can be misleading since true equilibrium may not be obtained.

Under alkaline ($\text{pH} > 7$), oxidizing conditions selenium in sediments should be present in its most oxidized form, selenate (Lakin, 1973; Howard, 1977). Because selenate is not strongly adsorbed and does not form insoluble compounds (Sindeeva, 1964; Leutwein, 1972), it is the most mobile form of selenium. In contrast, Geering et al. (1968) showed that selenite is strongly adsorbed by ferric oxides such as goethite. This adsorption decreases with increasing pH (Hingston et al., 1968). Thus only under alkaline ($\text{pH} > 7$) conditions will the selenite ion be mobile.

Under more reducing conditions ($E_H < 0.2$), elemental selenium, $\text{Fe}(\text{SSe})_2$, and FeSe_2 are the predicted solid phases of selenium (Figure 1.5). Selenite (adsorbed to iron oxides) is reduced to either the elemental state or selenide in the zones where sulfate reduction occurs. The stability field of elemental selenium is large and elemental selenium could be the dominant solid form of sedimentary selenium (see Figures 1.2 and 1.5). As the system becomes more reducing, elemental selenium can react with ferrous iron to form ferroselite or seleniferous pyrite (i.e., pyrite containing selenium, Howard, 1977). Alternatively, as the system becomes oxidizing, pyrite can be oxidized and ferroselite then formed from the released $\text{Fe}(\text{II})$ and the elemental selenium already present. This latter reaction is due to ferroselite

being more stable than pyrite in an oxidizing environment (Howard, 1977). Ferroselite has been found in uranium deposits in sandstone and occurs near the interface between oxidized and pyritic sandstones (Granger, 1966; Granger and Warren, 1969). At an $E_H > 0.1$ ferroselite should be oxidized, producing ferric oxides and elemental selenium (and eventually selenite). Formation of FeSe (achavalite; not shown in Figure 1.6) is unlikely because the stability field of FeSe is small in the pH range of marine sediments (Ben-Yaakov, 1973).

While thermodynamic calculations predict the oxidation state and solid phases of selenium in sediments, no information about the rates of conversion between the various selenium species is available. Observations in the laboratory demonstrate that the oxidation of selenite to selenate is slow, while the reduction of selenite to elemental selenium is fast (Rosenfeld and Beath, 1964). The oxidation of elemental selenium to selenite is slower than the reduction of selenite and is dependent upon the allotropic form and particle size of the elemental selenium (Rosenfeld and Beath, 1964; Geering et al., 1968). The differences in oxidation/reduction rates of selenium species could lead to the kinetic stabilization of certain unstable oxidation states and compounds in natural environments. While these studies are informative, the biological mediation of these processes has been shown to increase the rates of these reactions and produce thermodynamically

unstable forms of selenium (Levine, 1925; Koval'skii and Ermakov, 1970; Geering et al., 1968; Howard, 1977; Sarathchandra and Watkinson, 1981; Foda et al., 1983; and others)

In terms of elucidating diagenetic pathways, past studies of sedimentary selenium are not very informative since only total selenium concentrations are reported. These data are, however, the starting point for this research and will be discussed next.

Wiersma and Lee (1971) determined the selenium concentration in surficial sediments from 11 Wisconsin lakes; values range from 0.5 to 3.5 ug Se/g. Within these sediments, slightly higher concentrations occur in the upper 60 cm (1.8 to 2.4 ug Se/g) than in the deeper sections (0.8 to 1.4 ug Se/g, from 60 to 100 cm). A significant correlation ($r = 0.81$) between iron and selenium was observed. This correlation may be due to the adsorption of selenite to iron oxides prior to deposition. Selenium-sulfur phase associations (e.g., with pyrite) are also possible, although the low concentrations of sulfate in lake waters suggest that this is not likely. This prevents the accumulation of pyrite within lake sediments as compared to marine sediments (Nriagu and Soon, 1985; Davison et al., 1985).

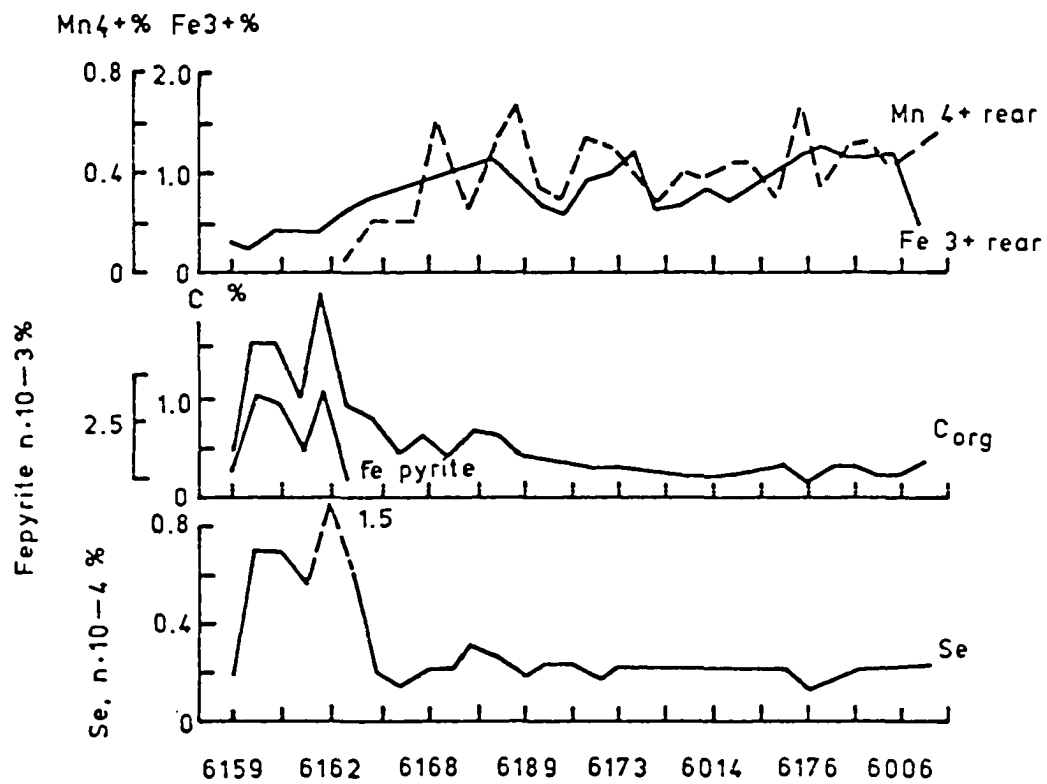
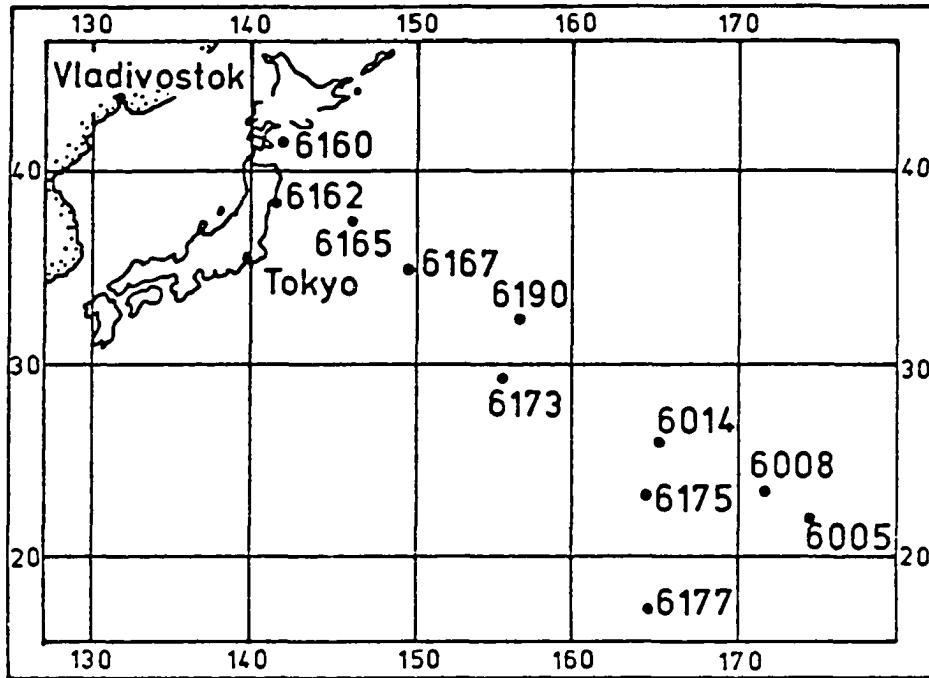
One of the first studies of sedimentary selenium in marine sediments was that of Sokolova and Pilipchuk (1973). They examined the distribution of selenium, organic carbon,

and pyrite-Fe in sediments from the coast of Japan to the Hawaiian Islands (Figure 1.6). Along this transect, the surface sediments are reducing (i.e., low E_H) near the coast of Japan, and become oxidized beyond the continental margin. The selenium content of the sediments varies from 0.1 to 1.7 ug Se/g (Figure 1.6). The highest selenium concentrations occur in reducing sediments, while selenium concentrations in oxidized sediments are lower by an order of magnitude. The association of selenium with pyrite-Fe and organic carbon is evident in the more reducing sediments. Selenium reaches a maximum value of 1.5 ug Se/g with corresponding organic carbon and pyrite-Fe maxima of 2.0% and 25 ug Fe/g. In oxidizing sediments, pyrite-Fe is undetectable, but a correlation between selenium and organic carbon still exists.

The correlation between selenium and organic carbon observed by Sokolova and Pilipchuk (1973) indicates that selenium is associated with sedimentary organic matter. This can occur either in the water column (reductive uptake by phytoplankton?) or during early stages of sedimentary diagenesis (via microbial uptake). The correlation between selenium and pyrite-Fe also suggests that selenium is incorporated into pyrite, possibly as a result of organic matter decomposition via sulfate reduction (Sokolova and Pilipchuk, 1973).

Tamari (1978) analyzed cores taken from the N. Pacific and the Sea of Japan for total sedimentary selenium and

Figure 1.6. Distribution of selenium, iron, pyrite and manganese in the surface sediments from Japan to Hawaii (from Sokolova and Pilipchuk, 1973).



other trace elements. He also treated sediments with sodium hydroxide to obtain information on selenium speciation and the sediment phases with which selenium is associated. Total sedimentary selenium concentrations in these cores range from 0.07 to 3.2 ug Se/g. The Pacific core exhibits a surface maximum (0.43 ug Se/g) and decreasing concentrations with depth (ca. 0.13 ug Se/g at 55 cm). In the Sea of Japan, one core exhibits a selenium minimum at the surface (0.32 ug Se/g), with a broad maximum at 30-50 cm (ca. 1.5 ug Se/g) and at 65 cm the selenium concentration in the core decreased to 0.79 ug Se/g. In a second core, the concentration of selenium displays little variation from the sediment surface to a depth of 90 cm (1.16 ± 0.17 ug Se/g, n=11). The vertical distribution of selenium in all cores is different from both aluminium and iron suggesting a non-detrital source. A slight positive relationship is observed between total carbon and total selenium in the three cores.

Tamari's (1978) sodium hydroxide leach removed less than 70% of the selenium in the surface sediments of these cores, and this fraction decreases with depth. In the surface sediments, it is possible that inorganic selenium is adsorbed to iron oxides. As the sediment becomes reducing with depth the dissolution of these iron oxides could lead to the subsequent release of adsorbed selenium. A NaOH leach has been shown to extract inorganic selenium (Cutter, 1985), but without proper pre-treatment this fraction may also contain a portion of humic-bound material (Gjessing, 1976)

containing organic selenide (Cutter, 1985). Therefore, Tamari's NaOH leach is not specific for inorganic forms of selenium. The amount of organically-bound selenide could be a significant portion of the total selenium in the leachate (Cutter, 1985).

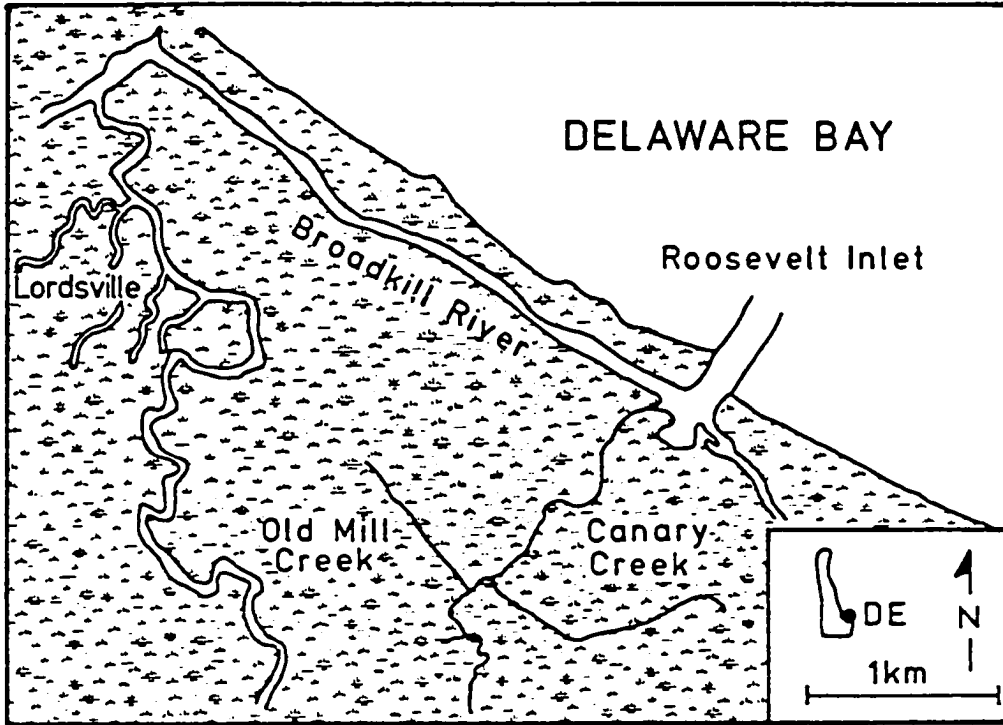
Recently, a technique has been developed to selectively leach inorganic selenium from sediments (Cutter, 1985). Using a 2M NaOH treatment, followed by elution through an XAD-8 column, selenite and selenate are separated from organic selenium and subsequently determined. The difference between total inorganic selenium and total selenium is operationally defined as "organic" selenium. "Organic" selenium actually is a combination of elemental selenium and selenide. The accuracy of this procedure was evaluated by comparison with the selective leaching procedure of Tessier et al. (1979), and use of radiotracers. The concentrations of selenite + selenate determined by Cutter's procedure are within 10% of the predicted concentrations. Using this procedure, Cutter (1985) showed that greater than 90% of the selenium extracted from estuarine and river sediments is associated with the "organic", reduced phase.

STUDY AREA

To examine the geochemistry of selenium in salt marsh sediments, this research was conducted in Delaware's Great Marsh, located near Lewes, Delaware on the southern shore of Delaware Bay (Figure 1.7). The sediments in the Great Marsh

Figure 1.7. Location map of study site Great Marsh, Lewes, Delaware. Samples were taken from Lordsville.

STUDY AREA



GREAT MARSH, LEWES, DELAWARE

were formed during the Holocene marine transgression (Strom and Biggs, 1972). The more recently deposited salt marsh material is underridden by lagoonal muds. The area is dominated by the marsh grass S. alterniflora and has been relatively undisturbed by human activity since the 1930's, when mosquito control ditches were built. Tidal inundations of the marsh occurs only during the highest tide of each month. Otherwise the marsh surface remains in contact with the atmosphere.

Aspects of the biogeochemistry of the Great Marsh system have been examined by Swain (1971), Lord (1980), Church et al. (1981), Boulegue et al. (1982), Lord and Church, 1983, and Luther et al. (1986). The seasonal cycling of sulfur, iron, and carbon in these sediments have been extensively studied by Lord (1980). The important biogeochemical aspects of this marsh system are summarized below.

The exposure of the marsh sediment surface to the atmosphere and infusion of oxygen during S. alterniflora photosynthesis causes iron and sulfur to be cycled seasonally between oxidized and reduced compounds. Lord (1980) divided the chemical cycle in the marsh sediments into 3 seasonal settings. In the spring/early summer, infusion of photosynthetic oxygen by S. alterniflora roots (to a depth of ca. 15 cm), causes the subsurface oxidation of pyrite. This process releases sulfate and protons into the pore waters, and facilitates the precipitation of iron

oxides and elemental sulfur. By late summer/early fall, the temperature of the marsh increases and sulfate reduction becomes the dominant reaction controlling the geochemistry of the marsh. Iron oxides, elemental sulfur, and protons are now consumed, with reduced iron (Fe^{+2}) and sulfide then building up in the pore waters. In the winter, both reduction and oxidation rates decrease, allowing the formation of sulfide phases (e.g., iron monosulfides and pyrite) due to diffusion of iron (II) and sulfide in the pore waters. The high concentration of dissolved sulfide (up to 7 mM) causes dissolved iron to be almost totally consumed via the precipitation of iron monosulfides and pyrite at this time. Below the oxic surface layers, pyrite accounts for between 70 to 80% of the total sulfur and reactive iron (Lord and Church, 1983). Due to the seasonally changing redox conditions, the marsh system is not sulfur limited, but with depth can be iron limited (Lord, 1980)

In short, the benefits of using a salt marsh environment for this research are that: 1) processes occur over a short depth range (0 to 40 cm); 2) redox changes occur over relatively short time scales; and 3) the information obtained may be useful in future studies of similar processes in other coastal or oceanic sediments. Using salt marshes as a model systems, the results of my study will have bearing on the coastal selenium cycle with respect to input/output processes at the sediment-water interface, oxidation-reduction reactions within sediments,

and the role of sediments as sites for changes in the speciation of dissolved selenium. Also, the relatively unpolluted environment of the Great Marsh enables the natural selenium cycle to be examined in the absence of major anthropogenic inputs (e.g., industrial) which might hinder data interpretation.

Chapter 2

The Determination of Selenium and Sulfur in Marine Sediments

INTRODUCTION

To study the geochemistry of selenium and sulfur, it is necessary to have analytical methods which are not only sensitive enough to detect trace concentrations, but also capable of determining the various oxidation states and chemical forms of selenium and sulfur. Such techniques exist for the study of sulfur in marine sediments (Cutter and Oatts, 1987), however only a few speciation techniques have been published for selenium in sedimentary material (Terada et al., 1975; Tamari, 1978; Cutter, 1985). Therefore, as part of this research the development of new analytical techniques for the further characterization of the solid phases of selenium was undertaken. It is the purpose of this chapter to discuss these procedures as well as the other methods used in this study. This chapter will be broken down into three sections: 1) sampling methods; 2) water analyses; and 3) sediment analyses.

SAMPLING METHODS

Cores (30 to 50 cm deep) were obtained by carefully driving a 6 cm diameter butyrate core liner into the marsh. Normally, three cores were obtained for each sampling period. By measuring outside and inside core lengths, depth

values were corrected for core compaction, which is assumed to be linear. The cores were immediately sealed from the atmosphere and returned to the laboratory (College of Marine Studies, Lewes, Delaware) for sectioning and squeezing. Once in the laboratory, the cores were extruded and sectioned in a nitrogen-purged glovebox (Lord, 1980) and the pore water obtained using Reeburgh (1967) sediment squeezers (0.4 μ m filtered). The extrusion and sectioning of the core in the glovebox was begun within one hour of sample collection. The temperature of the cores was kept as close to ambient marsh temperature as possible. Sampling intervals for the top 30 cm were 2.5 cm, and below 30 cm, intervals were increased to 5 cm. For pore water samples, several cores were squeezed at 5 cm intervals due to the low concentration of dissolved selenium. The first 1 to 2 ml of pore water were discarded, and the remainder collected in pre-cleaned Teflon bottles. The pore water was acidified to pH 1.5 with 6N HCl, and stored either under a nitrogen atmosphere or by quick freezing with liquid nitrogen (Troup et al., 1974; Loder et al., 1978). The total volume of pore water collected by this procedure ranged from 30 to 80 ml per 5 cm section. Pore waters were analyzed within 24 hr of collection. Sediment samples were frozen immediately after squeezing to prevent oxidative loss of reactive phases such as FeS.

Creek/estuarine water samples were collected by immersing a pre-cleaned linear polyethylene bottle below the water's surface. Due to the high concentration of particles

in these waters, samples were pre-filtered through a 1 μ m Gelman AE glass fiber filter in line with a 0.4 μ m Gelman filter cartridge. Filtered samples were collected in 1 L pre-cleaned borosilicate bottles. The samples were then acidified to pH 1.5 with concentrated HCl and stored at room temperature in the dark until analyzed.

All samples were brought back to Old Dominion University for analysis. Table 2.1 lists the parameters that were determined for sediment, pore water, and creek samples while Figure 2.1 presents a flow chart of pore water and sediment processing steps.

WATER ANALYSES

Experimental

Apparatus. The apparatus used for selenium determinations has been previously described by Cutter (1978; 1983). Figure 2.2 shows the apparatus used for the determination of selenite in liquid samples. This system can be used for samples with both high and low concentrations of dissolved selenium.

For low concentration samples, the stripping vessel (34/45 ground glass joint) can hold approximately 170 ml (100 ml of sample). For high concentrations samples, a small stripper system is employed. The small stripper is the same design as the larger unit except that a 29/42 ground-glass joint is used and the stripping vessel can hold approximately 70 ml. The injection port is a Teflon Swagelok

Table 2.1

List of Parameters Measured for this Study

Sediments (reference)	Pore Water (reference)
Total Selenium (1)	Total Selenium (2)
Selenate + Selenite (1)	Selenite (2)
Organic Selenide (3)	Selenate (2,3)
Elemental Selenium (3)	Organic Selenium (2,3)
Chromium Reducible Selenium (3)	
Elemental Sulfur (4)	
Acid Volatile Sulfur (5)	
Pyrite (5)	
Greigite (5)	
Total Carbon (6)	
Total Nitrogen (6)	
Total Sulfur (6)	
Reactive Iron (7)	

(1) Cutter, 1978; 1985

(2) Cutter, 1978; 1982; 1983

(3) This study

(4) Ferdelman and Luther (unpublished method)

(5) Cutter and Oatts, 1987

(6) Carlo Erba, 1985

(7) Tessier et al., 1979

Figure 2.1. Flow diagram for sample analyses (see Table 2.1 for specific techniques).

Flow Diagram for Sample Analyses

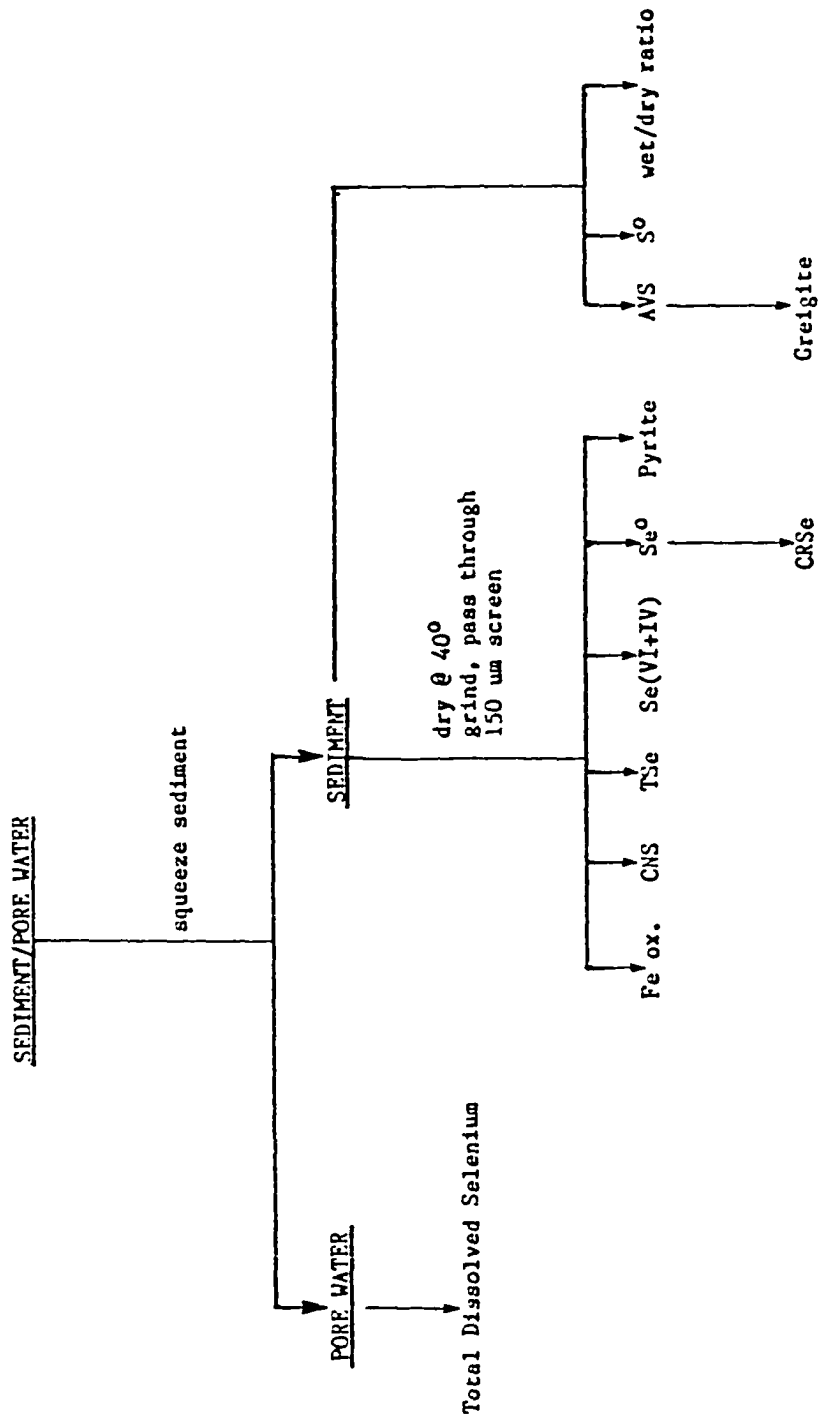
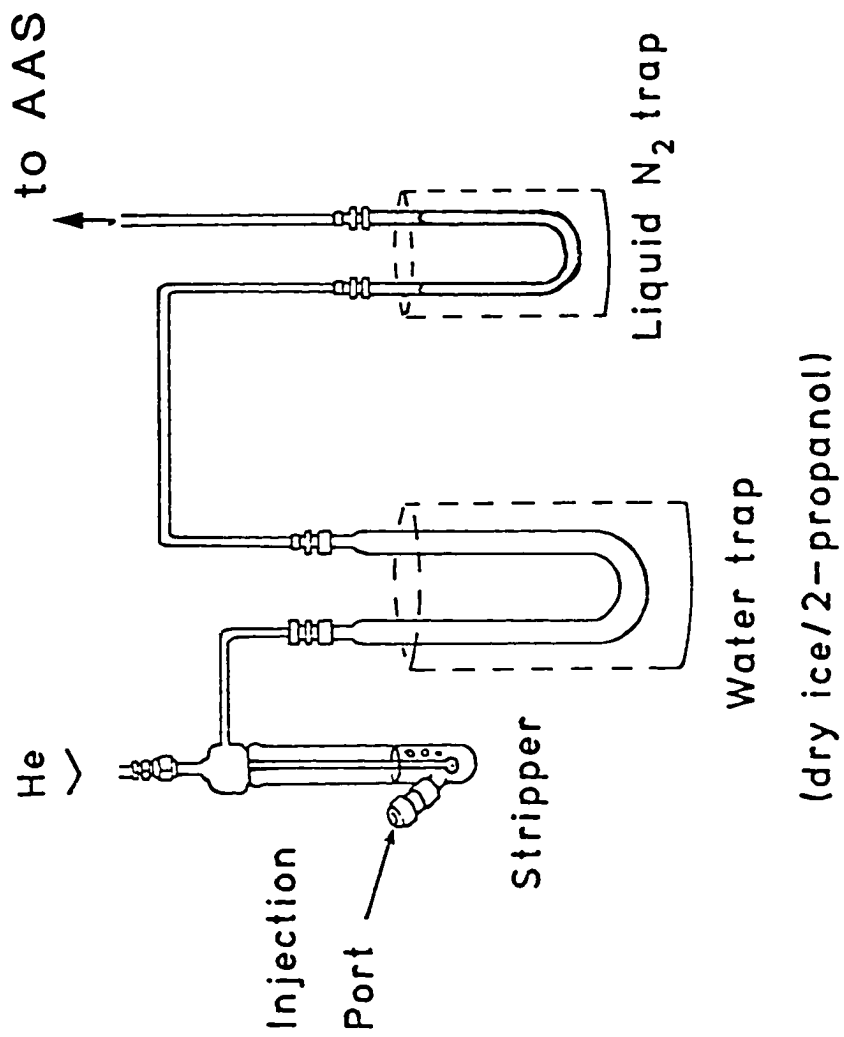


Figure 2.2. Apparatus for the stripping and trapping of volatilized inorganic selenium species.



fitting with a Teflon backed septum.

The stripping vessel is connected to a borosilicate glass U-tube (36 cm long, 14 mm i.d.) which is immersed in a dry ice/isopropanol bath. The U-tube acts as water trap and must be cleared of ice periodically (every 15-20 samples). The sample trap consists of a borosilicate U-tube (18 cm long, 6 mm o.d.) packed with dimethyl dichlorosilane-treated (DMCS) glass wool. The sample trap is immersed in liquid nitrogen for collection of hydrogen selenide. All tubing in the system is Teflon (6 mm o.d.) and all connections are made using Teflon Swagelok fittings.

The sample trap is connected directly into a quartz-tube burner which uses a air-hydrogen flame and is mounted in a Varian AA-1275 atomic absorption spectrometer (AAS). The dimensions of the burner head are 9 mm o.d. and 6.5 cm long (see Cutter (1978) for complete details). The following operating parameters are used: He stripping gas, 70 ml/min; burner gases, 200ml/min air and 70 ml/min H₂; lamp current, 8-10 mA; wavelength, 196.0 nm; and slit width, 1 nm. Spectrometer signals are processed and peak areas determined using a Hewlett-Packard 3392A digital integrator/plotter.

All glassware is cleaned with detergent, acetone, rinsed with deionized water and soaked in hot 7M HNO₃ overnight. The glassware is then rinsed with double deionized water (DDW) and dried. The glassware used for the stripping/trapping apparatus is silanized using DMCS to deactivate the glass surfaces (Grob, 1977). Plasticware is

treated similarly as the glassware except it is soaked in 1M HCl overnight instead of nitric acid.

Reagents and Standards. All reagents have been described previously (Cutter, 1978; 1983; 1985) and are of analytical grade.

Concentrated HCl (Baker) is bubbled for two hours with He to remove trace amounts of Cl₂. All working reagents are prepared daily, these include: (4% (w/v) sodium tetrahydridoborate (Alfa Products) in 0.08M NaOH, 2% (w/v) sulfanilamide (Baker), and 2% (w/v) potassium persulfate. Solutions of pH 1.6 and pH 12 are prepared using HCl and KOH, respectively.

Working standards of sodium selenite and sodium selenate (both from Alfa Products) are prepared daily from stock solutions of 1000 mg Se/L.

Amberlite XAD-8 resin, 16-50 mesh, (Supelco, Inc.) is rinsed three times with double deionized water (DDW) and decanted to remove the smallest resin particles. The resin is then rinsed three times with a pH 12 solution and stored cold in the pH 12 water solution until used. The XAD-8 column consist of 0.9 cm (i.d.) glass tube fitted with a Teflon stopcock. A DMCS-treated plug of glass wool is placed on the bottom of the column and 2.5 cm of cleaned resin is poured on top. The column + resin is rinsed (flowrate of 2 ml/min) with a 20 ml of pH 12 solution and then 20 ml of pH 1.6 solution.

Procedures: Dissolved selenium speciation. The determination of dissolved selenite, selenate, and organic selenide has been previously described by Cutter (1978; 1982; 1983). The technique involves selective formation of hydrogen selenide, liquid nitrogen-cooled trapping, and atomic absorption detection. Below is a description of this procedure for both high and low concentration samples using the large and small stripper system, respectively.

Large Stripper System

Selenite: A 100 ml sample is added to the bottom section of the stripping vessel and 52 ml of concentrated HCl is added. The system is connected to the gas bubbler and stripped with He for three minutes. The sample trap is then immersed in liquid nitrogen and 6 ml of tetrahydridoborate is added over a four minute time interval. The sample solution is stripped for a total of 10 minutes at which time the trap is removed from the liquid nitrogen. The resultant signal is processed via the digital integrator/plotter.

Selenite+Selenate: A 100 ml sample and 52 ml of concentrated HCl are added to a 400 ml beaker. The beaker is covered with a watch glass and boiled for 15 minutes. The solution is cooled to room temperature by placing it in an ice bath. After transferring the solution with rinsing into the bottom section of the stripper, the selenite procedure is then followed. This determination represents the concentration of selenite+selenite. The concentration of selenate is computed as the difference between the

concentrations of selenite+selenate and selenite.

Total Selenium: The selenite+selenate procedure is followed except 1.0 ml of the persulfate solution is added prior to boiling. The sample is then gently boiled for one hour. The sample is then transferred with rinsing to the bottom of the stripper and the selenite procedure is followed. This procedure yields the concentration of total selenium. $\text{Se}(-\text{II}+\text{O})$ is calculated as the difference between total selenium and selenite+ selenate.

Small Stripper System

Selenite: A 40 ml sample is added to the bottom section of the stripping vessel and 22 ml of concentrated HCl is added. The system is connected to the gas bubbler and stripped with He for two minutes. The sample trap is then immersed in liquid nitrogen and 3 ml of tetrahydridoborate is added over a three minute time interval. The sample solution is stripped for a total of 7 minutes at which time the trap is removed from the liquid nitrogen. The resultant signal is processed via the digital integrator/plotter.

Selenite+Selenate: A 40 ml sample and 22 ml of concentrated HCl are added to a 400 ml beaker. The beaker is covered with a watch glass and boiled for 15 minutes. The solution is cooled to room temperature by placing it in an ice bath. After transferring the solution with rinsing into the bottom section of the stripper, the selenite procedure is then followed. This determination represents the concentration of selenite+selenite. The concentration of

selenate is computed as the difference between the concentrations of selenite+selenate and selenite.

Total Selenium: The selenite+selenate procedure is followed except 0.5 ml of the persulfate solution is added prior to boiling. The sample is then gently boiled for 0.5 hour. The sample is then transferred with rinsing to the bottom of the stripper and the selenite procedure is followed. This procedure yields the concentration of total selenium. $Se(-II+O)$ is calculated as the difference between total selenium and selenite+selenate.

For pore water samples, the procedure for selenite+selenate determination is modified. An aliquot of sample (5 to 10 ml) is pH adjusted to 1.5 and then passed through a XAD-8 column at a flow rate of 2 ml/min. The eluant is collected in a 400 ml beaker. The column is rinsed so that the total volume collected (sample + rinses) is 40 ml. Determination of selenite+selenate entails boiling the sample, acidified with 22 ml of concentrated HCl, with 0.5 ml of a 2% (w/v) persulfate solution for 15 minutes. The sample is then analyzed for selenite as described above.

Reagent blanks consisting of DDW and all reagents used are run in triplicate for all species. Calibration is performed using the method of standard addition.

Discussion

The analytical figures of merits (e.g., accuracy, precision) for this selenium speciation procedure are listed

in the original publications of Cutter (1978; 1983). Accuracy (determined via the method of standard additions) is 98% and precision as relative standard deviation is 2.0% using 5 ng Se. The relative detection limit is 0.02 nM using a 100 ml sample.

Due to the low concentrations of dissolved selenium in the pore waters and the small sample volumes obtained by squeezing (< 80 ml), triplicate analyzes were not performed. Only a few samples had a high enough selenium concentration for speciation measurements to be performed.

For most uncontaminated natural waters, selenium determination via hydride generation is relatively free of interference (Cutter, 1983). However, a problem was encountered with pore water samples from the marsh. Pore water samples, spiked with selenate before boiling (i.e., the selenite+selenate procedure) showed no recovery, while samples spiked with selenite after boiling showed full recovery. This indicates that an interferent was effecting the quantitative reduction of selenate to selenite, and not the reduction of selenite to hydrogen selenide.

Inorganic interferents in the hydride method have been studied by Pierce and Brown (1977). Of possible interferents, iron was chosen for study because Lord (1980) showed that the pore waters of the Great Marsh can contain up to 1 mM of dissolved iron. Therefore, a selenate recovery experiment was performed using the selenite+selenate procedure and DDW containing either 1 mM ferrous- or ferric-

iron. In the presence of 1 mM ferrous-iron no recovery of selenate (2.5 ng Se) was obtained, while full recovery was obtained in the presence of 1 mM ferric-iron. Only with the addition of persulfate prior to boiling (i.e., total selenium procedure) was selenate fully recovered in the presence of 1 mM ferrous-iron. However, with the addition of persulfate, organic selenium would be converted to selenite. Therefore, organic selenium must first be removed in order to determine the concentration of selenite+selenate.

A procedure was developed, using XAD-8 resin (see above), to separate selenite+selenate from organic selenium so that the interferent can be eliminated using persulfate. The XAD-8 resin has been shown to remove organic material from acidified (pH 1.5) water samples (Roden and Tallman, 1982) and has been successfully used by Cutter (1985) for the separation of organic selenium from selenite+selenate from sediment leaches. Once the pore water sample is passed through the XAD-8 column the resultant analysis yields a selenite+selenate concentration.

SEDIMENT ANALYSES

Experimental

Apparatus. The apparatus for total selenium, selenium speciation, and elemental selenium determinations is described the above section. For particulate selenium determinations, final solution volumes are small so that the small stripper (total volume 70 ml) described above is

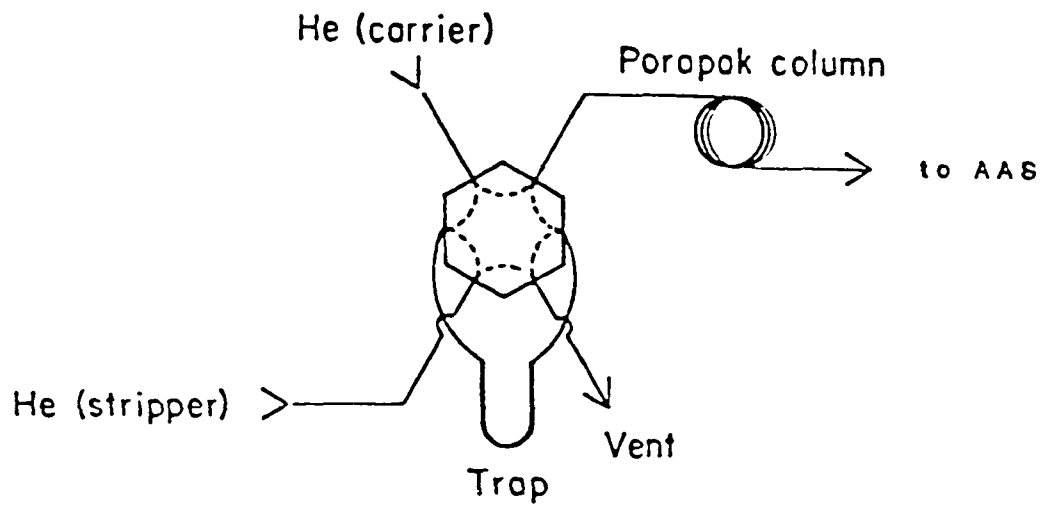
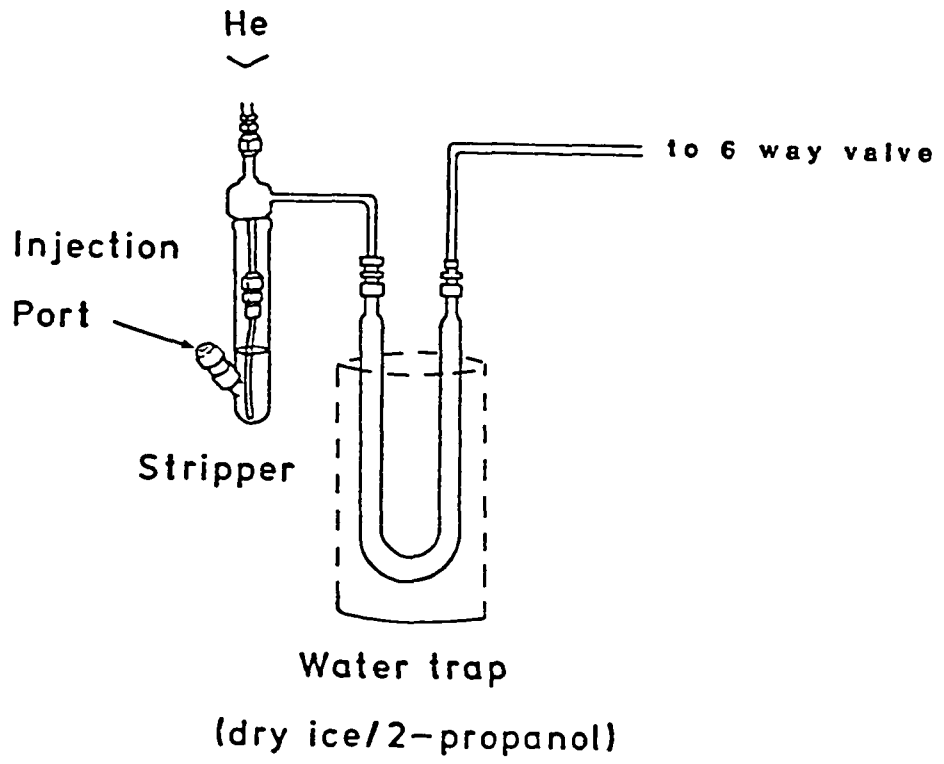
employed.

Selenium associated with pyrite or chromium reducible selenium (CRSe) is determined with modifications of the apparatus described above and in Cutter and Oatts (1987). Figure 2.3 shows the apparatus used for the determination of CRSe. It consists of a 40 ml borosilicate glass stripping vessel (24/25 ground glass joint) which is fitted with a Teflon bubbler consisting of a 1.5 cm piece of Gortex microporous Teflon tubing (Anspec Co.). The bubbler is inserted into a 6 mm o.d. Teflon tube connected to the stripper with a Teflon Swagelok fitting. The tip of the Goretex tubing is heat sealed. The injection port is a Teflon Swagelok fitting with a Teflon backed septum. A small magnetic stirrer is placed under the stripper to enhance mixing of the sediment slurry.

A water trap consisting of a borosilicate glass U-tube (36 cm long, 14 mm i.d.) is attached to the stripper. This U-tube is connected to a six way valve (Figure 2.3). The interior of the valve is stainless steel/Teflon and is pre-cleaned with acetone. A hydride trap, which consists of a borosilicate glass U-tube (6 mm o.d., 10 cm long) packed with DMCS-treated glass wool, is connected to the six-way valve. This trap is cooled in liquid nitrogen and collects hydrogen selenide evolved from the stripper. The six-way valve is configured so that the stripping gas and carrier gas can be purged through the liquid nitrogen trap. A Teflon column packed with acetone washed (de Souza et al., 1975)

Figure 2.3. Apparatus for the stripping and trapping of hydrogen selenide from sediment using chromium reduction.

—



Porapak-PS (6 mm o.d., 40 cm long, 50/80 mesh) was used for the separation of hydrogen selenide from hydrogen sulfide also produced during the treatment of the sediment with Cr(II). The column is interfaced directly in the quartz-tube burner mounted in an atomic absorption spectrometer (IL Model 241) via a Teflon Swagelok fitting. The column is kept at room temperature. The following operating parameters are utilized: He stripping gas, 75 ml/min; He carrier gas, 60 ml/min; burner gases, 200 ml/min air and 330 ml/min hydrogen. Signals from the spectrophotometer are recorded and processed on a Hewlett-Packard 3392A digital/integrator.

The apparatus used for the determination of particulate sulfur speciation (iron monosulfide, greigite, and pyrite) is fully described in Cutter and Oatts (1987). Briefly, the stripper and water trap are similar to the CRSe apparatus (no six-way valve, however). The hydrogen selenide trap used for selenium determinations is replaced by a borosilicate glass U-tube (16 cm long, 6 mm o.d.) packed with 2.5 cm of 50/80 mesh acetone washed Porapak QS. This trap/column is wrapped with Ni-Cr wire which is connected to a variable transformer, set to 50°C.

The trap/column is connected to a photoionization detector (HNU Systems) and electrometer (Model PI-52) interfaced to a Hewlett-Packard 3390A integrator. The following operating conditions are utilized: carrier/stripping gas, 60 ml/min He; detector temperature, 50°C; lamp intensity, 4 (using a 10.2-eV lamp).

Total sedimentary nitrogen, carbon and sulfur (NCS) are determined with a Carlo Erba ANA 1500 NCS analyzer. A Cahn Model 29 microbalance is used to weigh samples for NCS, CRSe, iron monosulfide, greigite, and pyrite analyses.

Iron, from the hydroxylamine-hydrochloride sediment leach, is determined by flame atomic absorption spectrometry (either a Perkin-Elmer 4000 or Varian AA-1275). A wavelength of 248.3 nm and slit width of 0.2 nm are used for this analysis. The instrument is used in the single beam mode with no background correction.

Glassware, used in all sample preparation and analysis, is cleaned as described previously.

Reagents and Standards. Most reagents are described in the previous section and in Cutter (1978; 1983; 1985) and Cutter and Oatts (1987). Nitric acid is trace metal grade (Baker Instra-Analyzed). Glass columns (described previously) are packed with 5 cm of XAD-8 resin instead of 2.5 cm as discussed in the water analyses section. A 1M sodium sulfite solution is adjusted to pH 7 using HCl. The chromium (II) solution is prepared by passing 1M chromium chloride (in 1M HCl) through a Jones reductor (Zhabina and Volkov, 1978). This Cr(II) solution is prepared daily and stored under nitrogen. The 5% (w/v) potassium iodide and 4% (w/v) sodium tetrahydridoborate (in 0.08M NaOH) solutions are also prepared daily.

A standard sulfide solution of 1 to 10 ug S/ml

(anhydrous Na₂S, Alfa Products) is prepared daily using nitrogen-purged DDW which is adjusted to pH 8 with NaOH. The solution is kept under nitrogen while being used. The selenium standard is described above. Elemental selenium standard was obtained from Pfaltz and Bauer, Inc., and is sold as the red form of elemental selenium.

Procedures: Sediment preparation. Sediments are stored frozen until preparation and/or analysis. Figure 2.1 presents a flow chart for sediment processing and analyses. Sediment samples analyzed for total selenium, selenite+selenate, elemental selenium, chromium reducible selenium, pyrite, total carbon/nitrogen/sulfur and iron oxides are dried at 40°C, ground using an agate mortar and pestle, and sieved through a 150µm nylon screen. Pyrite samples are further treated to remove elemental sulfur. An aliquot of the dried powder (ca. 200 mg) is placed in a polyethylene centrifuge tube with 10 ml carbon tetrachloride. The sample is sonicated for 10 minutes, centrifuged and the supernatant discarded. This procedure is repeated two times. The sample is dried at 80°C overnight. Samples for CRSe are pre-extracted with a pH 7 1M sodium sulfite to remove elemental selenium. Normally, the samples are the sediment residues left from the elemental selenium leach (see below). The leached sediment is washed three times with DDW and dried at 40°C. Because the sample is now a hardened pellet, it is re-ground using an agate mortar and

pestle. Sediment samples for iron monosulfide, greigite, and elemental sulfur are thawed just prior to analysis with a microwave oven and used directly. The wet to dry ratios of the sediment samples are determined on separate aliquots.

Total Selenium. Sediment (0.1g) is placed in a clean 50 ml pyrex beaker with 5 ml concentrated nitric acid, covered with a watch glass, and refluxed at a low temperature for three hours. At this time five drops of concentrated perchloric acid is added to the sample and the reflux continued for three hours. The watch glass is rinsed with DDW into the beaker. The contents of the beaker are brought to near dryness, but never to dryness. The above procedure is repeated again. At the end of the second reflux and evaporation, the sample is refluxed in 5 ml nitric acid (only) for an additional three hours and brought to near dryness. At this point 10 ml of 4M HCl is added to redissolve the residue. The sample is filtered through a 0.45-um membrane filter and stored in a pre-weighed 30 ml polyethylene bottle.

Aliquots (0.5-1.0 ml) of this digestion solution are diluted to 40 ml with DDW and analyzed for total selenium as described in the water analyses section. Sediments from selected depth intervals are digested and analyzed in triplicate, while each individual digest is analyzed for selenium in triplicate. Reagent blanks consisting of all reagents used are run through the entire procedure.

Sedimentary (selenite+selenate). Sedimentary (selenite+selenate) is determined by the method of Cutter (1985). In brief, a 0.5 gram of sediment is placed in a 50 ml Tefzel centrifuge tube, wetted with 2 ml of DDW and sonically disrupted (2 kHz) for three minutes. Two milliliters of a 2M NaOH solution are placed into the tube and the sample is leached in a sonic bath for 4 hours. The leachate is acidified to pH 1.6 - 1.8 with concentrated HCl (ca. 0.4 ml); small adjustments of the pH are made with dilute HCl or NaOH. The leachate is separated from the sediment by centrifugation (10,000 rpm for 10 min.) and the supernatant transferred into a 50 ml Teflon beaker. The sediment is rinsed with 1 ml of pH 1.6 solution, respun, and the supernatant added to the Teflon beaker; this rinse procedure is repeated two additional times. The leachate is then passed through a prepared Amberlite XAD-8 resin column (flow rate of 2 ml/min) to remove "organic" selenium (Roden and Tallman, 1982; Cutter, 1985). The eluant is collected in pre-weighed 30 ml polyethylene bottles.

Selenite+selenate is determined in this solution by subjecting 1-2 ml aliquots to the total dissolved selenium procedure described above using boiling time of 15 minutes. The concentration of Se(-II+0) in a sediment is computed as the difference between the concentrations of total selenium and selenite+selenite.

Elemental selenium. A 0.30g dried sample is placed in a 50

ml Tefzel centrifuge tube, 5 ml of 1M Na₂SO₃ (pH 7) is added, and the solution is sonically disrupted (2 kHz) for two minutes. The tube is capped and placed in a ultrasonic bath for eight hours. The resultant slurry is centrifuged at 10,000 rpm for ten minutes and the supernatant is decanted into a 50 ml Teflon beaker. The sediment is then rinsed with 1 ml of the sulfite solution, centrifuged, and again decanted into the Teflon beaker. A total of three rinses are used (save sediment pellet for CRSe procedure). The sulfite supernatant is filtered through a 47 mm Nuclepore membrane filter (0.45 um) into a pre-weighed 50 ml glass beaker. Two milliliters of concentrated HNO₃ are added to the filtered solution, the beaker is covered with a watch glass and placed on a hot plate. The solution is refluxed at a low temperature for one hour. The watch glass is rinsed with DDW into the beaker and the solution is then slowly evaporated. The sample should be evaporated to near dryness, but never to dryness. When the sample is near dryness, approximately 0.3 ml of DDW is added. The solution is evaporated down to near dryness and 0.3 ml of DDW is added again. After the second addition of DDW and dryness step, the sample is removed from the hot plate and cooled. Ten milliliters of 4M HCl are added to the beaker and the beaker weighed. The residue is allowed to dissolve and resultant solution mixed thoroughly. The solution is then poured into a 30 ml polyethylene bottle for storage.

In order to analyze the sample, a 0.50 ml aliquot is

diluted to 40 ml with DDW and subjected to the total dissolved selenium procedure.

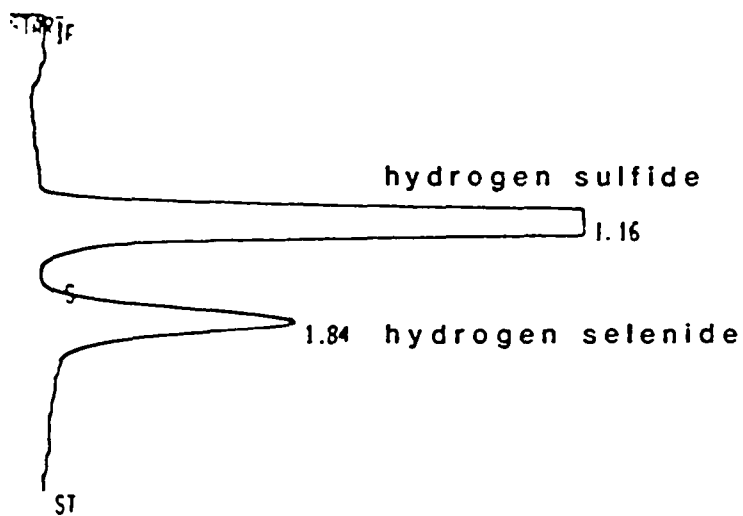
Chromium Reducible Selenium. The sediment from the elemental selenium procedure is rinsed with 5 ml of DDW, centrifuged and the DDW discarded. The DDW rinse is repeated two times. The rinsed sediment pellet is dried and re-ground.

Dried sediment (ca. 0.070 g) is added to the stripper bottom along with a magnetic stir bar. The sample is wetted with 15 ml of DDW and purged for 90 seconds. The six-way valve is set to the strip/trap setting and the magnetic stirrer started. After purging, 4 ml of concentrated HCl is injected. The trap is immersed in liquid nitrogen and 10 ml of acidic-Cr(II) is added. All injections are made using a glass syringe with a platinum needle. After a 25 minutes of stripping and trapping, the valve is switched to the trap/column setting and the trap is removed from the liquid nitrogen. Using the conditions stated above, hydrogen selenide should elute at approximately 1.76 minutes (Figure 2.4).

Calibration of the system is done by attaching the small selenium stripper system (described in the water analyses section and Cutter, 1978) to the six-way valve column apparatus. It is necessary to pre-condition the column three times with 122 ng Se(IV) in order to obtain consistent response factors. Hydrogen selenide is generated

Figure 2.4. Typical chromatogram showing the separation of hydrogen selenide and sulfide (see text for operating conditions).

ID 19 42 6



RUN # 52
ID 19.42

SEP/30/85 22:39:37

RT	AREA	TYPE	AR/HT	AREA%
1.16	3.1504E+07	SPB	0.136	84.540
1.84	5761300	BB	0.203	15.460

TOTAL AREA= 3.7265E+07
MUL FACTOR= 1.0000E+00

from a standard solution of selenite using the dissolved selenite procedure described above. However, the hydrogen selenide is chromatographed using the Porapak-PS column. A typical calibration curve is shown in Figure 2.5.

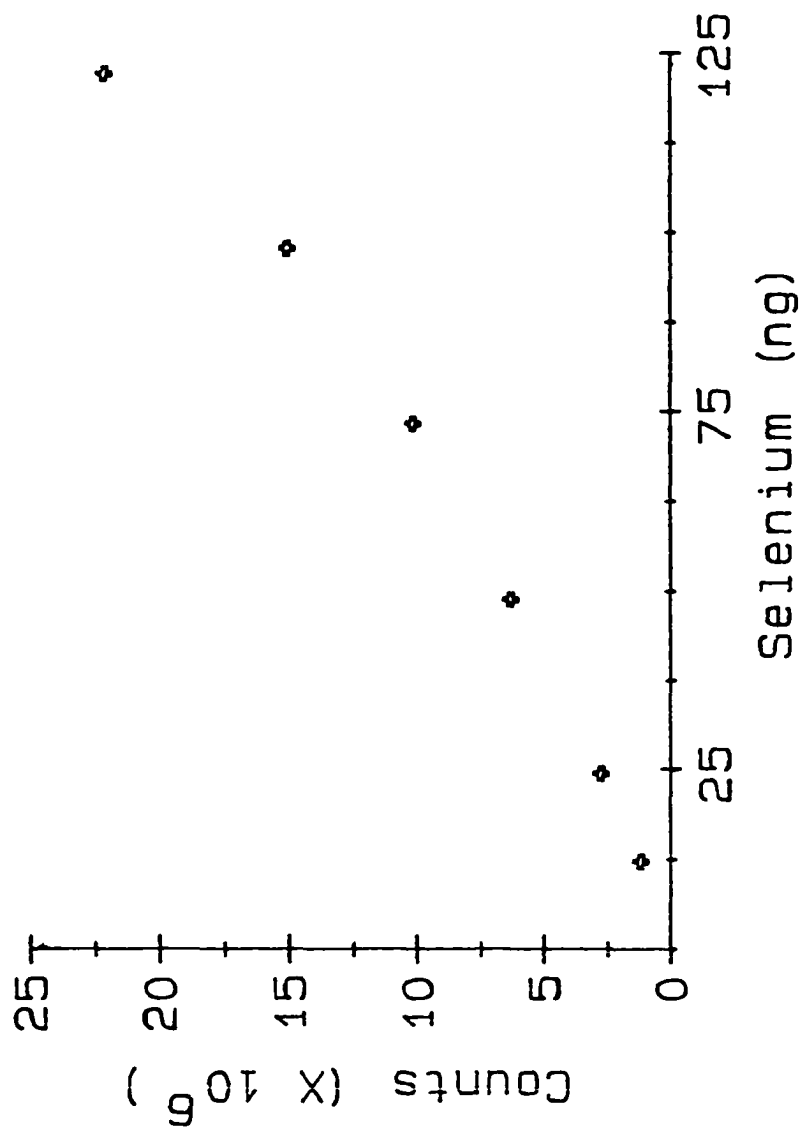
Iron Monosulfide, Greigite, and Pyrite. The determination of acid volatile, greigite, and pyrite sulfur utilizes the methods for the selective generation of hydrogen sulfide described by Zhabina and Volkov (1978) and Cutter and Oatts (1987).

Elemental Sulfur. Elemental sulfur is determined using a method developed by Ferdelman and Luther (unpublished) at the University of Delaware. This technique takes advantage of the reaction between elemental sulfur and sulfite, which forms thiosulfate quantitatively. Thiosulfate is determined with a Princeton Applied Research model 174A polarograph using a model 303 static drop mercury electrode (Luther et al., 1985).

Carbon, Nitrogen and Sulfur. Total particulate carbon, nitrogen, and sulfur are determined on dried and ground sediment using a Carlo Erba ANA 1500 NCS Analyzer.

Iron oxides. Iron oxides (total reactive iron) are determined by a modification of the method by Tessier et al. (1979). Approximately 0.50 g of sediment is placed into a 50 ml Tefzel centrifuge tube along with 10 ml of 0.04M hydroxylamine-hydrochloride (in 25% acetic acid). The tube

Figure 2.5. Typical calibration curve for chromium reduction technique using Porapak-PS column (see text for operating conditions).



is capped and sonicated for one hour. The tube is then placed in a 90°C water bath for seven hours. The slurry is stirred once every hour. After seven hours, the slurry is cooled and then centrifuged for 10 minute at 10,000 rpm. The supernatant is decanted into a 50 ml Teflon beaker. The sediment is rinsed with 5 ml of DDW, centrifuged, and decanted. This procedure is repeated twice. The combined supernatant is filtered through a 47 mm 0.45 um Nuclepore filter and the filtrate placed in a pre-weighed 30 ml polyethylene bottle.

Iron analysis is performed by flame atomic absorption spectrometry (Varian AA-1275 Atomic Absorption Spectrometer, AAS). Operational conditions are taken from the Varian Operation Manual. The method of standard addition is used for calibration. Certain depth intervals were leached in triplicate while all samples were determined by the AAS in triplicate and corrected for reagent blanks.

Discussion

Total Selenium. The analytical figures of merits for this procedure are discussed in Cutter (1985). The accuracy of the method was determined by comparison with National Bureau of Standard reference material and shown to recover 100% of the reported selenium (Cutter, 1985). The average procedural precision is less than 7% (RSD) for triplicate analyses while the detection limit is 10 ng Se/g using a 0.20 g sample.

Sedimentary (selenite+selenate). The accuracy of this method was determined by comparison to the method of Tessier et al (1979) and using radiotracer experiments; agreement was found to be within an average of 95% (Cutter, 1985). Certain sediment samples were analyzed in triplicate to assess the precision of the method. Precision is better than 8.7% (RSD) at a concentration of 40 ng Se/g (n=3), while the detection limit is 0.44 ng Se/g using a 0.500 g sediment sample.

As noted in the dissolved selenium section above, difficulties were encountered when trying to determine selenite+selenate in marsh pore waters. A similar problem was also encountered with sedimentary (selenite+selenate), but only selenite could not be determined. Once again, iron is likely to be the interferent since the concentrations of iron oxides reach up to 1% Fe.

A possible technique to remove this interference, would be to pass the leachate, acidified to 4M with HCl, through a column packed with an anion exchange resin (Amberlite AG1X8, 100-200 mesh). Cutter (unpublished data) has shown that procedure removes iron interference from particulate digests, with full recovery of selenite and selenate. Unfortunately, this modification was not developed for this study in time to be used for the sedimentary (selenite+selenate) determinations.

Elemental Selenium. The approach used for the determination

of elemental selenium involves the reaction between elemental selenium and sodium sulfite at pH 7 to form soluble sodium selenosulfate (Warren, 1968). For the determination of elemental selenium four basic criteria had to be met: 1) the technique must be amenable to the hydride/AAS method for selenium analysis, 2) the leaching procedure must quantitatively solubilize the elemental selenium present in the sediment, 3) the leach must not solubilize other forms of selenium (e.g., organic selenides, ferroselite, and selenite+selenate) and 4) the analysis must be precise ($< \pm 10\%$, RSD). These criteria are discussed below.

An experiment was performed to check if sodium sulfite can quantitatively solubilize elemental selenium and if the resultant solution can be determined by the hydride/AAS system. A known amount of elemental selenium was placed into a beaker with 1M sodium sulfite. The beaker was heated for one hour at a low setting. Because the solution can not be analyzed directly (upon the addition of tetrahydridoborate, elemental sulfur precipitates), the sulfite solution was treated with nitric acid (see above procedure). For this and subsequent experiments, commercially available elemental selenium was used. Since its purity was not reported, the standard was subjected to the total selenium digest which is calibrated using the primary selenite standard. Data on the recovery of elemental selenium using the sulfite treatment are presented in Table 2.2. From these data, it is apparent

Table 2.2

Recovery of Se⁰ using Sodium Sulfite

mg Se added ^a	mg Se recovered ^b	% Recovered
3.1	3.0 ± 0.1	97 ± 2
3.1	3.2 ± 0.1	103 ± 4
3.4	3.5 ± 0.1	103 ± 2
4.6	5.4 ± 0.8	117 ± 17
4.7	5.0 ± 0.2	106 ± 3
		Average: 105 ± 6

a - the selenium added is based on the purity of the elemental selenium standard which was determined by the nitric-perchloric digest procedure.

b- each sample is determined in triplicate.

that elemental selenium can be quantitatively solubilized ($104.6 \pm 3.5\%$) by sodium sulfite.

In order to check the recovery of elemental selenium in actual sediments, an aliquot of marsh sediment was spiked with a known amount of elemental selenium standard and leached with the sulfite solution. The sediment/elemental selenium mix was also digested using the nitric-perchloric procedure (see above). A recovery of $90.6 \pm 8.6\%$ ($n=3$) was obtained (Table 2.3). It should be pointed out that the concentration of elemental selenium in the sediment mix is over three orders of magnitude higher than natural concentrations of selenium (mg/g versus ug/g). Because the concentration of elemental selenium in marsh sediment is much lower it should therefore be completely solubilized using the same solution/sediment ratio.

Although this experiment showed that most of the elemental selenium was solubilized it is possible that other forms of selenium are leached and also extracted. In particular, treating sediments with pH 9 sulfite may liberate sedimentary (selenite+selenate) and organic selenium. The pH of a 1M sodium sulfite solution is nine, and as such some fraction of the particulate selenite+selenate might also be leached from the sediments during the elemental selenium procedure (Hingston et al., 1968; Cutter, 1985). To check this, marsh sediment containing a known amount of sedimentary (selenite+selenate) was leached with sulfite at pH 9. In addition, the potential pH effect was

Table 2.3

Recovery of Se⁰ from Marsh Sediment^a using a Sodium Sulfite Leach and Nitric-Perchloric Digest

Nitric-Perchloric Digest
(mg Se/g)

1.79 ± 0.08

1.85 ± 0.13

1.54 ± 0.13

average: 1.72 ± 0.11 (n=3)^b

Sulfite Leach at pH 9
(mg Se/g)

1.53 ± 0.04

1.66 ± 0.17

1.49 ± 0.11

average: 1.56 ± 0.11 (n=3)^b

Recovery = 90.7 ± 8.6%

a-Sediment sample used: DMC smII, 11-13 cm,

Total Selenium: 0.48 ± 0.028 ug Se/g

Elemental Se : 0.18 ± 0.017 ug Se/g

b - "n" is the number of samples processed, while each sample is analyzed in triplicate.

examined by leaching the same sediment with sulfite adjusted a to pH 7. Table 2.4 contains the results of these experiments. The data show that at pH 9, 0.34 ± 0.022 ug Se/g is leached from the sediment, while at pH 7 only 0.19 ± 0.026 ug Se/g is recovered. The difference between these values is 0.15 ug Se/g or 92% of the sedimentary (selenite+selenate) concentration of 0.17 ± 0.004 ug Se/g originally in the sediment. This data indicates that a 1M sodium sulfite solution at pH 9 solubilizes the majority of the sedimentary (selenite+selenate), while a pH 7 solution appears to be more selective for elemental selenium.

To further verify that little or no sedimentary (selenite+selenate) is leached at pH 7, an experiment was performed in which the sediment was extracted with pH 7 water and the leachate analyzed for total selenium. The results in Table 2.4 show that only a small portion of the sedimentary (selenite+selenate) ($7.1 \pm 2.9\%$, n=3) was solubilized. Thus, it appears that the use of pH 7 sulfite does not contaminate the elemental selenium fraction with sedimentary (selenite+selenate).

Finally, the effect of the sulfite leach on organic selenium was examined. Since organic selenium is not determined directly, organic carbon was used as an indicator. A marsh sediment was leached with sodium sulfite (at pH 9) and analyzed for total carbon, nitrogen and sulfur before and after leaching. Although the previous experiments show that a pH 7 sulfite solution must be used, a pH 9

Table 2.4

Sulfite and Water Leach Results of Marsh Sediment^a
at pH 7 and 9

I) Sulfite Leach at pH 7 (ug Se/g)

- 1) 0.19
- 2) 0.16
- 3) 0.18
- 4) 0.19
- 5) 0.20
- 6) 0.23

average: 0.19 ± 0.026 (n=6)

II) Sulfite Leach at pH 9 (ug Se/g)

average: 0.34 ± 0.022 (n=1)

III) Water Leach at pH 7 (ug Se/g)

- 1) 0.017
- 2) 0.0084
- 3) 0.0095

average: 0.012 ± 0.005 (n=3)

Sediment sample used: 6/26/86, 10-12.5 cm

Total Selenium = 0.60 ug Se/g
Selenite+Selenate = 0.17 ug Se/g

a - "n" is the number of samples processed, while each sample is run in triplicate.

solution should solubilize more organic carbon than one at pH 7 (Gjessing, 1976). Therefore, the results of this experiment will likely indicate the maximum amount of organic selenium that can be solubilized. After leaching, the sediment was rinsed four times with DDW, dried, re-ground, and analyzed for NCS.

The results in Table 2.5 show that within the analytical errors complete recoveries of carbon and nitrogen are obtained. The losses in total sulfur are expected since sodium sulfite solubilizes elemental sulfur in a similar manner to elemental selenium (Ferdelman and Luther, unpublished method). The carbon and nitrogen results imply that very little organic selenium would be mobilized by the sulfite leach. A simple calculation was performed to estimate the theoretical amount of selenium released by sulfite given an amount of organic carbon solubilized. The ratio of selenium to carbon is fairly uniform in Great Marsh sediments ($\text{Se/C} \times 10^{-6}$ (molar) = 1.27 ± 0.36 , n=67). Assuming that 3% (2X the standard deviation of the carbon analyses) of the organic carbon (average OC = 6.38%) is solubilized, only 0.016 ug Se/g would be leached. This concentration is small in comparison to the concentrations found in these sediments (see Chapter 4).

The analytical precision of the sulfite leach procedure averages 12% (RSD, n=3), and may be due to the amount of sample handling (i.e., transfer steps and the drying step). The detection limit of this procedure is

Table 2.5

Carbon, Nitrogen, and Sulfur Recoveries after Sulfite Leach

	% Before Leach ^a	% After Leach ^a	Recovery, %
Carbon	4.83 ± 0.05	4.91 ± 0.07	101.7 ± 1.8
		5.07 ± 0.14	104.9 ± 3.1
Nitrogen	0.364 ± 0.004	0.369 ± 0.006	101.4 ± 2.0
		0.397 ± 0.010	109.1 ± 3.0
Sulfur	1.69 ± 0.04	1.31 ± 0.06	77.5 ± 4.0
		1.20 ± 0.04	71.0 ± 2.9

a - each sample is run in triplicate.

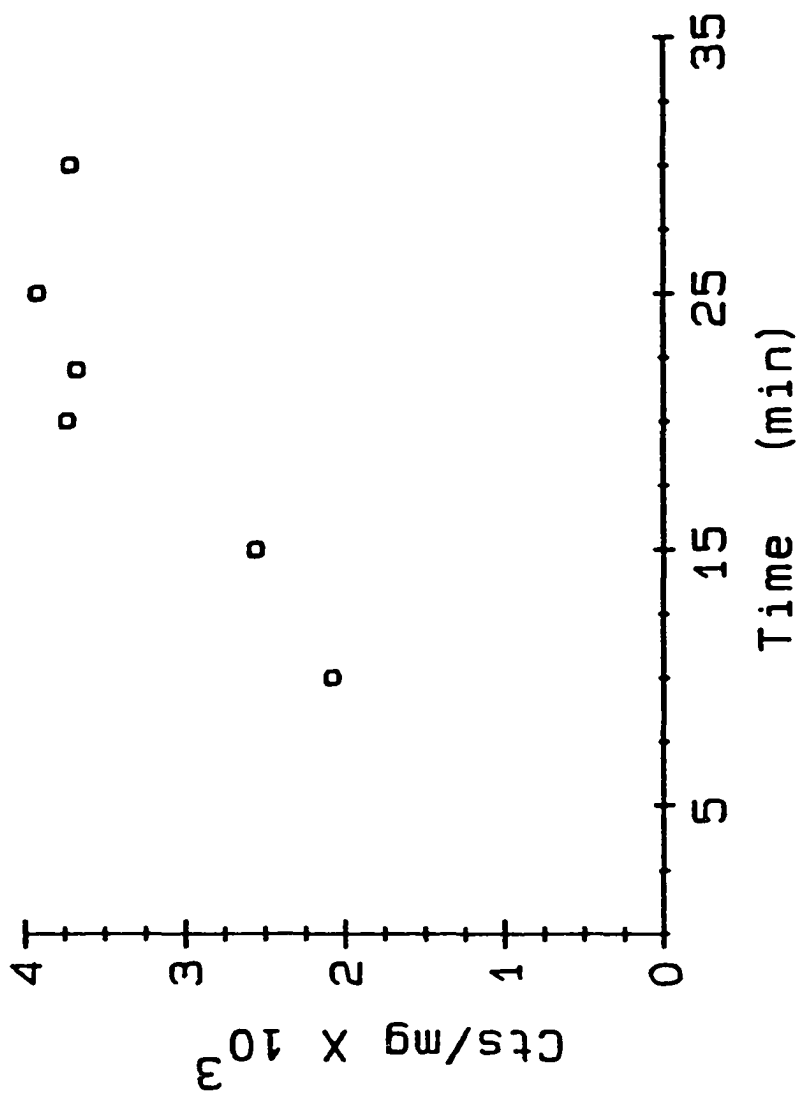
2.7 ng Se/g using a 0.30g sediment sample. Overall, the results in Tables 2.2, 2.3, 2.4 and 2.5 show that sodium sulfite is a reasonably accurate and precise leach for the extraction of elemental selenium from marsh sediments.

Chromium Reducible Selenium. The determination of chromium-reducible selenium is an adaptation of the pyrite method proposed by Zhabina and Volkov (1978) and Cutter and Oatts (1987). Selenium determined via chromium reduction is most likely a mixture of ferroselite (FeSe_2) and selenium associated with pyrite (FeSSe). Analytically, the separation of ferroselite and pyrite-Se would be difficult due to their similar chemical properties. Therefore, selenium determined by this procedure is termed "chromium reducible selenium" (CRSe).

The recovery of CRSe versus stripping/reaction time was first investigated. For this work, a marsh sediment was used to determine the maximum recovery. The data in Figure 2.6 shows that maximum recovery occurs after a 20 minute strip/trap time. This time is similar to that which is used for the analysis of pyrite using chromium reduction (Cutter and Oatts, 1987). Therefore, 25 minutes is used to make the procedure relatively time independent.

The above experiment gives the maximum recovery of CRSe, however it necessary to determine the percent recovery of CRSe or ferroselite. Because there is no commercial ferroselite standard, synthesis of a standard was

Figure 2.6. Recovery of CRSe (as hydrogen selenide) with increasing Cr(II) reaction/strip time. For this experiment a marsh sediment sample was analyzed for various times until maximum recovery was obtained (ca. 20 minutes). Integrator counts were then normalized to sediment weight for each reaction time.



undertaken. Ferroselite was prepared by placing freshly precipitated iron sulfide in a solution of sodium selenosulfate (Warren, 1968). The slurry was stirred for four days under nitrogen at 35°C. The mixture was filtered and the ferroselite dried at room temperature. The identification of ferroselite was confirmed by X-ray diffraction by G. Luther at the University of Delaware.

The synthetic ferroselite was spiked into a marsh sediment sample and analyzed for total sedimentary selenium (as above) and CRSe. The spiked sediment sample was pre-extracted with sodium sulfite to remove elemental selenium remaining after synthesis. The amount of selenium recovered by the Cr(II) reduction is 0.21 ± 0.030 mg Se/g (n=7), while the nitric perchloric digest (i.e., total selenium) yielded 0.26 ± 0.014 mg Se/g (n=3). Thus the chromium method appears to recover $80.8 \pm 12.4\%$ (RSD = 15.4%) of the spiked ferroselite. The large analytical uncertainty is most likely due to the inhomogeneity of the sediment mix (1 mg Se(0) into 3 gm sediment) and the small sample size used for this experiment (1 to 3 mg sediment).

Three other forms of selenium were used to check the specificity of the chromium reduction procedure. Selenite (24.4 ng Se) and organic selenide (48.8 ng Se as seleno-methionine) were subjected to the chromium reduction method. No detectable hydrogen selenide was generated from either compound. Marsh sediment, spiked with elemental selenium was also analyzed by the chromium method. A poor and variable

recovery of elemental selenium was observed (average of 27%, n=19). Since the variable and non-quantitative recovery of elemental selenium would obviously hamper the determination of CRSe, elemental selenium is first removed using sodium sulfite (e.g., as part of the elemental selenium procedure).

The detection limit for CRSe is 0.060 ug Se/g using a 40 mg sediment sample. The precision for the CRSe determination is 10% (RSD) at 0.010 ug Se/g (n=4).

Iron Oxides. The method for leaching iron oxides involves the combined action of reducing the oxide with hydroxylamine hydrochloride and keeping the dissolved metal in solution with acetic acid Tessier et al. (1979). Because the leach is performed on untreated sediment (i.e., no prior removal of the exchangeable, carbonate or iron monosulfide phases) the concentrations are considered to be total reactive or non-residual iron (Chester and Hughes, 1967; Agemiam and Chau, 1976; Salomons and Forstner, 1984). This phase would be expected to undergo major diagenetic alterations due to the changing redox conditions within the sediment and would be a major source of iron for pyritization. The detection limit for this analysis is 0.015% Fe (2X the standard deviation of the blank) using 0.500 g sediment sample, while precision averaged 4% (RSD, n=3).

Chapter 3

Sulfur Geochemistry in the Great Marsh

INTRODUCTION

While the main objective of this dissertation is the elucidation of the geochemical cycle of selenium in a salt marsh system, a concurrent study of sulfur's geochemistry was also undertaken because of their chemical similarities (see Chapters 1 and 5). Using newly developed analytical techniques (Cutter and Oatts, 1987), sedimentary sulfur speciation was examined in sediments of the Great Marsh. In this chapter, I will present a qualitative and quantitative model of the seasonal variations of sedimentary sulfur. This chapter will be followed by a similar discussion pertaining to the geochemistry of selenium in these sediments. Finally in Chapter 5, a comparison of both data sets will be presented. To start this chapter, I will first briefly discuss pertinent background material on the sulfur cycle that was not covered in Chapter 1.

The sulfur cycle in coastal marine sediments has received considerable attention due to sulfate's pivotal role in anaerobic respiration and the resultant formation of authigenic sulfide minerals (Goldhaber and Kaplan, 1974). Thus, the cycling of sulfur in anoxic environments also affects the biogeochemical cycling of carbon and trace elements, as well as the maintenance of biological activity (Howarth, 1984). Furthermore, it is proposed that reduced

sulfur serves as an energy source for chemolithotrophic bacteria (Howarth, 1984). This energy, from the oxidation of sulfide, can be used by a number of organisms which fix CO₂ as organic biomass. Bacterially produced sulfide can also react with a number of metal cations, iron being the most abundant in marine sediments. Of the possible iron-sulfur compounds, pyrite (FeS₂) is the only thermodynamically stable phase in marine sediments (Berner, 1967). A variety of pyrite synthesis schemes have been proposed (see review by Rickard, 1975), including the reaction of mackinawite (FeS_{0.94}) with elemental sulfur or polysulfides, the dissociation of greigite (Fe₃S₄), and the direct reaction of ferrous iron and polysulfides. As a result, mackinawite and greigite may be important intermediates in pyritization. Moreover, it has been demonstrated that the commonly observed "framboidal" form of pyrite requires greigite as an intermediate (Sweeney and Kaplan, 1973). Laboratory studies indicate that pyrite formation via mackinawite and greigite proceeds more slowly than direct precipitation (Rickard, 1975). However, demonstrating the existence of certain pyrite intermediates in the environment has been hampered by the lack of sensitive and selective analytical techniques. Recently developed methods (Cutter and Oatts, 1987) are now able to discriminate between the various forms of sedimentary sulfur (elemental sulfur and sulfur in mackinawite, greigite, and pyrite) at detection limits suitable for the examination of natural sediments.

The role of sulfate reduction in the cycling of both sulfur and carbon in salt marsh environments has been the focus of several studies. Howarth and Teal (1979) found that pyrite formed rapidly in upper marsh sediments, and that it represented the major fraction of sedimentary sulfur. In contrast, King et al. (1985) conclude that acid volatile sulfides and elemental sulfur are the short-term products of sulfate reduction in the salt marsh. Both these studies employed ^{35}S -labelled sulfate to measure sulfate reduction rates to determine the fate of bacterially produced sulfide. This technique must be used with caution since isotope exchange between the different sulfur phases has been observed (Jorgensen et al., 1984). In addition, processes were examined only on short time scales (days), and in one study (King et al., 1985), only the upper 10 cm of sediment were investigated. Lord and Church (1983) exploited the seasonal redox cycling of a Delaware salt marsh in order to examine sulfate reduction and pyritization. To obtain the rate of pyritization they derived a diagenetic modeling using porewater and solid phase constituents to fit observed pyrite profiles.

This examination of sedimentary sulfur is complimented by a parallel study of dissolved sulfur speciation in the marsh (Luther and Church, submitted), which greatly benefits both studies. In this manner the cycling of sedimentary sulfur and the mechanisms of pyritization, can be examined

through a careful analysis of all sulfur pools in the marsh sediment.

RESULTS AND DISCUSSION

Total carbon, nitrogen, and sulfur

Sulfate reduction in a salt marsh is driven by the large inputs of organic matter to the marsh environment (Howarth, 1984). Consequently the formation of iron sulfide minerals is also affected by this organic matter input (Berner, 1970). Organic carbon values in the surface sediments (0-3 cm) averaged 8.32%, while those below 30 cm averaged 4.53% (Table 3.1). In contrast to other marine sediments where the major organic carbon input is detritus, organic carbon in salt marsh sediments is formed in-situ by S. alterniflora (Valiela et al., 1976). In Figure 3.1 carbon/nitrogen (atomic) ratios with depth are shown for the five sampling periods. As is generally seen in marine sediments, the carbon/nitrogen ratios increase with depth, indicating that nitrogen-rich organic material is being selectively remineralized. In the upper 15 cm of sediment where the majority of the biological productivity occurs (Roman and Daiber, 1984), seasonal trends are not readily apparent in the carbon and nitrogen data. It is unclear why the 12/85 data is inconsistent with the others, but anomalies in this core appear in the other data as well. For this reason, the December 1985 results will only be treated qualitatively.

TABLE 3.1
Great Marsh Solid Phase Sulfur Data

Depth (cm)	Org. C (%)	Tot. N (%)	Tot. S (%)	FeS ←	Fe ₃ S ₄ (mg S/g)	S(O) →	FeS ₂	Fe,ox ^a (mg Fe/g)
Sampling date: 4/4/85								
0-2.9	9.43	0.86	0.65	ND	0.03	0.40	1.57	13.3
2.9-5.8	11.7	1.02	0.97	0.14	0.02	2.91	1.65	5.32
5.8-8.6	12.7	1.38	1.01	0.29	0.13	2.67	3.32	NA
8.6-11.5	9.44	0.67	1.18	NA	0.02	2.69	3.98	2.01
11.5-14.4	7.62	0.57	1.32	0.35	0.06	3.93	4.93	1.40
14.4-17.3	5.57	0.39	1.53	0.24	1.19	0.61	8.23	1.49
17.3-20.2	5.82	0.37	1.06	0.24	0.31	0.44	6.84	2.35
20.2-23.0	6.27	0.42	0.88	0.20	0.25	0.56	5.04	1.99
23.0-25.9	6.16	0.38	1.06	0.14	0.24	0.68	6.51	1.24
25.9-28.8	4.11	0.29	1.12	NA	NA	NA	7.17	1.48
28.8-32.3	4.48	0.32	1.32	0.04	0.39	0.64	7.30	2.18
32.3-35.7	4.32	0.30	1.49	0.08	NA	NA	8.85	2.19
Sampling date: 6/19/85								
0-2.7	8.08	0.76	0.53	0.03	0.02	0.34	2.09	9.90
2.7-5.5	9.54	0.82	0.70	0.03	0.07	0.93	0.85	2.90
5.5-8.2	9.15	0.77	0.73	0.05	0.08	0.98	1.07	1.70
8.2-10.9	5.45	0.41	1.72	0.03	0.01	0.97	12.6	1.70
10.9-13.7	8.05	0.65	0.89	0.05	0.01	2.44	1.86	1.80
13.7-16.4	7.43	0.58	1.16	0.07	1.76	2.67	2.55	0.80
16.4-19.1	5.26	0.36	1.64	0.05	0.86	0.57	12.2	2.20
19.1-21.8	5.76	0.38	0.92	0.14	0.71	0.71	6.34	1.70
21.8-24.6	8.94	0.57	1.16	0.25	0.07	0.73	4.73	1.20
24.6-27.3	6.00	0.41	0.94	0.03	NA	NA	5.55	1.40
27.3-30.0	5.61	0.39	1.32	0.02	0.41	0.44	9.21	1.90
30.0-34.4	4.19	0.30	1.42	0.05	NA	NA	10.3	3.00
34.4-38.8	3.40	0.24	0.75	0.06	NA	NA	5.07	1.80
38.8-42.0	3.20	0.21	0.91	0.10	NA	NA	7.75	1.80
Sampling date: 12/5/85								
0-3.2	7.70	0.61	1.23	.003	0.07	NA	3.06	3.9
3.2-6.4	7.16	0.83	1.15	0.06	0.05	NA	2.28	1.4
6.4-9.6	6.04	0.75	1.94	0.05	0.03	NA	9.83	1.5
9.6-12.8	5.10	0.40	1.10	0.01	0.17	NA	3.90	1.5
12.8-16.1	6.56	0.58	0.95	0.02	0.06	NA	3.08	1.1
16.1-19.3	6.08	0.52	1.42	0.02	0.17	NA	6.33	0.9
19.3-22.5	5.23	0.40	1.64	0.02	0.77	NA	9.59	1.4
22.5-25.7	6.76	0.49	1.17	0.04	1.18	NA	3.97	1.7
25.7-28.9	5.08	0.40	0.79	0.15	0.44	NA	2.28	1.4
28.9-32.1	4.86	0.43	0.71	0.08	NA	NA	3.25	1.1
32.1-35.3	4.94	0.43	1.43	0.04	0.42	NA	7.90	1.9
35.3-38.6	3.30	0.31	1.30	0.04	NA	NA	8.28	2.6
38.6-41.7	3.33	0.30	1.23	0.02	NA	NA	8.61	1.8
41.7-48.1	3.12	0.31	1.07	0.02	NA	NA	9.98	1.6
48.1-54.5	3.60	0.41	1.48	0.02	NA	NA	5.63	2.1

Table 3.1 (continued)

Depth (cm)	Org. C (%)	Tot. N (%)	Tot. S (%)	FeS ←	Fe ₃ S ₄ (mg S/g)	S(O) →	FeS ₂	Fe,ox ^a (mg Fe/g)
Sampling date: 3/26/86								
0-3.0	7.78	0.73	0.55	ND	0.02	0.34	1.12	7.83
3.0-6.0	8.52	0.80	0.61	ND	0.02	0.77	0.51	3.30
6.0-9.0	10.1	0.96	1.70	0.03	0.06	4.71	1.75	2.91
9.0-12.0	9.11	0.79	1.21	0.02	0.06	3.42	2.64	2.07
12.0-15.0	8.76	0.62	0.95	ND	0.02	1.06	2.96	1.38
15.0-18.0	6.30	0.51	1.58	0.09	1.35	0.46	11.2	2.00
18.0-21.0	5.19	0.38	1.50	0.05	0.51	0.35	10.2	1.95
21.0-24.0	4.74	0.32	0.64	0.20	0.50	0.97	3.45	1.74
24.0-27.0	8.88	0.56	1.35	0.18	0.27	0.94	4.96	1.79
27.0-30.0	7.14	0.48	1.14	0.10	0.51	NA	4.70	1.17
30.0-33.0	4.65	0.33	1.98	0.01	0.32	0.76	12.1	2.06
33.0-36.0	5.01	0.37	1.70	0.02	0.32	NA	9.91	3.01
36.0-39.0	4.21	0.31	1.22	0.01	0.88	NA	6.80	2.02
39.0-45.0	3.71	0.26	1.13	0.04	0.70	NA	6.16	1.84
Sampling date: 6/26/86								
0-2.9	7.99	0.76	0.77	.004	0.03	3.67	1.97	5.66
2.9-5.9	8.94	0.80	0.86	.004	0.03	1.06	1.11	2.93
5.9-8.8	6.63	0.54	0.98	0.01	0.02	1.36	2.49	1.59
8.8-11.7	8.31	0.71	0.92	0.01	0.03	1.22	0.88	1.82
11.7-14.7	6.09	0.55	1.04	0.01	0.13	0.53	2.14	1.08
14.7-17.6	4.83	0.37	1.54	0.02	0.78	0.64	8.05	1.87
17.6-20.5	4.82	0.33	0.81	0.10	0.41	0.38	4.31	1.79
20.5-23.4	5.54	0.41	0.65	0.35	0.19	0.57	1.93	1.75
23.4-26.4	6.90	0.44	0.92	0.14	0.06	0.76	4.44	1.25
26.4-29.3	5.34	0.36	1.76	.004	0.05	NA	10.8	1.62
29.3-31.6	5.98	0.42	1.61	ND	0.07	0.42	8.68	2.01
31.6-34.0	6.12	0.42	1.16	ND	0.05	NA	5.45	0.87

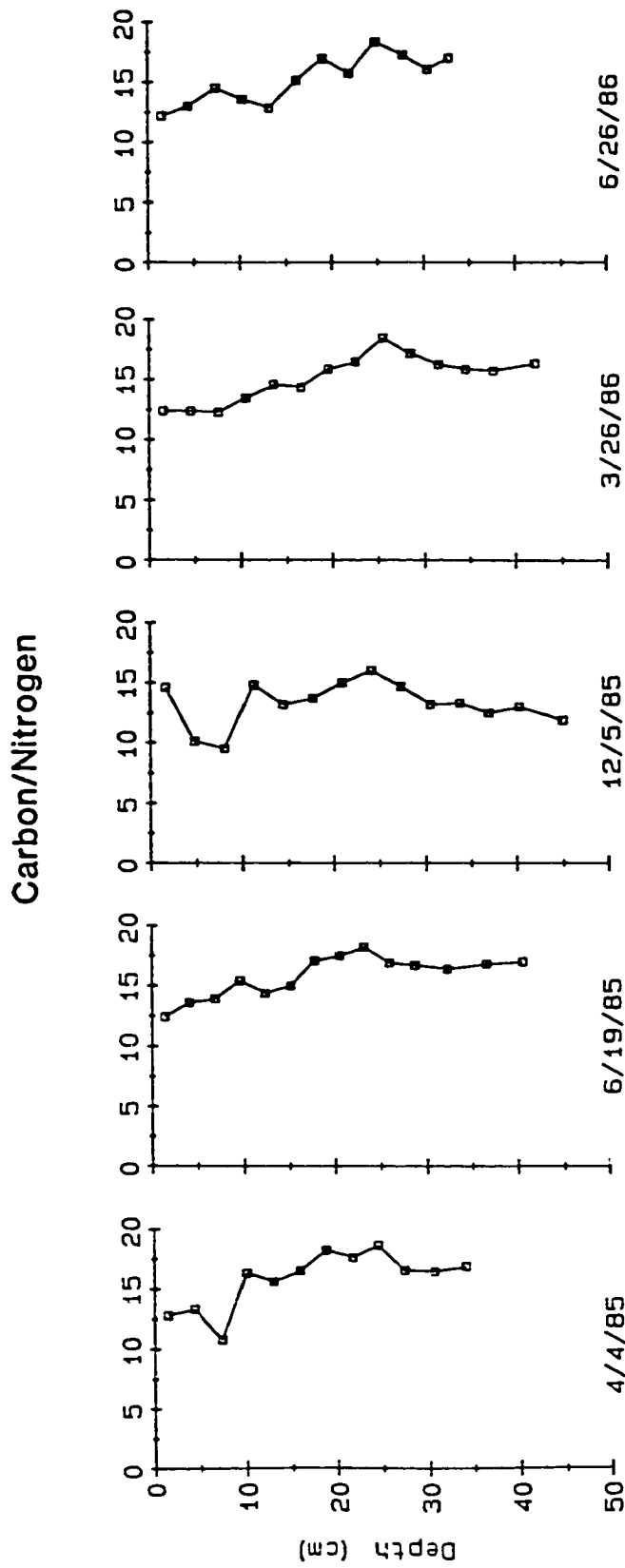
All values on a dry weight basis

NA - Not Analyzed

ND - Not Detectable

^a Reactive iron oxides

Figure 3.1. Carbon:nitrogen ratios (atomic) in sediments from the Great Marsh. Sediments were sectioned at 2.6 to 3.0 cm intervals, and C/N data are plotted versus the mean depth of each section.

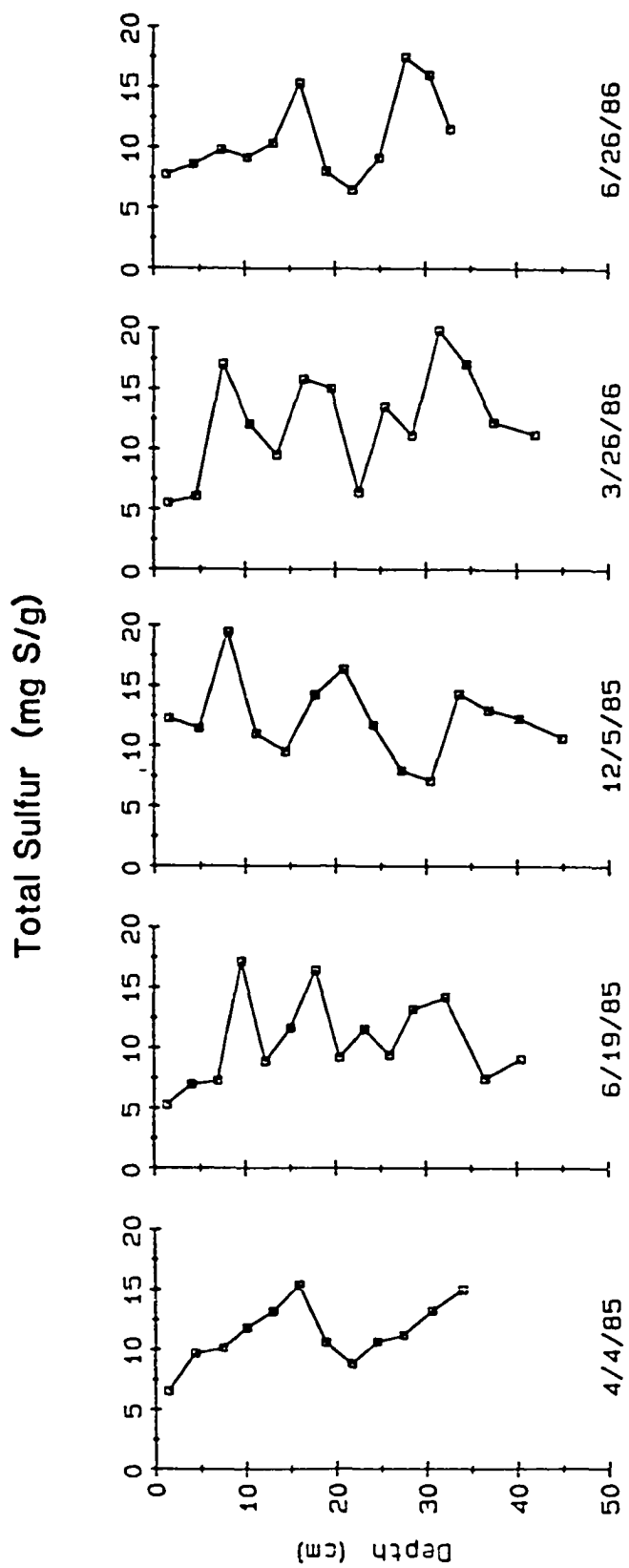


Total sulfur displays a general increase with depth (Figure 3.2), averaging 6.3 mg/g in surface sections and 13.5 mg/g in the deeper sediment (12/85 data not included). However in comparison to nitrogen and carbon, total sulfur shows considerably more variation with depth in all cores. These changes in total sulfur are due primarily to variations in pyrite concentrations (discussed below). At the sediment surface, carbon/sulfur (atomic) ratios average 36.1, a value considerably higher than that for many marine sediments (7.41, Berner and Raiswell, 1983). This elevated ratio is due to the high organic carbon content of the marsh sediment. In the upper 15 cm, sedimentary C/S ratios decrease rapidly, and below 30 cm the C/S ratio is relatively constant with an average of 9.31. The increase in sedimentary sulfur with depth (Figure 3.2) and the relatively constant C/S ratio below 25 cm suggests that most sulfide incorporation occurs through the oxidation of organic carbon in the upper marsh sediment via sulfate reduction. This conclusion is similar to that of other salt marsh studies (Howarth and Teal, 1979; Lord and Church, 1983; Howes et al., 1984).

Iron monosulfide

Iron sulfides which are soluble in weak hydrochloric acid are termed acid volatile sulfides (AVS), and under the conditions of early diagenesis are thought to be primarily amorphous iron sulfide and mackinawite (Goldhaber and Kaplan, 1974). While greigite is typically included in the

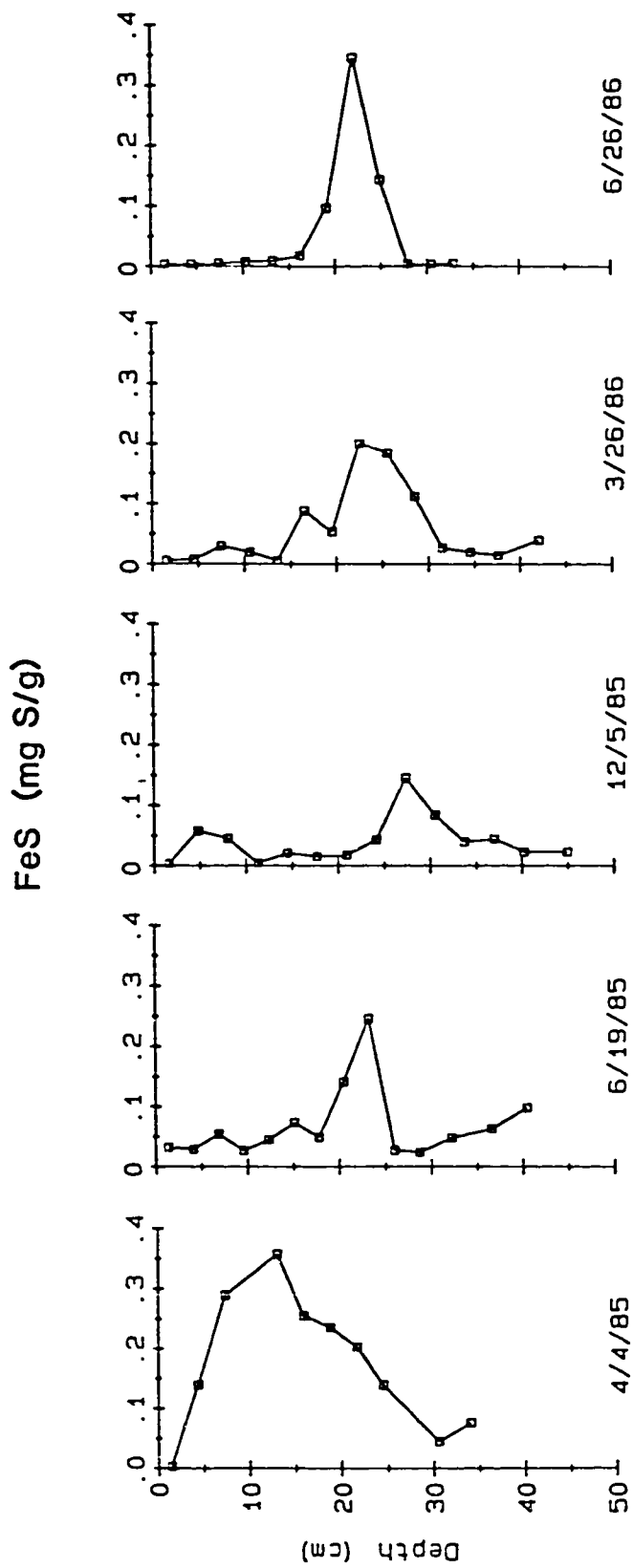
Figure 3.2. Depth distribution of total sulfur in the Great Marsh. Concentrations are on a dry weight basis. Sediments were sectioned at 2.6 to 3.0 cm intervals, and total sulfur data are plotted versus the mean depth of each section.



AVS fraction (e.g., Rickard, 1969; King et al., 1985), the analytical methods used here can discriminate between simple iron monosulfides and greigite. Thus, in this chapter the AVS fraction will be referred to as iron monosulfide. Iron monosulfide is the initial product formed by the reaction of bisulfide and ferrous iron, and in the presence of elemental sulfur is transformed to greigite (Sweeney and Kaplan, 1973) and pyrite (Berner, 1970). Iron monosulfide may also be lost through oxidation to ferrous- and ferric-iron, and elemental sulfur.

Since iron monosulfide is thermodynamically unstable under most conditions, it is expected to be a transient intermediate in salt marsh sediments. Indeed, large temporal changes are apparent in the concentration and distribution of FeS in the marsh (Figure 3.3). Winter/Spring time (April, December 1985 and March 1986, Figure 3.3) FeS concentrations are elevated and the maxima are found closer to the sediment surface than in the summer (June 1985 and 1986, Figure 3.3) when oxygen injection via *S. alterniflora* photosynthesis is at a maximum. Thus, the abundance and distribution of FeS appears to be a sensitive integrator of redox conditions in the marsh. In this manner, the 1986 drought (December to April) and corresponding oxidation of the upper sediment is apparent in the deeper FeS maximum in March 1986 as compared to April of the previous year. The highest concentration of FeS occurred in April 1985 and June 1986, and accounted for 2.5% and 5% of the total sulfur, respectively. Generally

Figure 3.3. Depth distribution of iron monosulfide in the Great Marsh. Concentrations are on a dry weight basis. Sediments were sectioned at 2.6 to 3.0 cm intervals, and FeS data are plotted versus the mean depth of each section.



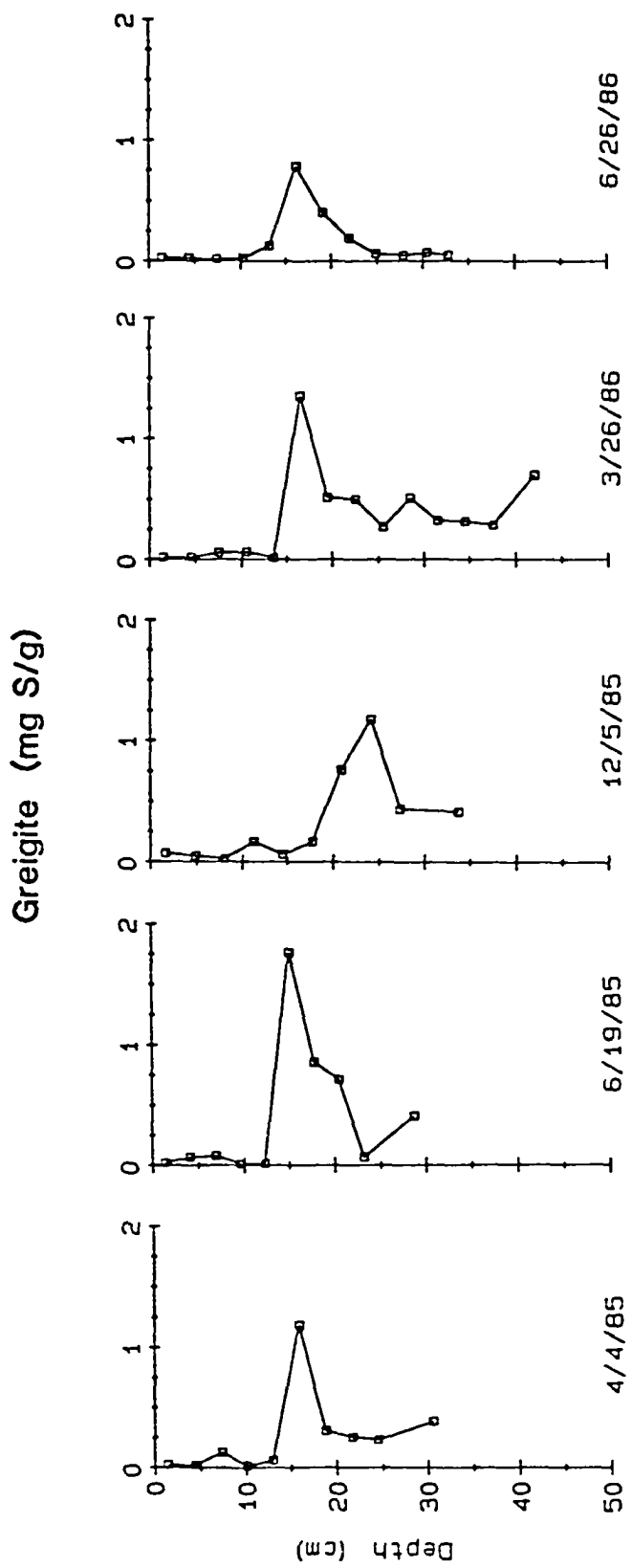
iron monosulfide accounted for 3% or less of the total sedimentary sulfur. For the five sampling periods, the depth of the FeS maximum coincides with predicted mackinawite saturation using solubility calculations (Berner, 1967; Boulegue et al., 1982; Lord and Church, 1983), and the dissolved iron and bisulfide data of Luther and Church (submitted).

Greigite

Like mackinawite, greigite is thermodynamically unstable in oxic conditions and is a proposed intermediate in pyrite formation (Goldhaber and Kaplan, 1974). For the synthesis of framboidal pyrite, Sweeney and Kaplan (1973) have shown that a greigite intermediate is essential. Further, the kinetic studies of Rickard (1975) indicate that this synthetic pathway would be slow relative to that of direct precipitation which produces individual pyrite crystals. Using solubility calculations and the identification of framboidal pyrite by electron microscopy in Great Marsh sediments, Lord and Church (1983) postulated that greigite should be present. The data in Figure 3.4 confirm their hypothesis, and show that the distribution of greigite is not as temporally variable as that of iron monosulfide (Figure 3.3). Indeed, greigite appears to be poised at the interface between the upper sediment which cycles from oxic to anoxic and the deeper, permanently anoxic sediment.

The highest concentration of greigite was observed in

Figure 3.4. Depth distribution of greigite (Fe_3S_4) in the Great Marsh. Concentrations are on a dry weight basis. Sediments were sectioned at 2.6 to 3.0 cm intervals, and greigite data are plotted versus the mean depth of each section.



June 1985 (15% of total sulfur), with the concentration of this phase otherwise ranging from 5-10% of the total sulfur (Table 3.1). The greigite peak corresponds with the deeper pyrite maximum (to be discussed below), and with the exception of the first core, is at a shallower depth than that of FeS (Figures 3.3 and 3.4). The positions of the greigite maxima are consistent with solubility predictions (Berner, 1967; Boulegue et al., 1982; Lord and Church, 1983). In this case, porewaters should become saturated with respect to greigite at lower bisulfide concentrations than that for iron monosulfide (i.e., greigite should precipitate closer to the surface).

Elemental sulfur

While some data for elemental sulfur have been available for salt marsh ecosystems (e.g., King et al., 1985), they have not been complete enough for a seasonal description. Lord (1980) estimated the concentration of elemental sulfur to be the difference between total sulfur and pyrite-sulfur (in the upper 20 cm, 5-12 mg S/g). This operational definition would include organic sulfur in the S(0) fraction (FeS makes a minor contribution to total sulfur). As will be apparent shortly, independent determinations of elemental sulfur show that this operational definition overestimates the concentration. Elemental sulfur can be formed through the oxidation of dissolved bisulfide or solid phase iron sulfides. Further oxidation removes elemental sulfur, as does the formation of

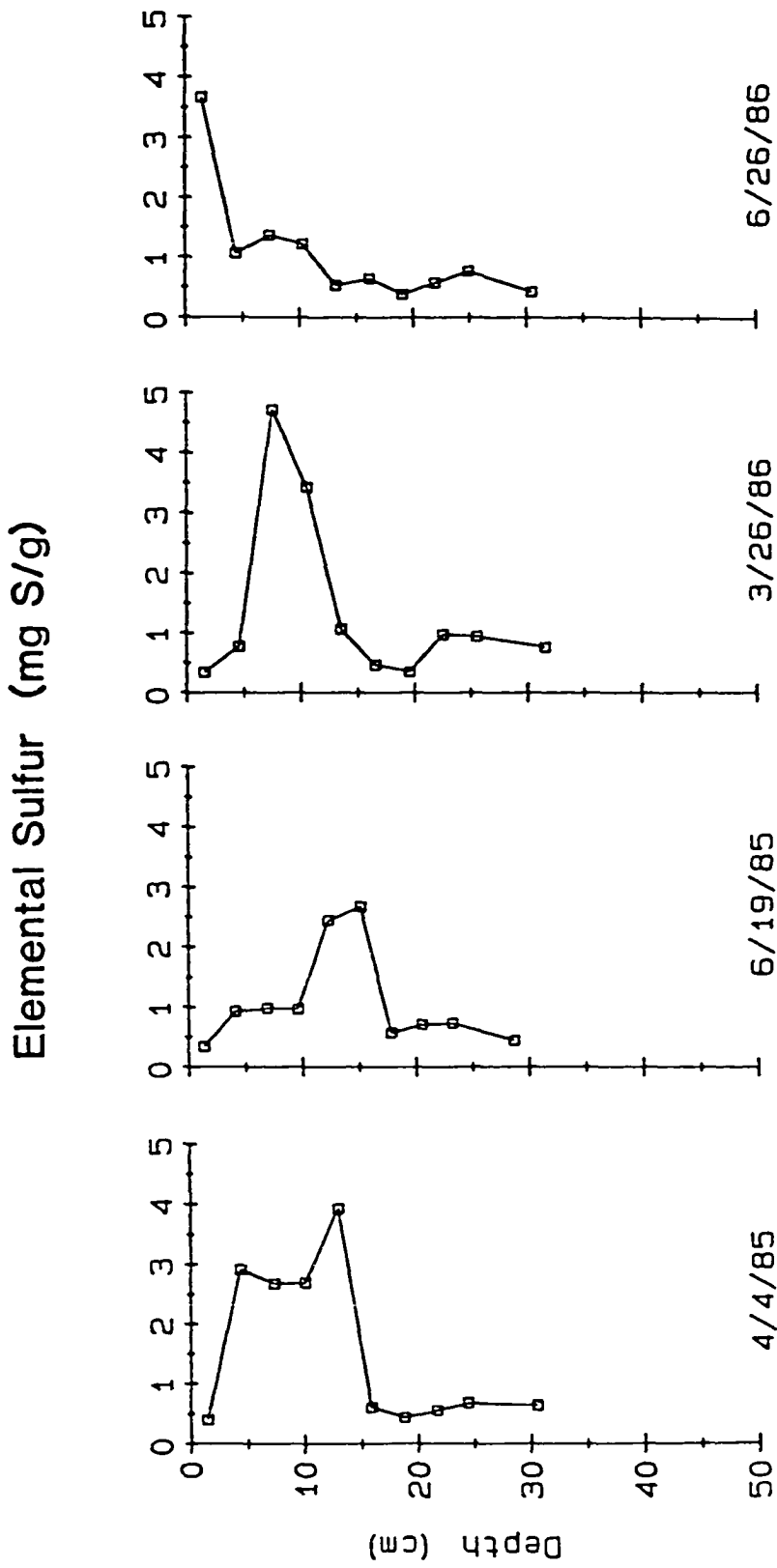
greigite and pyrite (Goldhaber and Kaplan, 1974).

The four profiles of elemental sulfur (Figure 3.5) show that this sulfur form is restricted to the seasonally oxic portion of the marsh sediment (0-15 cm). Correspondingly, elemental sulfur displays the greatest abundance in the late winter/early spring when oxygen from the S. alterniflora roots is beginning to be introduced. In June 1986 S(0) reached 47% of the total sulfur, with maxima during the other sampling periods ranging from 23-30% of the total sulfur. Qualitatively, these elemental sulfur results are similar to those observed by Troelsen and Jorgensen (1982) in shallow coastal sediments, although the concentrations of S(0) in Great Marsh sediments are approximately a factor of 10 higher. Troelsen and Jorgensen (1982) found elemental sulfur maxima in the sediments' oxidized surface layer, and observed that the concentration of S(0) increased as the sediment became more oxidized in the winter. Overall the abundance and distribution of elemental sulfur, like iron monosulfide, is coupled to seasonal redox changes in the marsh, and thus the formation/destruction of iron sulfide phases. This conclusion will be examined more thoroughly below.

Pyrite

As the thermodynamically stable form of iron sulfide in marine sediments, the abundance and distribution of pyrite ultimately controls the burial of both sulfur and iron, as well as other trace metals (Boulegue et al., 1982). With

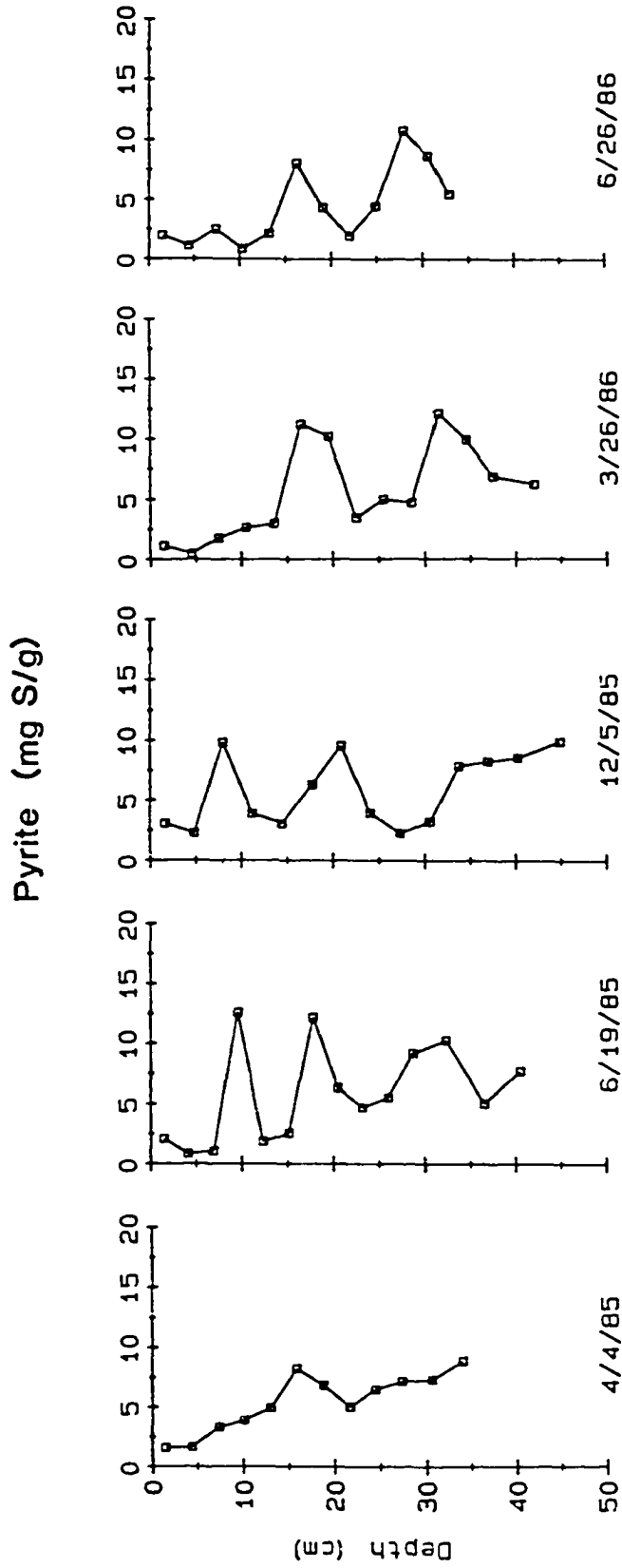
Figure 3.5. Depth distribution of elemental sulfur in the Great Marsh. Concentrations are on a dry weight basis. Sediments were sectioned at 2.6 to 3.0 cm intervals, and S(0) data are plotted versus the mean depth of each section.



respect to sulfur, the importance of pyrite is clearly seen when comparing the total sulfur profiles (Figure 3.2) to those in Figure 3.6 for pyrite. The variations in total sulfur with depth are primarily due to variations in pyrite (with the one exception being the upper sulfur maximum in the 3/86 core which is due to elemental sulfur). Below 20 cm pyrite comprises an average of 56.7% of the total sedimentary sulfur for all cores. In the sediment below 15 cm where anoxic conditions persist throughout the year (Boulegue et al., 1982; Lord and Church, 1983), two pyrite maxima and an intervening minimum are observed in four of the five profiles (maxima centered approximately at 18 cm and 30 cm, Figure 3.6). In view of the sediment accumulation rate in the Great Marsh (0.47 cm/yr, Church et al., 1981) and the slow rates of pyritization at this depth (Lord and Church, 1983), the existence of two pyrite maxima (or, a pyrite minimum at 22 cm) likely reflects a depositional artifact rather than a diagenetic effect. Given the sediment accumulation rate, the deep pyrite minimum corresponds to the 1930's when mosquito ditches were dug in the marsh, and thus may be a result of oxidative pyrite loss due to this process.

In contrast to the deep sediment (>15 cm), pyrite in the upper marsh sediments (0-15 cm) shows more variation with time (Figure 3.6). Between April and June 1985 a pyrite maximum develops and persists into December (Figure 3.6). Although these data show a one point maximum, the analyses

Figure 3.6. Depth distribution of pyrite (FeS_2) in the Great Marsh. Concentrations are on a dry weight basis. Sediments were sectioned at 2.6 to 3.0 cm intervals, and pyrite data are plotted versus the mean depth of each section.

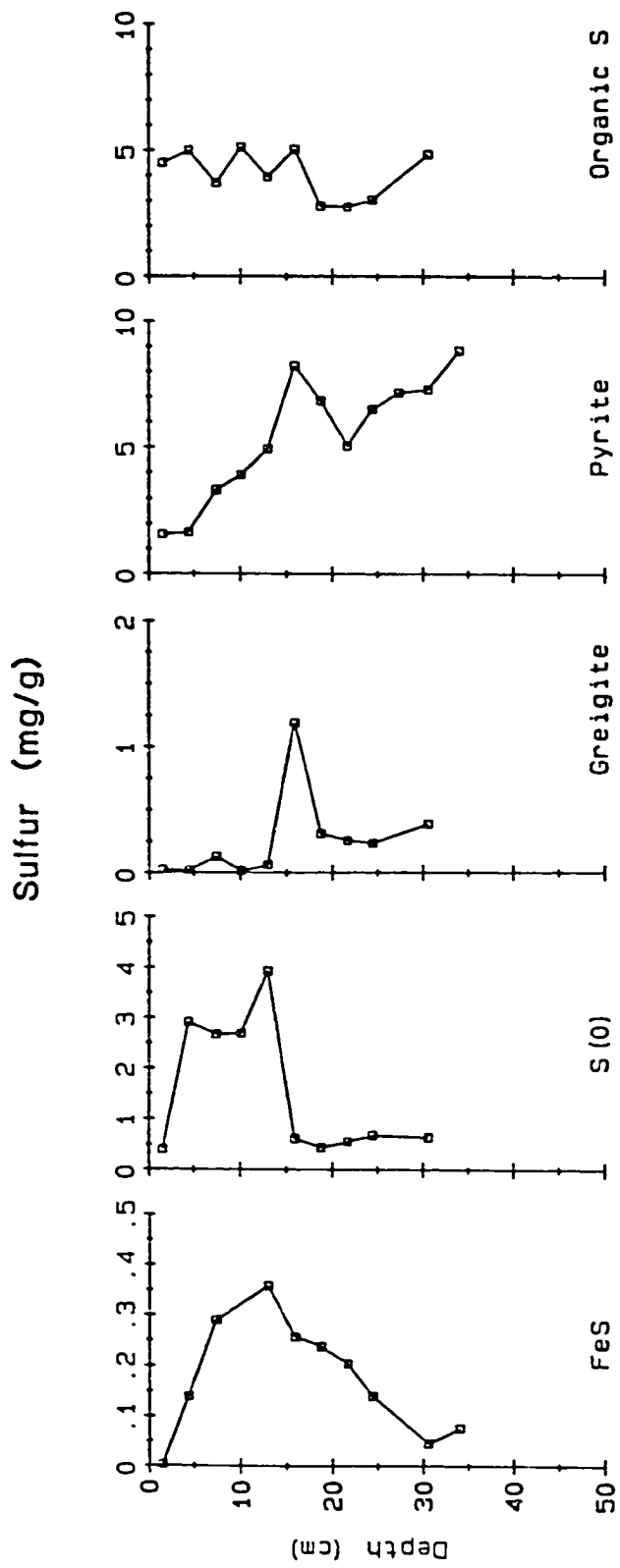


were repeated in triplicate with the same result. While a duplicate core was not taken in June 1985, analyses of duplicate cores from other periods show excellent agreement (within 10%). Thus we are reasonably confident that this pyrite maximum is not an artifact. By March 1986 the shallow pyrite maximum has disappeared, the loss mechanism presumably being oxidation (see Luther et al., 1982; and Luther and Church, submitted). Such rapid rates of pyrite formation and oxidation have been reported in other marshes (e.g., Howarth and Teal, 1979), and in the Great Marsh (Lord and Church, 1983). In June 1986 there is a slight indication of another subsurface pyrite peak (Table 3.1 and Figure 3.6). Based upon the data presented by Luther and Church (submitted), this slight subsurface maximum on June 26, 1986 is actually the remnants of a larger pyrite peak (5-7.5 cm) which underwent oxidative degradation during the monthly tidal inundation of the marsh. Thus, their results indicate that the June 1985 subsurface pyrite maximum (Figure 3.6) is not an isolated phenomenon, but one which is repeated the following year. In this respect it is important to note that the June 19, 1985 core was obtained before the monthly flooding. Furthermore, the pyrite data presented by Luther and Church (submitted) demonstrate that pyrite undergoes even more rapid formation and destruction than the results in Figure 3.6 would suggest.

As Lord and Church (1983) have noted, the formation of pyrite in the Great Marsh occurs in two distinct regimes.

The upper sediment (0-15 cm) displays large variations in pyrite which reflect rapid rates of formation and destruction. The deeper pyrite maxima (below 15 cm, Figure 3.6) are indicative of a slower pyritization. This observation corresponds to the two pathways of pyritization proposed by Goldhaber and Kaplan (1974), in which single pyrite crystals are formed rapidly through direct precipitation of ferrous iron and polysulfides, and framboidal pyrite is produced by a slower reaction with a greigite intermediate. Rickard (1975) has examined the mechanisms and kinetics of pyrite formation in marine sediments. His work shows that rapid pyritization has a second order dependence on iron monosulfide surface area, and a first order dependence on protons, total dissolved sulfide, and elemental sulfur surface area. The mechanism entails the dissolution of iron monosulfide and elemental sulfur to form ferrous ions and polysulfides, and the subsequent precipitation of pyrite. In this manner, the upper marsh sediment is ideal for rapid pyritization since all of the reactants are in abundance. To show this, all of the sulfur phases for the April 1985 core are plotted together in Figure 3.7. Although Luther and Church (submitted) do not have data for this period, their seasonal porewater results indicate that the upper marsh sediment also has low pH (4.2-6.0), which is needed for rapid pyritization. Pyritization in the deeper sediments is slower (Lord and Church, 1983), and the overlapping greigite and

Figure 3.7. Depth distributions of all inorganic sulfur species for the April 4, 1985 sediment core from the Great Marsh. Data points are plotted at the mid-depth of each section and represent the average concentration for each interval.



pyrite peaks (Figure 3.7) tend to confirm the slow reaction pathway proposed by Sweeney and Kaplan (1973). A qualitative confirmation of this scenario could be obtained by examining pyrite textures with depth (i.e., one would expect to observe single crystals near the surface and framboids at depth). Unfortunately such data are not available. However, using the data presented here a quantitative examination of pyritization in the marsh is possible.

A quantitative assessment of pyritization

The rates of pyritization in the Great Marsh have been determined by Lord and Church (1983) using a diagenetic model. In their work the rate of subsurface pyritization is taken to be equal to the sulfate reduction rate (i.e., the production rate of bisulfide is assumed to be limiting), and the deeper ($z > 15$ cm) rate of pyritization is limited by the availability of ferrous iron (i.e., the rate of formation of iron monosulfide and greigite). The data presented here allow the net transformation rates of sulfur phases in the upper sediment to be calculated. This examination will particularly focus on the production of subsurface pyrite between April and June 1985. As noted above, the rapid formation of pyrite requires a source of iron and sulfur. In the upper 15 cm of sediment, sulfur for pyritization is available in the pools of elemental sulfur and iron monosulfide, as well as from in-situ sulfate reduction. Correspondingly, the sources of pyritic iron can be iron oxyhydroxides, iron monosulfide, and dissolved porewater

iron (II), all of which are found in the upper sediments. From April to June 1985 the growth of a subsurface pyrite maximum (Figure 3.6) is accompanied by a decrease in elemental sulfur and FeS concentrations (Figures 3.3 and 3.5). By integrating the concentrations of S(0) in the upper 15 cm of sediment for each core and computing the concentration changes over 76 days (April 4 to June 19), one obtains a loss rate for elemental sulfur of $3.2 \text{ umole S/cm}^3\text{d}$ (assuming a sediment density of 1.8 g/cm^3 ; Lord, 1980). In a similar manner, the loss of iron monosulfide is computed to be $0.6 \text{ umole S/cm}^3\text{d}$. Over this same depth range, the rate of pyrite formation is calculated to be $4.2 \text{ umole S/cm}^3\text{d}$. The uncertainty of these rates is estimated to be $\pm 10\%$ and is related to analytical and spatial variabilities. These rates will be used below to estimate the net sulfate reduction rate in these sediments.

With respect to a sulfur mass balance, the gain in pyritic sulfur exceeds the losses of elemental sulfur and iron monosulfide-sulfur (i.e., 4.2 versus $3.2 + 0.6 = 3.8 \text{ umole S/cm}^3\text{d}$). This difference must represent pyritic sulfur that came from sulfate reduction during the 76 day period. Thus, the estimated sulfate reduction rate for this spring period is $0.4 \text{ umole S/cm}^3\text{d}$. This rate is similar to the yearly average calculated by Lord and Church (1983) for the same site ($0.13 \text{ umole S/cm}^3\text{d}$), as well as the sulfate reduction rates for other salt marshes (e.g., Howarth and Teal, 1979; Howarth and Giblin, 1983). The observed

pyritization rate ($4.2 \text{ umole S/cm}^3\text{d}$) is over an order of magnitude higher than that calculated by Lord and Church (1983) for the upper sediment. This apparent discrepancy may be explained by the fact that the rate estimated here is for a specific time period (76 days), and not a yearly average as Lord and Church calculated (i.e., the pyritization rate may be slower through the rest of the year). In support of this contention, the rate of pyritization in the upper 15 cm of sediment does slow considerably between the June and December 1985 ($0.39 \text{ umole S/cm}^3\text{d}$, calculated as above). However, it is also important to remember that the pyritization rates observed in this study are likely underestimates due to the large temporal changes in pyrite. The data presented by Luther and Church (submitted) show large losses of pyrite on time scales of several days. Thus, between our sampling periods pyrite could have formed and been recycled several times.

Based on the stoichiometry of pyrite (1Fe:2S) and the rate of pyritization, an integrated loss of solid phase iron on the order of $2.1 \text{ umole Fe/cm}^3\text{d}$ would be anticipated between April 4 and June 19, 1985. Data for iron oxides are presented in Table 3.1, and in a manner similar to that for sulfur phases, an iron loss of $2.5 \text{ umol Fe/cm}^3\text{d}$ can be computed. While this value is close to stoichiometric predictions, the contribution of iron from iron monosulfide must also be considered. If the monosulfide loss is included, the total loss of reactive iron from phases other

than pyrite is $3.1 \text{ umole Fe/cm}^3\text{d}$. Since the loss of iron from reactive oxides and monosulfide is greater than the increase of pyritic iron, a gain in porewater iron of $1.0 \text{ umole Fe/cm}^3\text{d}$ would be expected between April and June 1985. Luther and Church (submitted) report elevated porewater iron concentrations in June 1985, but data are not available for April 1985. Since dissolved ions can migrate by diffusion and advection, an exact estimate of the iron increase would be difficult. Overall, changes in sulfur and iron inventories of the upper sediments appear to match the rapid pyritization schemes postulated by other workers (e.g., Goldhaber and Kaplan, 1974; Rickard, 1975). While the focus here has been the formation of pyrite in salt marsh sediments, its removal through oxidation is also apparent in our data. This aspect of the sulfur cycle is covered in the paper by Luther and Church (submitted).

Below 15 cm pyrite accumulates more slowly, and Lord and Church (1983) postulate that the rate is limited by the formation of iron monosulfide and greigite from refractory iron phases in the sediment. The greigite data in Figure 3.4 allow their postulate to be examined by comparing the rate of greigite loss to that of pyrite formation. The average concentration of iron monosulfide is approximately 10% that of greigite in sediments below 15 cm. Thus for the calculations below, only greigite will be considered in the formation of pyrite. Using a rate equation from Lord and Church (1983):

$$d(\text{pyrite})/dt = K' (H^+)^2 (HS^-)^{1.5} (Fe_r) \quad (1)$$

where K' is the rate constant ($1.4 \times 10^{16} L^{1.5}/mole^{1.5} yr$), H^+ is the hydrogen ion activity (pH=7), HS^- is the dissolved sulfide concentration (ca. 1.7 mM), and Fe_r is the concentration of refractory iron (2 mg Fe/g); the rate of pyrite formation below 15 cm is calculated to be 0.96 $\mu mole S/cm^3 yr$.

To estimate the rate of greigite loss, the diagenetic model of Burdige and Gieskes (1983) can be applied to the greigite data where concentrations exponentially decrease with depth (ca. below 15 cm, refer to Figure 3.4). Although not all profiles exhibit an exponential decrease with depth as the June 1986 profile does, this approach should provide an indication of importance of greigite in pyrite formation. In this application, it is also assumed that the only processes which affect greigite below 15 cm are burial via sedimentation and loss through pyritization. Further, the loss of greigite via pyritization is assumed to be first order with respect to greigite (Rickard, 1975). At steady state these processes can be described using the following diagenetic equation:

$$-w(dC/dz) - k_{red}C = 0, \quad (2)$$

where k_{red} is the first order removal rate constant (/yr), w is the sedimentation rate (cm/yr), C is the concentration of greigite (mg S/g), and z is depth (cm, positive downward). The solution to this equation is:

$$C = C_0 e^{-B(z-15)}, \quad (3)$$

where $C=C_0$ at $z=15\text{cm}$ (i.e., this is the boundary condition) and B is equal to k_{red}/w . Employing a modified form of equation 2, a plot of $\ln [\text{Fe}_3\text{S}_4]$ versus depth yields a straight line whose slope is equal to k_{red}/w . Using greigite data below 15 cm from all but the 12/85 core, such a best fit line gives $C_0=0.8$ mg S/g, $B=0.107/\text{cm}$, and a linear correlation coefficient of 0.61 for $n=24$. With a sedimentation rate of 0.47 cm/yr (Church et al., 1981), k_{red} then equals 0.051/yr. Integrating the greigite removal rate ($=k_{\text{red}}C$) from 15-30 cm results in a depth averaged greigite removal rate of 1.14 $\mu\text{mole S}/\text{cm}^3\text{yr}$. Lord and Church (1983) report that pyrite in the deeper marsh sediment has framboidal texture, and since the rate of greigite loss is roughly equivalent to the rate of pyrite formation, these results support the laboratory studies of Sweeney and Kaplan (1973). Specifically, a tight coupling between greigite and framboidal pyrite would be expected during the slow formation of pyrite.

CONCLUSIONS

The use of newly developed analytical techniques has allowed a detailed examination of sedimentary sulfur cycling in Delaware's Great Marsh. Within the marsh two well-resolved zones of pyritization are observed. In the upper sediment where seasonal redox cycling occurs, the co-occurrence of elemental sulfur, iron monosulfide, low pH, and reactive iron lead to high rates of pyrite formation

during certain times of the year. The sedimentary sulfur speciation data from this zone confirm the rapid pyritization mechanisms proposed by Rickard (1975). Similarly, in the deeper sediments where pyrite formation slows, the diagenetic modeling illustrates the importance of a greigite intermediate during pyritization.

While most of the focus of this paper has been on inorganic sulfur species in the sediment, the amount and behavior of organic sulfur can be approximated by the difference between total sulfur and the sum of the inorganic sulfur fractions. In Figure 3.7 a plot of organic sulfur for April 1985 is shown. Unlike the inorganic forms, organic sulfur in the marsh is relatively resistant to degradation. However, organic sulfur can consist of many compounds (e.g., sulfate esters, sulfur amino acids), and only a gross characterization is provided by these operationally defined results. Detailed analyses of the actual organic sulfur species would likely result in a clearer understanding of organic sulfur cycling.

CHAPTER 4

Selenium Geochemistry in the Great Marsh

INTRODUCTION

The potential usefulness of examining the speciation of sedimentary selenium was introduced in Chapter 1. The benefits of using a similar approach for sulfur was demonstrated in Chapter 3. Determining the speciation of sedimentary sulfur allowed a detailed study of the reactions and pathways sulfur undergoes during early diagenesis. Also, kinetic information was obtained by modeling changes in the different sulfur pools during the year. In this chapter, the early diagenesis of selenium in a salt marsh is investigated. As with sulfur, the different solid phases of selenium were determined to more fully understand the processes affecting sedimentary selenium. If redox cycling of selenium occurs, a salt marsh environment should be useful in elucidating these processes (see Chapters 1 and 3). Following this chapter, a comparison between the geochemistries of selenium and sulfur will be presented to highlight potential similarities in the diagenetic pathways affecting these two chemically similar elements.

RESULTS AND DISCUSSION

The oxidation-reduction reactions of carbon, sulfur, and iron in the Great Marsh proceed according to pathways typically seen in other coastal and marsh sediments

(Jorgensen, 1977; Aller, 1980; Lord and Church, 1983; Giblin and Howarth, 1984; King et al., 1985; Chanton, 1985). The marsh redox cycle discussed in Chapter 3 and summarized in Table 4.1 will be used in the discussion of the geochemistry of selenium in the Great Marsh. Ancillary data used in describing these cycles (Table 4.2), such as pore water sulfate, chloride, pH, and sulfide, were provided by J. Scudlark and G. Luther of the University of Delaware. Overall, the marsh redox cycle follows a seasonal trend with different reactions dominating at different times of the year (Table 4.1, also see for example, Lord and Church, 1983; Giblin and Howarth, 1984; Luther et al., 1986).

The transport of selenium through a marsh may include the import of selenium from creek waters and deposition from the atmosphere, and the export of selenium via pore fluids, gaseous emissions, and surface water runoff. Within the sediments, oxidation/reduction processes could transform the different chemical forms of selenium, and affect their transport through the marsh system. A general schematic model of selenium pathways in a salt marsh is shown in Figure 4.1.

In the following sections, data on selenium in the sediments, pore waters and creek water will be presented. Using these data, the sources and sinks of selenium to the marsh will be examined, and a qualitative and quantitative description of selenium geochemistry will be developed.

Table 4.1

SEASONAL MARSH CYCLE

1985

APRIL

- O₂ infusion via Spartina roots is low; plants are still dormant.
- Oxide veneer present in upper layers.
- Precipitation of iron sulfide below 3 cm; up to 0.36 mg AVS/g between 11-14 cm.

JUNE

- O₂ infusion via Spartina roots in upper 12 cm.
- Below ca. 12 cm marsh system is reducing (H₂S, up to 2.5 mM, below 11cm).
- pH minimum (< 4.5) between 2-5 cm.
- Iron sulfide concentration is low (<0.05 mg AVS/g) in upper 12 cm.

DECEMBER

- Spartina plants are beginning to be less active.
- Microreducing zones present in upper 10 cm.
- Slight sulfate excess above 10 cm.
- Small AVS max (0.15 mg AVS/g) centered around 27 cm.

Table 4.1 (continued)

1986

MARCH

- Spartina are still inactive, plant shoots are just emerging.
- Oxide veener present in surface section.
- Large sulfate excess in upper 5 cm, below 9 cm sulfate is depleted.
- pH minimum (<4.5) at 3 cm.
- Broad AVS max (0.2 mg AVS/g) centered around 22 cm.
- Sulfide buildup to > 1mM below 12 cm.

JUNE

- Spartina plants are active, O₂ infusion via roots.
- Large sulfate excess in upper 10 cm, below 10 cm sulfate depletion.
- pH minimum (4.4) centered around 3 cm.
- Sharp AVS max (0.35 mg AVS/g) centered around 20 cm.
- Slight sulfide buildup starting around 12.5 cm.

Table 4.2

Pore Water Ancillary Data^a

Depth (cm) pH SO₄⁼(mM)^b HS⁻(mM)

Sampling date: 6/18/85

0-2	5.7	-1.0	ND
2-4	4.2	+8.1	ND
4-6	4.5	+8.5	ND
6-8	5.2	+4.5	ND
8-10	5.8	+1.8	ND
10-12	6.0	+2.6	ND
12-14	6.3	+0.7	0.1
14-16	6.6	-7.0	0.7
16-18	NA	-8.0	1.2
30-32	6.6	-11.0	2.7

Sampling date: 12/11/85

0-2.5	6.5	-12.8	ND
2.5-5	5.9	+1.4	ND
5-7.5	6.1	+1.3	ND
7.5-10	6.3	+1.5	ND
10-12.5	6.5	-3.7	ND

Sampling date: 3/27/86

0-3	6.9	+99.5	ND
3-5.5	4.6	+31.5	ND
5.5-8.5	7.4	+1.6	ND
8.5-11	7.5	+4.7	ND
11-14	7.4	-2.0	ND
14-16	7.3	-8.0	1.1
16-18.5	7.3	-4.0	NA
21-24	7.0	-1.3	2.4
27-30	6.9	-1.5	NA
37-40	6.8	+0.8	NA

Table 4.2 (continued)

Depth (cm)	pH	SO ₄ ⁼ (mM) ^b	HS ⁻ (mM)
Sampling date: 6/17/86			
0-2.5	5.4	+44.9	ND
2.5-5	4.4	+52.3	ND
5-7.5	4.6	+42.4	ND
7.5-10	6.4	NA	ND
10-12.5	7.0	+7.7	0.1
12.5-15	7.2	-2.1	0.3
15-17.5	7.4	-4.2	NA
17.5-20	7.2	-6.3	NA
20-22.5	7.2	-4.5	NA
22.5-25	7.3	-3.8	NA

a - Data courtesy of G. Luther and J. Scudlark
of the Univ. of Delaware.

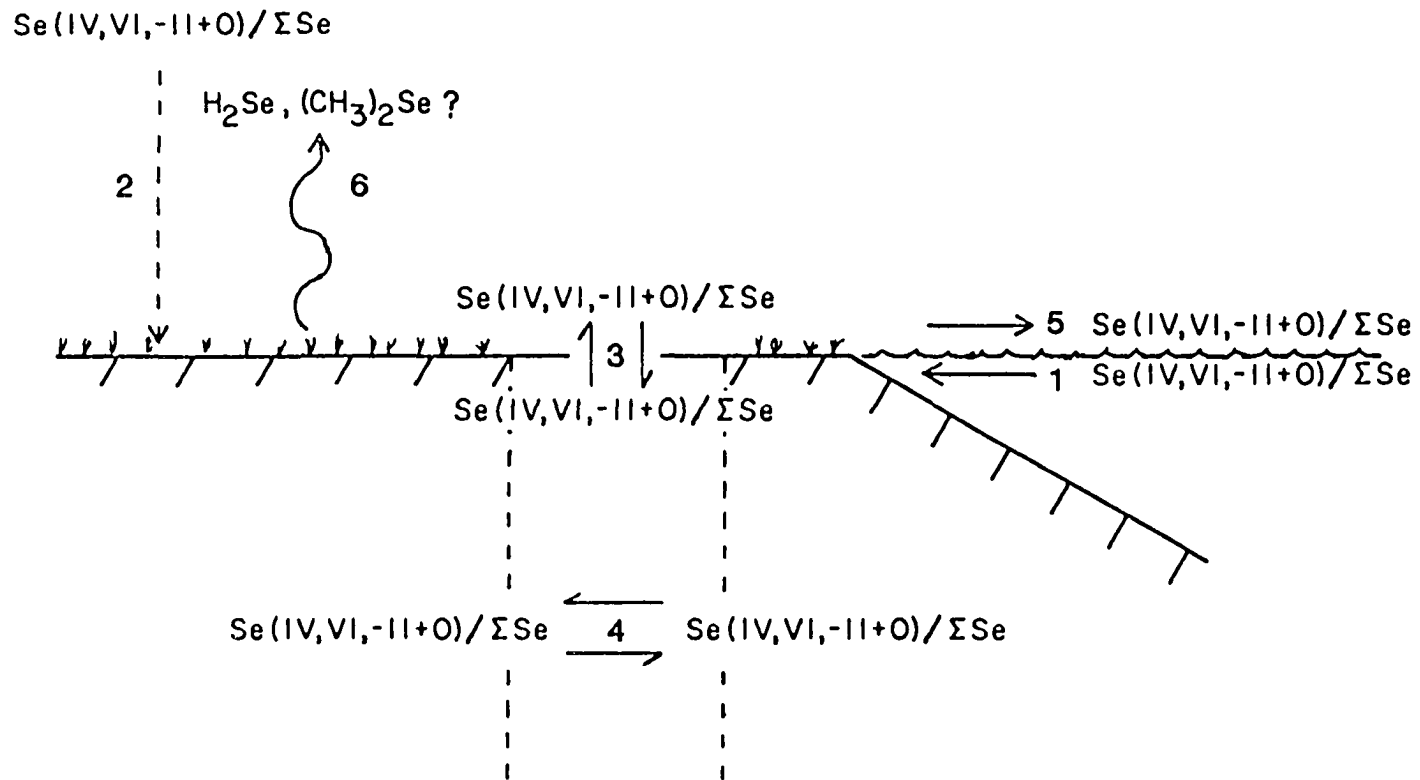
b - (-) sulfate deficit
(+) sulfate excess

ND - Not Detected

NA - Not Analyzed

Figure 4.1. Schematic representation of selenium's geochemical cycle in a salt marsh environment. The major speciation of selenium is represented as a ratio to the total selenium, and may be in the dissolved or particulate state. Major processes include: (1) Input from flood tides; (2) Input from atmospheric deposition; (3) Removal/recycling at the sediment surface; (4) Diagenetic reactions within the sediment; (5) Export by ebb tides; (6) Gaseous emissions to the atmosphere.

Selenium's Geochemical Cycle in a Salt Marsh



Dissolved Selenium in Pore and Creek Waters

The pore water selenium data for the 4/4/85, 6/19/85, 12/5/85, 3/26/86, and 6/26/86 sampling dates are given in Table 4.3 and plotted versus depth in Figure 4.2. It should be kept in mind throughout these discussions that the depth stated within the text is actually the mid-point for a specific depth interval.

In April 1985 a broad pore water maximum of 37.6 pg Se/g (H₂O), centered around 19 cm, is observed (Figure 4.2). Above and below this maximum, concentrations are near the detection limits (< 5 pg Se/g (H₂O)). By June 1985, a sharp pore water maximum of 153 pg Se/g (H₂O) forms (Figure 4.2). This maximum is centered around a depth of 14 cm, and quickly drops to undetectable levels at a depth of 20 cm. Unfortunately, no other samples were obtained below 22 cm to determine if concentrations remained undetectable. From June 1985 to December 1985, concentrations of pore water selenium in the upper 15 cm decrease to 35 pg Se/g (H₂O) (Table 4.3, Figure 4.2). Below this depth, concentrations are undetectable. In March 1986 selenium concentrations (Figure 4.2) in the entire core are at the detection limit, while in June 1986 concentrations (Table 4.3, Figure 4.2) in upper 15 cm increase to 310 pg Se/g (H₂O). This sharp maximum is centered at 10 cm, and below this depth concentrations of pore water selenium gradually decrease (Figure 4.2).

Limited selenium speciation data were obtained for the June 1985 and June 1986 pore water samples. In June 1985

Table 4.3

Great Marsh Pore Water Selenium Data

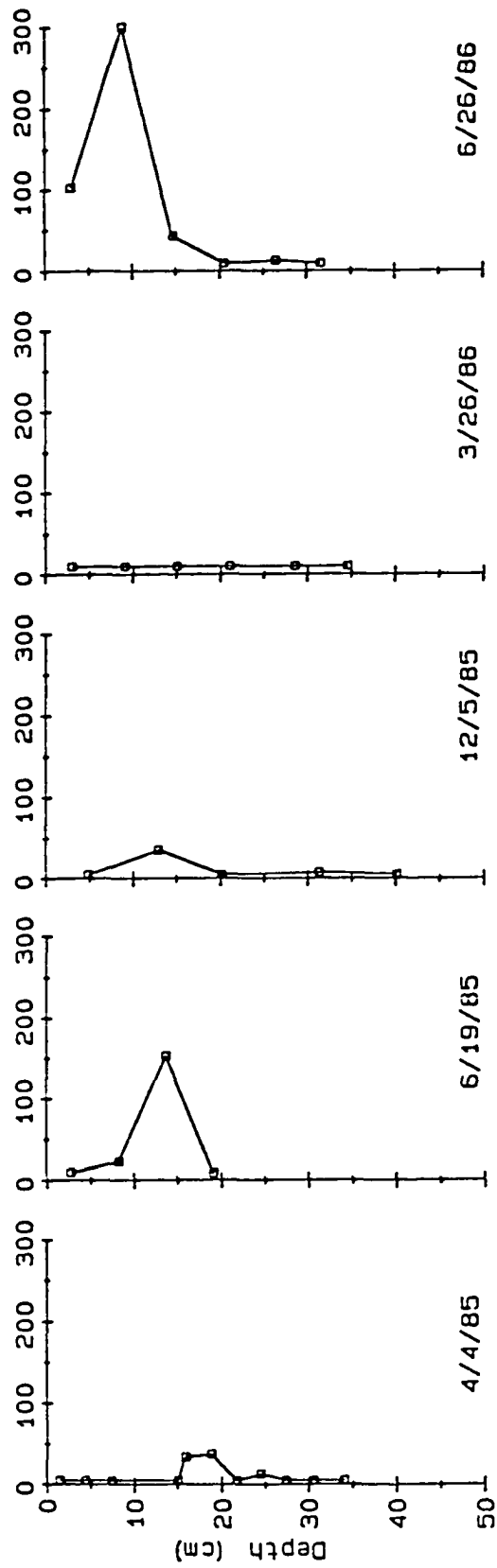
Depth (cm)	TSe pg Se/g (H ₂ O)	Depth (cm)	TSe pg Se/g (H ₂ O)
Sampling date: 4/4/85		Sampling Date: 3/26/86	
0-11.5	ND	0-6	ND
11.5-14.4	15.0	6-12	ND
14.4-17.3	33.8	12-18	ND
17.3-20.2	37.6	18-24	ND
20.2-23.0	ND	27-30	ND
23.0-25.9	12.8	33-36	ND
25.9-35.7	ND		
Sampling date: 6/19/85		Sampling date: 6/26/8	
0-5.5	9.4	0-5.9	103
5.5-10.9	23.1	5.9-11.7	311
10.9-16.4	153	11.7-17.6	42.9
16.4-21.8	8.2	17.6-23.4	ND
		23.4-29.3	12.6
		29.3-34.0	ND
Sampling date: 12/5/85			
0-8	ND		
8-16	35.1		
16-24	ND		
24-32	7.4		
32-48	ND		

ND - Not Detectable

Figure 4.2. Depth distribution of total pore water selenium in the Great Marsh. Sediments were sectioned and squeezed at specific intervals (see Table 4.3) and data are plotted versus the mean depth of each section.

Total Porewater Selenium

(pg Se/g H₂O)



two depth intervals (11-14cm and 14-17cm) were analyzed for selenite. Only the 11-14 cm depth interval has detectable selenite (37.5 pg Se/g (H₂O)), and this accounts for 25% of the total selenium. Speciation data for the June 1986 core are also limited. Due to an unidentified interferent (see Chapter 2), selenite was not determined. However, selenite+selenate was determined in all pore waters from this core. In the top 6 cm, selenite+selenate is 52 pg Se/g (H₂O) or 51% of the total selenium, while below this depth the concentration of selenite+selenate is undetectable. The concentration of organic selenium, calculated as the difference between total selenium and selenite+selenate (see Chapter 2), increases with depth and accounts for 100% of the total selenium below the surface section.

Creek waters adjacent to the marsh show little variation in the concentration of total dissolved selenium (Table 4.4) over the course of this study. Concentrations range from 77.4 pg Se/g (H₂O) in June 1986 to 86.1 pg Se/g (H₂O) in March 1986. The average total dissolved selenium of 81.3 ± 3.8 pg Se/g (H₂O) (n=4) is similar to those determined in other estuaries (Measures and Burton, 1978; Takayanagi and Wong, 1984a; 1984b; Takayanagi and Cossa, 1985; Cutter, unpublished manuscript).

In summary, profiles of pore water dissolved selenium show distinct seasonality (Table 4.3, Figure 4.2). The changes in the concentration of pore water selenium appear related to the redox characteristics of the marsh

Table 4.4

Creek Water Total Dissolved Selenium

Sampling Date	Total Selenium (pg Se/g)
4/4/85	81.3 ± 0.4
6/19/85	No Sample
12/5/85	78.9 ± 1.3
3/26/85	86.1 ± 6.3
6/26/86	77.4 ± 1.6
Average:	80.9 ± 6.6

environment (Table 4.1). Maximum concentrations are observed in June 1985 and 1986 when the marsh is most oxidizing, with low or undetectable concentrations when the marsh is reducing (April and December 1985 and March, 1985). Speciation data indicate that dissolved selenate+selenite comprises ca. 50% of the total dissolved selenium at the surface of the marsh and this fraction decreases in concentration with depth. While the pore water dissolved selenium concentrations change dramatically over the period of this study (Figure 4.2), adjacent creek waters have fairly constant dissolved selenium concentrations (Table 4.4).

Chemical Forms of Sedimentary Selenium

The different chemical forms of sedimentary selenium in conjunction with total sedimentary selenium (Table 4.5, Figures 4.3 to 4.7) help form a coherent picture of the reactions selenium undergoes during early diagenesis of the salt marsh sediment. Unfortunately, there are very few, if any, literature values on the different chemical forms of selenium with which to compare the data (see Chapter 1). Therefore, possible pathways will be postulated, based on known reactions of selenium and related thermodynamic data. Total sedimentary selenium will be examined first to set the stage for the discussion of the different chemical forms of selenium which follows.

TABLE 4.5
Great Marsh Solid Phase Selenium Data

Depth (cm)	TSe (ug/g)	Se(IV+VI) ^a (ug/g)	Se ⁰ (ug/g)	CRSe (ug/g)	Org-Se (ug/g)
Sampling date: 4/4/85					
0-2.9	0.70±0.02	0.038±0.007	0.37±0.03	ND	0.30±0.04
2.9-5.8	0.58±0.02	ND	0.26±0.01	ND	0.29
5.8-8.6	0.59±0.10	0.028±0.007	0.34±0.01	ND	0.31±0.02
8.6-11.5	0.46±0.02	ND	0.21±0.03	ND	0.23
11.5-14.4	0.45±0.02	0.028±0.007	0.32±0.01	ND	0.10±0.02
14.4-17.3	0.41±0.02	0.030±0.005	0.18±0.01	ND	0.20±0.02
17.3-20.2	0.50±0.02	0.015±0.007	0.24±0.02	ND	0.24±0.03
20.2-23	0.44±0.02	ND	0.28±0.02	ND	0.15
23-25.9	0.30±0.01	ND	0.13±0.01	ND	0.15
25.9-28.8	0.30±0.02	ND	0.12±0.02	ND	0.16
28.8-32.3	0.33±0.04	0.025	0.11±0.01	0.038±0.006	0.16±0.05
32.3-35.7	0.32±0.03	ND	0.07±0.02	0.031	0.22
Sampling date: 6/19/85					
0-2.7	0.44	0.011	0.30	ND	0.13±0.05
2.7-5.5	0.42±0.02	0.025±0.005	0.30±0.01	ND	0.09±0.01
5.5-8.2	0.52±0.03	0.053	0.32±0.03	ND	0.14±0.05
8.2-10.9	0.43±0.02	0.10±0.01	0.26±0.03	ND	0.07±0.03
10.9-13.7	0.47±0.05	0.13±0.02	0.24±0.02	ND	0.10±0.06
13.7-16.4	0.33±0.01	0.11±0.02	0.18±0.02	0.058±0.009	ND
16.4-19.1	0.42	0.042±0.006	0.23±0.02	0.064±0.006	0.08±0.02
19.1-21.8	0.53±0.05	0.052	0.28±0.03	ND	0.20±0.06
21.8-24.6	0.49±0.01	0.028	0.27±0.02	ND	0.19±0.18
24.6-27.3	0.35±0.01	0.036	0.22±0.02	ND	0.10±0.01
27.3-30.0	0.31±0.03	0.034±0.001	0.14±0.01	ND	0.13±0.03
30.0-34.4	0.29	0.021±0.004	0.13±0.01	ND	0.14±0.02
34.4-38.8	0.26±0.02	0.018	0.12±0.01	ND	0.13±0.02
38.8-42.0	0.21±0.03	0.009±0.001	0.08±0.01	ND	0.13±0.03
Sampling date: 12/5/85					
0-3.2	0.46	0.032±0.004	NA	NA	NA
3.2-6.4	0.40±0.03	0.063±0.04	NA	NA	NA
6.4-9.6	0.48±0.03	0.050	NA	NA	NA
9.6-12.8	0.46±0.01	0.066±0.004	NA	NA	NA
12.8-16.1	0.57±0.02	0.066±0.004	NA	NA	NA
16.1-19.3	0.57±0.01	0.056±0.005	NA	NA	NA
19.3-22.5	0.57±0.01	0.039±0.002	NA	NA	NA
22.5-25.7	0.74±0.03	0.027±0.002	NA	NA	NA
25.7-28.9	0.50±0.03	0.017±0.001	NA	NA	NA
28.9-32.1	0.42±0.02	0.029±0.002	NA	NA	NA
32.1-35.3	0.41±0.02	0.025±0.002	NA	NA	NA
35.3-38.6	0.41±0.02	0.012±0.003	NA	NA	NA
38.6-41.7	0.43±0.02	0.009±0.001	NA	NA	NA
41.7-48.1	0.37±0.03	0.013±0.001	NA	NA	NA

TABLE 4.5 (continued)

Depth (cm)	TSe (ug/g)	Se(IV+VI) ^a (ug/g)	Se ^o (ug/g)	CRSe (ug/g)	Org-Se (ug/g)
Sampling date: 3/26/86					
0-3	0.74±0.07	0.046±0.004	0.36±0.03	ND	0.34±0.07
3-6	0.79	0.059	0.38±0.02	ND	0.35±0.07
6-9	0.95±0.10	0.068±0.009	0.32±0.02	0.007	0.55±0.10
9-12	0.98±0.03	0.15±0.01	0.54±0.04	ND	0.28±0.05
12-15	0.64	0.037±0.003	0.31±0.01	ND	0.29±0.02
15-18	0.78±0.02	0.058±0.002	0.31±0.03	0.037	0.38±0.03
18-21	0.72±0.08	0.019±0.002	0.22±0.01	0.19±0.03	0.30±0.08
21-24	0.66±0.06	0.031±0.003	0.28±0.03	0.051	0.31±0.07
24-27	0.88±0.11	0.041±0.001	0.26±0.02	ND	0.59±0.11
27-30	0.64±0.04	0.045±0.004	0.16±0.02	0.027	0.41±0.05
30-33	0.50±0.02	0.039±0.002	0.14±0.01	ND	0.33±0.03
33-36	0.45±0.03	0.026±0.002	0.14±0.03	0.044	0.24±0.04
36-39	0.35±0.01	0.027±0.003	0.11±0.03	0.049	0.17±0.03
39-45	0.37±0.03	0.017±0.003	0.06±0.01	0.075	0.21±0.03
Sampling date: 6/26/86					
0-2.9	0.60±0.04	0.047±0.003	0.32±0.02	ND	0.23±0.05
2.9-5.9	0.70	0.11±0.01	0.37±0.02	ND	0.22±0.05
5.9-8.8	0.64±0.04	0.17	0.22±0.001	ND	0.24±0.04
28-11.7	0.79±0.03	0.17±0.01	0.35±0.04	ND	0.27±0.05
11.7-14.7	0.60±0.04	0.17±0.01	0.19±0.02	ND	0.25±0.05
14.7-17.6	0.66±0.03	0.064±0.003	0.26±0.01	ND	0.34±0.03
17.6-20.5	0.47±0.01	0.045	0.22±0.03	ND	0.20±0.02
20.5-23.4	0.65±0.03	0.047±0.002	0.26±0.02	ND	0.34±0.04
23.4-26.4	0.55±0.04	0.043±0.003	0.18±0.02	ND	0.32±0.05
26.4-29.3	0.45	0.023±0.003	0.12±0.01	ND	0.30±0.02
29.3-31.6	0.48±0.01	0.030±0.004	0.093±0.015	0.021	0.34±0.02
31.6-34.0	0.41±0.01	0.030±0.004	0.10±0.02	ND	0.28±0.02

All values on a dry weight basis

NA - Not Analyzed

ND - Not Detectable

^a Sedimentary (selenite+selenate)

Figure 4.3. Depth distribution of total sedimentary selenium in the Great Marsh. Sediments were sectioned at 2.6 to 3.0 cm intervals, and total selenium data are plotted versus the mean depth of each section.

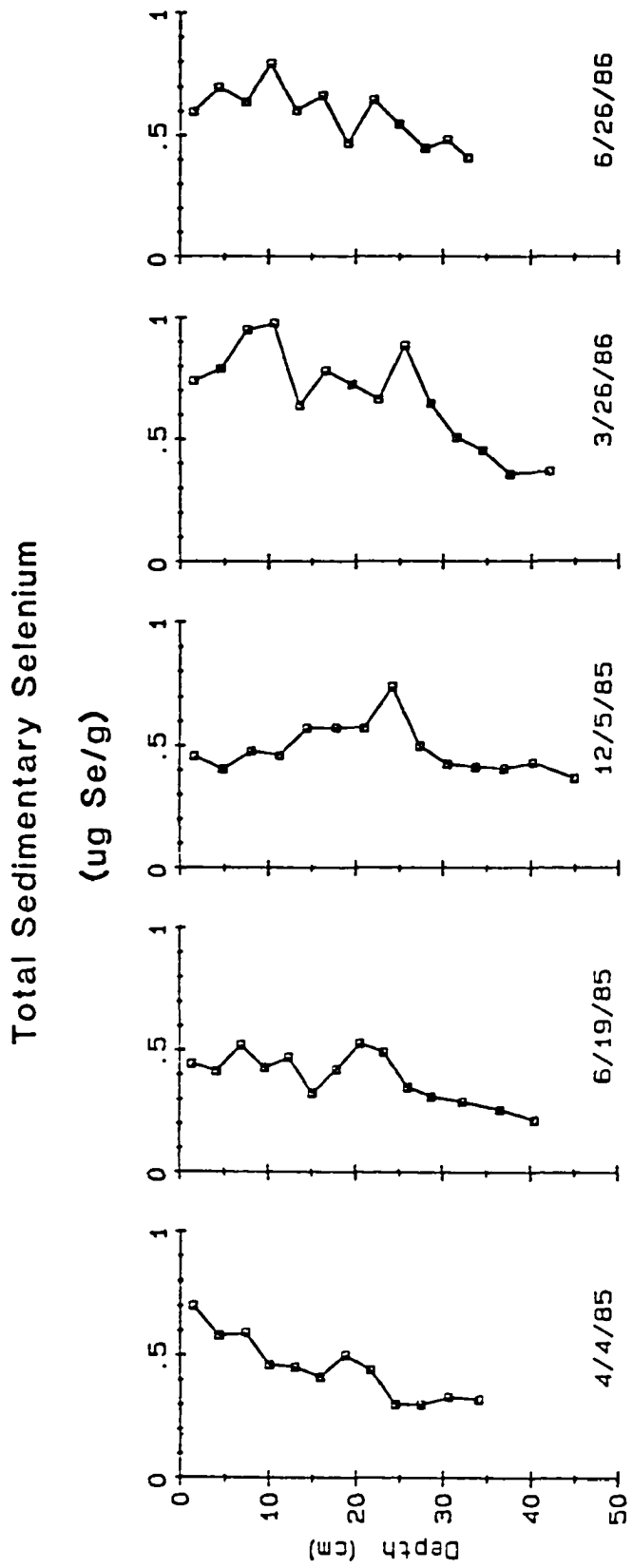


Figure 4.4. Depth distribution of sedimentary (selenite+selenate) normalized to total sedimentary selenium in the Great Marsh. Sediments were sectioned at 2.6 to 3.0 cm intervals, and the data are plotted versus the mean depth of each section.

Sedimentary (selenite+selenate)
(% of total selenium)

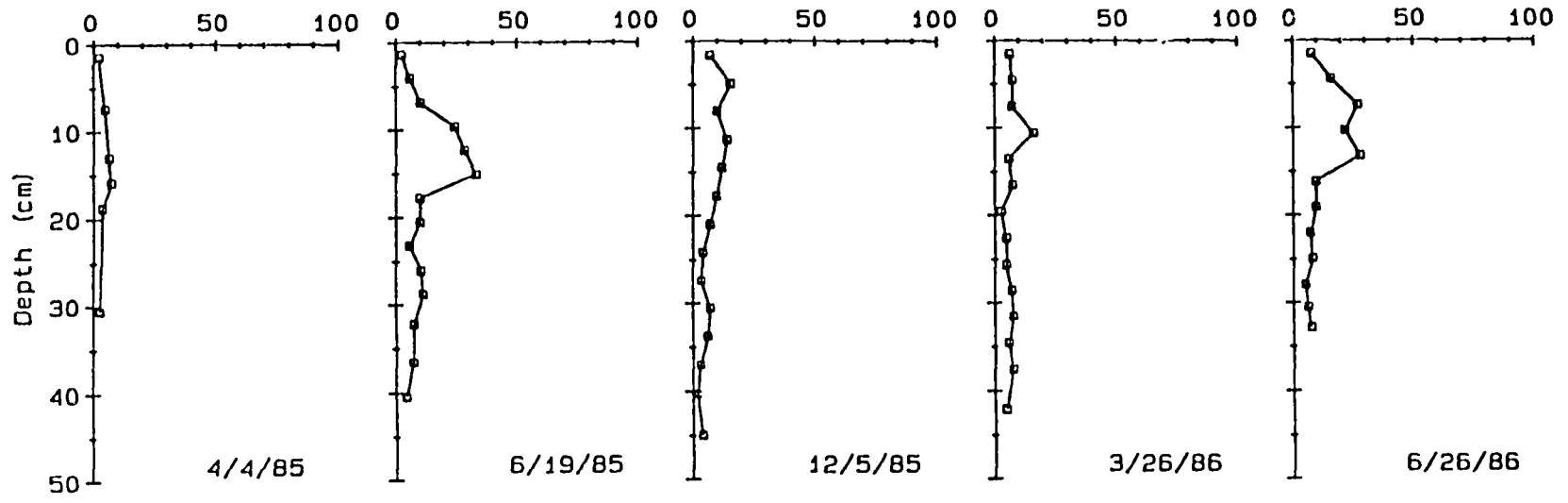


Figure 4.5. Depth distribution of elemental selenium normalized to total selenium in the Great Marsh. Sediments were sectioned at 2.6 to 3.0 cm intervals, and the data are plotted versus the mean depth of each section.

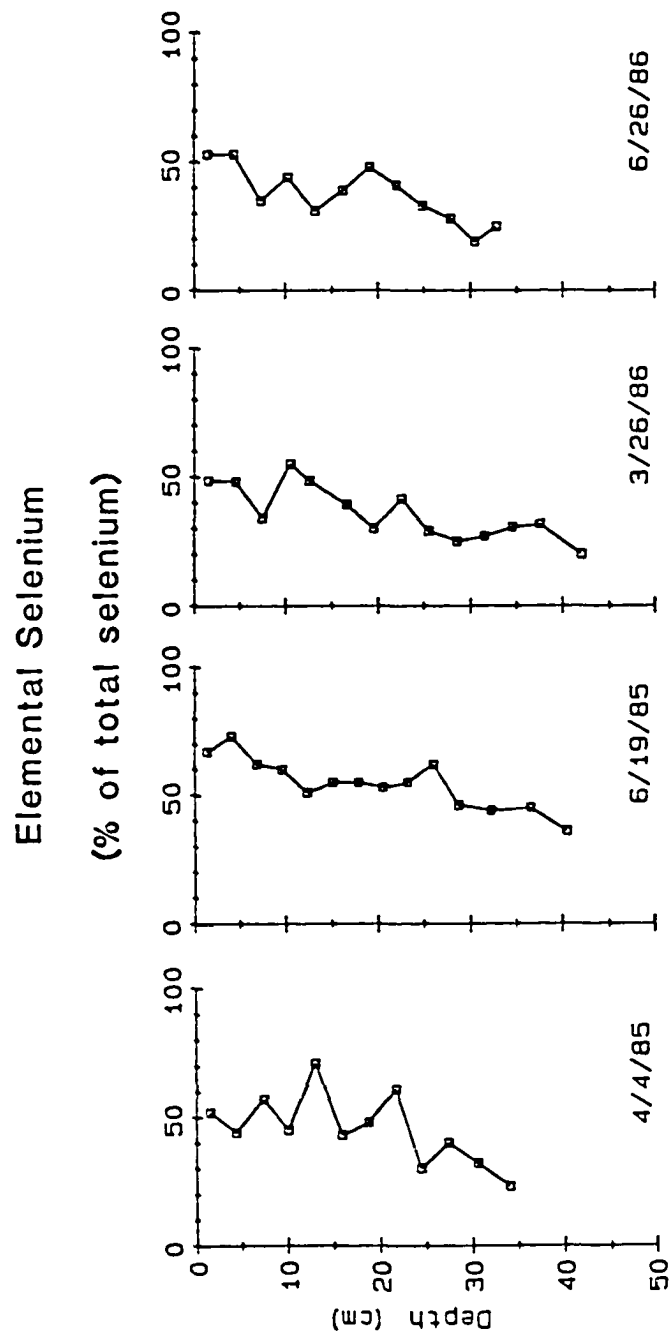


Figure 4.6. Composite depth distribution of elemental selenium concentrations in the Great Marsh. Sediments were sectioned at 2.6 to 3.0 cm intervals, and the data are plotted versus the mean depth of each section.

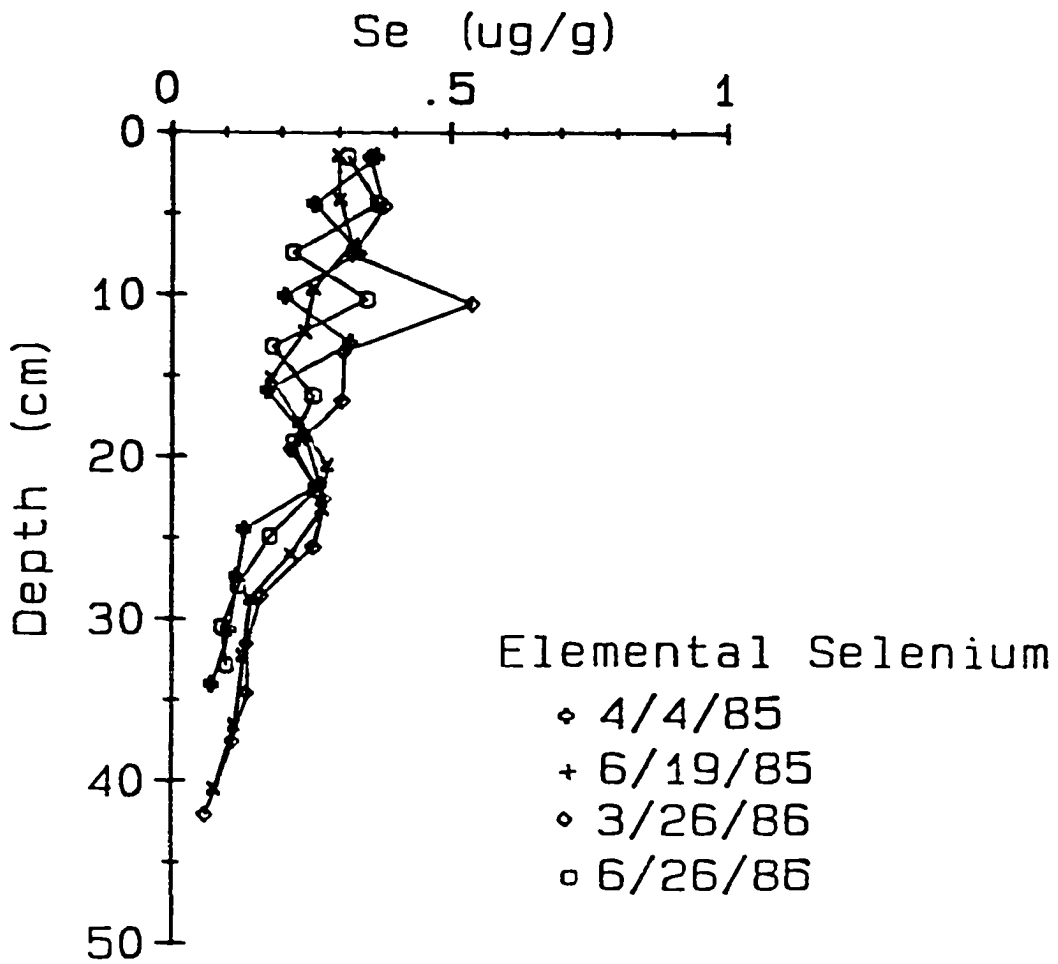
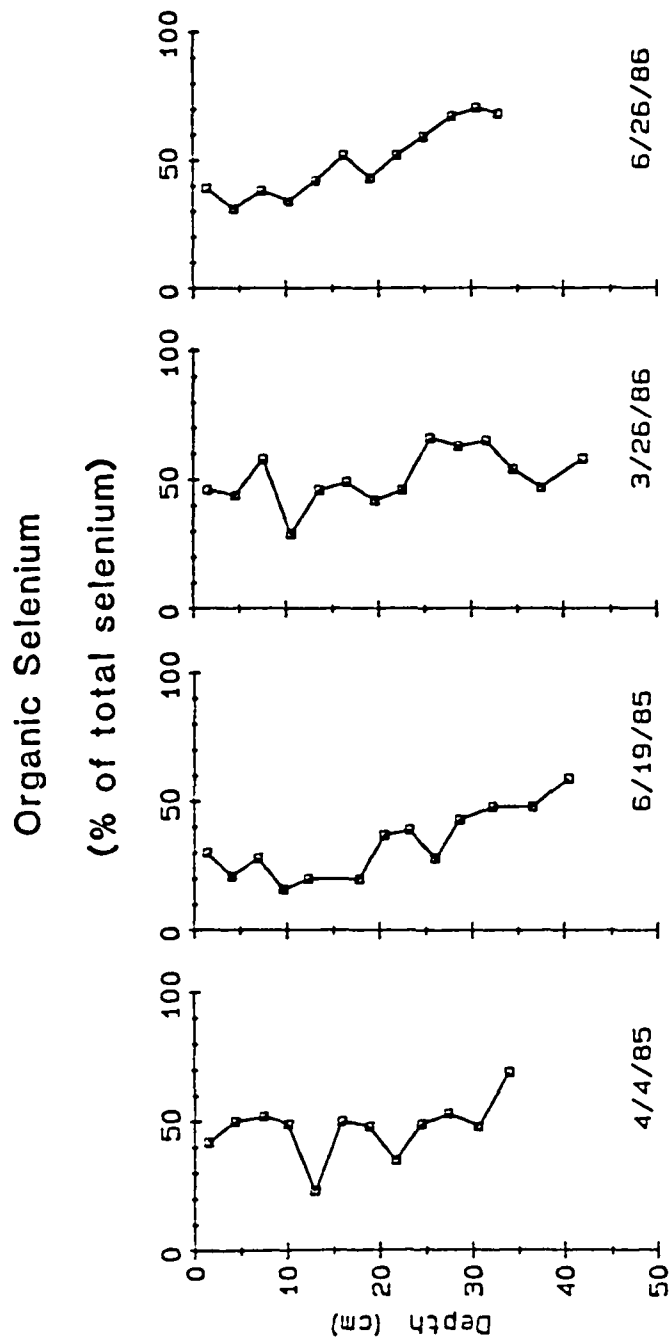


Figure 4.7. Depth distribution of organic selenium normalized to total selenium in the Great Marsh. Sediments were sectioned at 2.6 to 3.0 cm intervals, and the data are plotted versus the mean depth of each section.



Total Sedimentary Selenium

The concentrations of total sedimentary selenium during April, June, and December 1985, and March and June 1986 are listed in Table 4.5 and plotted versus depth in Figure 4.3. Concentrations of total sedimentary selenium in all cores show a general decrease with depth. The April 1985 profile has a surface selenium concentration of 0.70 ug Se/g and decreases steadily to 0.32 ug Se/g by 34 cm (because all profiles have data at 34 cm, this depth will be used as a reference level for these discussions). A broad sub-surface selenium maximum of 0.50 ug Se/g is seen between 15 and 25 cm. In June 1985, surface selenium values have declined to 0.44 ug Se/g. Below this, concentrations decrease to 0.29 ug Se/g at 34 cm, except for a broad maximum (0.53 ug Se/g) at around 21 cm.

The December 1985 profile (Figure 4.3) shows the smallest concentration decrease with depth. The sedimentary selenium concentration at the surface is 0.46 ug Se/g and decreases slightly to 0.41 ug Se/g at 34 cm. In March 1986, the concentration of surface selenium has increased to 0.74 ug Se/g and eventually decreases to 0.45 ug Se/g by 34 cm. In the June 1986 profile (Figure 4.3), total selenium decreases from a surface concentration of 0.60 ug Se/g to 0.41 ug Se/g at 34 cm. The profile is more variable with depth than the other four profiles making careful interpretation difficult. The reason for this variability is not clear since the analytical precision averages 7%

(relative standard deviation) for individual depth intervals.

Overall, the concentration of total sedimentary selenium ranges from 0.21 to 0.95 ug Se/g for all depths. Surface concentrations exhibit an average concentration of 0.59 ± 0.14 ug Se/g (n=5), while concentrations average 0.37 ± 0.08 ug Se/g (n=5) at a depth centered around 34 cm. Below 34 cm concentrations of sedimentary selenium decrease slightly to between 0.21 to 0.43 ug Se/g. In general, the concentrations of total sedimentary selenium determined in these cores are similar to those reported for other non-polluted fresh water and marine sediments (see Chapter 1). A discussion of the sources and sinks of total sedimentary selenium will be presented later.

Sedimentary (selenite+selenate)

The sedimentary (selenite+selenate) data are presented in Table 4.5. The concentrations are normalized to total selenium (% of the total sedimentary selenium) and plotted versus depth in Figure 4.4.

In April 1985 sedimentary (selenite+selenate) is less than 8% of the total selenium, with concentrations ranging from 0.038 to 0.015 ug Se/g (Table 4.5). No distinct trend is obvious in the profile (Figure 4.4). As spring progresses to summer, the profile changes dramatically. The June 1985 profile (Figure 4.4) shows a gradual increase in the concentration of sedimentary (selenite+selenate) from the

surface (0.011 ug Se/g, 2.4% of the total selenium) to a maximum at a depth of 12 cm (0.13 ug Se/g, 28.3% of the total selenium). However, when normalized to total selenium, the 15 cm section (Figure 4.4) has the greatest percentage of sedimentary (selenite+selenate) (33% of the total selenium). Below 18 cm, sedimentary (selenite+selenate) accounts for less than 10% of the total selenium, with concentrations ranging from 0.009 to 0.052 ug Se/g (Table 4.5, Figure 4.4).

The winter profile of sedimentary (selenate+selenite) in December 1985 (Figure 4.4) exhibits lower concentrations compared to the June 1985 profile. Concentrations increase from 0.032 ug Se/g (10% of the total selenium) at the surface to a broad maximum of 0.066 ug Se/g (13% of the total selenium) between 5 and 14 cm. Below this maximum, concentrations and percentages of sedimentary (selenite+selenate) decrease gradually to 0.025 ug Se/g (7% of the total selenium) at 34 cm (Table 4.5, Figure 4.4). From December 1985 to March 1986, concentrations of sedimentary (selenite+selenate) do not change appreciably (Table 4.5).

By June 1986 the sedimentary (selenite+selenate) concentrations increase throughout the upper 15 cm of the core (Table 4.4, Figure 4.5). The concentration in the surface section is 0.047 ug Se/g (7.9% of the total selenium) and increases gradually to a broad maximum of 0.17 ug Se/g (23% of the total selenium) at 13 cm. The sedimentary (selenite+selenate) concentrations then rapidly

decrease to 0.046 ug Se/g at 20 cm, which accounts for less than 10% of the total selenium. Below 30 cm the concentrations decrease to 0.030 ug Se/g (7% of the total selenium).

The spatial and temporal distribution of sedimentary (selenite+selenate) (Table 4.5, Figure 4.4) appears to be related to the changes in the redox environment of the marsh (Table 4.1 and 4.2, also see Figure 3.3). When the marsh is reducing (e.g., April 1985), FeS forms (see Figure 3.3) and the sedimentary (selenite+selenate) is generally less than 10% of the total selenium (Table 4.5, Figure 4.4). Oxidizing conditions (e.g, June 1985), as indicated by low or undetectable concentrations of FeS in the upper 15 cm of the marsh (Table 4.1, also Figure 3.3), exhibit concentrations of sedimentary (selenite+selenate) up to 33% of the total selenium (Table 4.5, Figure 4.4). Moreover, sedimentary (selenite+selenate) is predominantly found in the seasonally oxic portion of the sediment (0-15 cm). Below 15 cm, in the permanently anoxic sediment, sedimentary (selenite+selenite) is < 10% of the total selenium.

Elemental Selenium

Concentrations of elemental selenium are given in Table 4.5 for the April 1985, June 1985, March 1986, and June 1986 cores. The data are normalized to total selenium and plotted versus depth in Figure 4.5. The distributions of elemental selenium in all cores are similar. Concentrations uniformly

decrease with depth without apparent seasonal features (Figure 4.6, Table 4.5).

Surface concentrations of elemental selenium (Table 4.5) average 0.34 ± 0.03 ug Se/g (n=4) or 58% of the total selenium, below which concentrations decrease to an average of 0.10 ± 0.02 ug Se/g (n=4) or 50% of the total selenium at 34 cm. In the June 1985 profile however, elemental selenium (Figure 4.5) accounts for up to 73% of the total sedimentary selenium near the surface and decreases to 36% at 36 cm.

Because elemental selenium occupies a large region in E_H/pH stability field diagrams (see Chapter 1), Geering et al. (1968), Lakin (1973), and Howard (1977) and others predicted that elemental selenium should be the dominant form of selenium in sediments. The elemental selenium data presented here (Table 4.5, Figure 4.5) confirm this suggestion. Further, the elemental selenium data for the Great Marsh indicate that seasonal redox changes do not affect elemental selenium to the extent that elemental sulfur was controlled (see Chapter 3).

Chromium Reducible Selenium

Chromium reducible selenium is an operationally defined fraction of sedimentary selenium. This fraction should contain selenium in either the mineral ferroselite ($FeSe_2$) or pyrite (FeS_2) (see Chapters 1 and 2). For the purpose of this and other discussions, this fraction will be termed chromium reducible selenium (CRSe). The concentrations

listed in Table 4.5 were normalized to total selenium and are presented in Table 4.6.

The data for CRSe are very limited in number since the concentrations of CRSe in most samples were below the detection limit of the method (≤ 0.009 ug Se/g). In general, concentrations of chromium reducible selenium are extremely low to undetectable at most depths (Table 4.5). Overall, concentrations range from 0.010 to 0.19 ug Se/g and account for 0.7 to 25% of the total sedimentary selenium. When detectable, the depths centered around 15 cm and deeper sections below 30 cm contain the majority of the CRSe (Tables 4.5 and 4.6). The CRSe data is in contrast to the pyrite data presented in Chapter 3. While pyrite is dominant phase of sulfur, CRSe is a minor fraction of the total sedimentary selenium.

Acid Volatile Selenium

Attempts were made to determine acid volatile selenium from the marsh sediments. Howard (1977) suggests that FeSe (achavalite) could form during the alkaline oxidation of FeS-Se⁰ or FeS-HSe⁻. The FeSe (acid volatile selenide) fraction would be similar to acid volatile sulfide (Berner, 1967; Goldhaber and Kaplan, 1974).

Fourteen sediment sections (June 1985) were analyzed, and no acid volatile selenium was detected (detection limit of < 0.009 ug Se/g). The absence of acid volatile selenium indicate that this phase of selenium is either not stable in

Table 4.6

Chromium Reducible Selenium

Depth ^a (cm)	%CRSe ^b
Sampling date: 4/4/85	
0-28.8	ND
28.8-32.3	12
32.3-35.7	9.6

Sampling date: 6/19/85	
0-13.7	ND
13.7-16.4	18
16.4-19.1	15
19.1-42.0	ND

Sampling date: 3/26/86	
0-6	ND
6-9	0.7
9-15	ND
15-18	4.7
18-21	25
21-24	7.7
24-27	ND
27-30	4.2
33-36	9.8
36-39	11
39-45	25

Sampling date: 6/26/86	
0-29.3	ND
29.3-31.6	4.7
31.6-34	ND

- ND - Not Detectable (see Table 5)
- a - Specific Intervals in Table 5
- b - Chromium Reducible Selenium
normalized to Total Selenium

these sediments or not stable during storage. These conclusions are in agreement with the calculations by Howard (1977).

Organic Selenium

Organic selenium is calculated as the difference between total sedimentary selenium and the sum of the measured inorganic forms of selenium (i.e., elemental selenium, chromium reducible selenium, and selenite+ selenate). The concentrations of organic selenium from the April 1985, June 1985, March 1986, and June 1986 sampling periods are listed in Table 4.5. The concentrations are normalized to total selenium and plotted versus depth in Figure 4.7. Because organic selenium is calculated as a difference, the errors associated with these values are large (Table 4.5) and interpretation should be made with caution. Direct determinations of organic selenium compound in sediments is definitely needed.

The concentrations of organic selenium (Table 4.5), except for the March 1986 data, exhibit no distinct trend with depth. Concentrations range from 0.078 to 0.34 ug Se/g and are near constant with depth in each core with only slight variations between cores (Table 4.5). Concentrations for the March 1986 core (Table 4.5) range from 0.17 to 0.59 ug Se/g, but it is unclear why the March 1986 data are more variable. Although the depth distribution of organic selenium appears to be near constant with depth (Table 4.5),

certain trends can be noted by normalizing the concentrations to the total selenium data (Figure 4.7).

In April 1985 the amount of organic selenium is $47 \pm 11\%$ ($n=12$) of the total selenium (Figure 4.7) throughout the entire core. A similar trend is seen in the March 1986 profile (Figure 4.7) with an average of $51 \pm 11\%$ ($n=12$) of the total selenium as organic selenium. The June 1985 and 1986 profiles (Figure 4.7) show a depletion of organic selenium in the upper 20 cm of the marsh. Below 20 cm organic selenium in the two profiles approaches or surpasses 50% of the total selenium. The apparent seasonal variability in the percent organic selenium (Figure 4.7) may be an artifact of the calculation which defines this fraction. Specifically the profile of elemental selenium and the apparent seasonal changes are mirror images of the seasonal changes in sedimentary (selenite+selenate), which is the only selenium fraction to show seasonal variability.

Input of Selenium to the Marsh

In this section a more rigorous examination of the import of selenium to the marsh will be made. Subsequently, the internal cycling of sedimentary (selenite+selenate) within the marsh, and the export of selenium from the marsh will be reviewed using both mass balance calculations and diagenetic modeling.

As seen in Figure 4.2, the concentration of total sedimentary selenium varies between 0.21 and 0.95 ug Se/g

and shows no distinct seasonal trend. These concentrations are up to an order of magnitude higher than the estimated crustal abundance of selenium (0.09 ug Se/g, Turekian and Wedepohl, 1961). The major process for the incorporation of selenium into marsh sediments is presumably the biotic uptake of selenium by plants from creek waters (Peterson and Butler, 1962; Rosenfeld and Beath, 1964; Wrench, 1978; Foda et al., 1983). Other processes, such as the adsorption of selenite (from creek and rain waters) onto iron oxides or organic matter, the deposition of particulate selenium from creek water and the atmosphere, and anthropogenic inputs (atmospheric and creek water) may also be important.

Many researchers have found a correlation between organic matter and selenium (see Chapter 1). A correlation between organic matter and selenium might indicate biotic uptake of selenium or possible scavenging of selenium onto organic matter. Regression analysis shows only a weak positive correlation between organic carbon and either total selenium ($r = 0.55$, $n = 67$) and organic selenium ($r = 0.30$, $n = 51$) in the sediments from the Great Marsh. Thus, either additional mechanisms besides plant uptake and incorporation are helping to enrich these sediments with selenium, or processes are fractionating organic carbon and selenium during sedimentary diagenesis. Overall, the ultimate source of selenium to this marsh is postulated to be the atmosphere (from both wet and dry deposition) and adjacent creek waters (which contains both dissolved and particulate selenium).

Although it is difficult to quantify these inputs, estimates will be made to determine their relative importance.

Using a present day wet depositional flux of 15.0 ng Se/cm²yr (Cutter and Church, 1986) and a dry deposition flux of 2.7 ng Se/cm²yr (Ross, 1985), a total atmospheric flux of 17.7 ng Se/cm²yr is obtained. It should be pointed out that the wet deposition flux is taken from samples collected at a location about 2 km from the marsh site, and although the data set is limited, it should be sufficiently accurate for this work. However, the dry deposition flux is taken from data compiled by Ross (1985) for an intermediate (urban/remote) location, and may vary by a factor of three.

Taking the average selenium concentration (C) in the top 2.5 cm section to be 0.59 ug Se/g ($\pm 26\%$, n=5), a sedimentation rate (w) of 0.47 cm/yr (Church et al., 1981), a porosity (ϕ) of 0.85 (Lord and Church, 1983), and a sediment dry density (p) of 1.8 g/cm³ (Church, personal communication), the mass accumulation rate, R (Berner, 1980), can be calculated using:

$$R \text{ (ug/cm}^2\text{yr)} = C w p (1-\phi). \quad (1)$$

Assuming steady state, this equation predicts 74.9 ng Se/cm²yr are deposited at the marsh surface. Thus atmospheric deposition (wet and dry) can account for only 24% of this input, and by difference, 76% (57.2 ng Se/cm²yr) of the input must be from creek waters. These calculations indicate that both atmospheric and creek water inputs are important sources of selenium to the marsh.

It should be noted here that the changes in the concentration of total selenium with depth are assumed to be diagenetically controlled (i.e., if these inputs of selenium have been constant over the past 70 yrs; at a depth of 34 cm and using a sedimentation rate of 0.47 cm/yr) and not related to source variations. This assumption is most likely valid for two reasons. First, the concentration of total dissolved selenium in the creek waters showed little variation and averages 81.3 pg Se/g (H₂O). This selenium concentration is well within the range of data from other unpolluted estuaries (Measures and Burton, 1978; Cutter, 1982; Takayanagi and Cossa, 1985). Therefore, increasing selenium input to the marsh with time from creek waters appears unlikely. Second, the atmospheric flux is close to the value estimated by Ross (1985) for remote continental areas (6 ng Se/cm²yr). While, Weiss et al. (1971) found no increase in the concentration of selenium in ice core samples from Greenland. Assuming steady state deposition over the last 72 years and no diagenetic loss of selenium, it is possible to estimate the past atmospheric (and creek water) inputs to the marsh. Taking the average concentration of total selenium at 34 cm (0.37 ± 0.08 ug Se/g) and the data used above (i.e., p, ϕ, and w) the input of total selenium is calculated to be 47 ng Se/cm²yr. If the atmospheric deposition of selenium has been a constant percentage of the total selenium input to the marsh (24%), then the old (post-1910) atmospheric input is calculated to

be 11.3 ng Se/cm²yr or 36% lower than the present day atmospheric flux. Within the analytical and spatial variability (\pm 20%), the present and past atmospheric fluxes are quite similar. This further supports the contention that source variations have probably not affected the inputs of selenium to the marsh over the past 72 years.

The biological uptake and incorporation of selenium into marsh sediments was estimated using literature data on the concentration of selenium in plants and plant biomass and productivity in the Great Marsh. Unfortunately, there are no estimates of the selenium concentration in S. alterniflora from this marsh. However, Peterson and Butler (1962) and Leutwein (1972) present data that suggest a concentration of total selenium in higher plants on the order of 1 ug Se/g plant. Using biomass data (live plants per unit area) from Hardisky et al. (1984), an inventory of selenium in plants of the Great Marsh of 0.015 ug Se/cm² is calculated. This value most likely underestimates (by a factor of ca. 3) the inventory of selenium because it does not include belowground biomass (Good et al., 1982). However, the calculated amount of selenium in live biomass is more than two orders of magnitude lower than the standing stock of total sedimentary selenium (5.04 ug Se/cm²). Total plant production rates (above and belowground) for the Great Marsh were determined by Roman and Daiber (1984). They measured an average plant production rate for short S. alterniflora of 0.57 g plant/cm²yr (on a dry weight basis).

Assuming 1 ug Se/g plant, a selenium incorporation rate of 0.57 ug Se/cm²yr is obtained. This rate is approximately 8X higher than the input of selenium needed to account for the input of sedimentary selenium (0.075 ug Se/cm²yr, see above). These calculations indicate that biological fixation could be a dominant mechanism for incorporating selenium into the marsh sediments. Furthermore, live biomass appears to account for a only small percentage of the total amount of selenium in the Great Marsh.

It is interesting that the organic selenium data (see Table 4.5) does not reflect this source. If plant growth is the dominant mechanism for the incorporation of selenium into the marsh, the organic selenium data should exhibit higher concentrations in the surface 15 cm and decrease with depth below 20 cm (i.e., between the surface and 15 cm, the majority of the S. alterniflora roots are found). This might be related to a rapid cycling of selenium through the plants or a sampling artifact. During sample preparation, the marsh sediment was separated from the root material. This might underestimate the concentration and phase distribution of selenium in the surface section (0 to 15 cm) of the marsh. However, the amount of selenium in the plants is a small fraction of the total sedimentary selenium and would most likely not affect the distribution of selenium with depth. The cycling of selenium through the plants can be calculated by dividing the standing crop of selenium in live biomass (0.015 ug Se/cm²) by the production rate (0.57 ug Se/cm²yr).

This yields a mean residence time of selenium in the plants of 10 days. This calculation indicates rapid selenium recycling through the marsh grass. Selenium lost from the grasses maybe transferred to the sediments, surrounding waters as litter, or released to the atmosphere.

Internal Cycling of Selenium in Marsh Sediments

The seasonal behavior of sedimentary (selenite+ selenate) can be caused by both abiotic and biotic processes. Internal sources of sedimentary (selenite+ selenate) include elemental and organic selenium. Whereas the oxidation of elemental selenium has been studied (see below), the oxidation or conversion of organic selenium has received less attention (Cutter, 1982). The oxidation of elemental selenium by oxygen has been studied by Schulek and Koros (1960) and Gattow (1964, as cited in Geering et al., 1968). These researchers show that the susceptibility of elemental selenium to oxidation is dependent upon its allotropic form and particle size. The red and black amorphous allotropes of selenium are the most easily oxidized while the grey hexagonal allotrope is the most inert. Geering et al. (1968) state that the red or black forms of elemental selenium would be the likely allotropes in sediments because red amorphous elemental selenium initially precipitates from solution. Geering et al. (1968) further show that elemental selenium is oxidized by both abiotic and biotic pathways, but the rate of oxidation is

faster in the presence of micro-organisms. Howard (1977) demonstrates that elemental selenium is slowly oxidized to selenite as FeS is oxidized to Fe(OH)₃; these experiments were conducted in a sterile environment. In more recent experiments, Sarathchandra and Watkinson (1981) show that a strain of Bacillus megaterium, isolated from soils, can oxidize elemental selenium to selenite. The above information indicates that the oxidation of elemental selenium to sedimentary (selenite+selenate) is biologically (microbially) mediated, although abiotic pathways do exist.

The seasonal decrease in sedimentary (selenite+selenate) (Figure 4.4) can be due to a combination of pore water and gaseous fluxes, biological uptake to organic forms of selenium, and conversion to either elemental selenium or other selenium phases (e.g. CRSe). Howard (1977) demonstrates in laboratory experiments that when selenite is added to a reducing environment containing Fe⁺³, HS⁻, and CaCO₃, elemental selenium is produced. Howard (1977) concludes that once elemental selenium is formed, only a small fraction will be reoxidized to selenite during the oxidation of HS⁻ with oxygen. Biotic uptake of selenite has been documented by Peterson and Bulter (1962) for higher plants, and by Foda et al. (1983) for bacteria. Bacteria can reduce selenite to elemental selenium (Levine, 1925; see Koval'skii and Ermakov, 1970) or to organic selenides in proteins (Shamberger, 1983). A decrease in (selenite+selenate) could also be due its conversion to gaseous forms.

Reamer and Zoller (1980) show that selenite, and to a lesser extent selenate and elemental selenium, are converted to volatile methylated species by micro-organisms in sewage sludge and soils. Overall, it appears that a host of abiotic and biotic mechanisms could account for the loss and gain of sedimentary (selenite+selenate).

The internal transformation of sedimentary (selenite+selenate) can be quantified using a mass balance approach. For each sampling period the standing stock ($\mu\text{g Se/cm}^2$) of sedimentary (selenite+selenate) is determined by calculating the depth integrated concentrations (Table 4.5) from the surface to 20 cm. These areas were determined using a digitizing planimeter. The apparent conversion rate of sedimentary (selenite+selenate) is calculated by subtracting the standing stock of one profile from the previous profile and dividing this value by the time between sampling. It must be pointed out that the rates of sedimentary (selenite+selenate) conversion as calculated in this manner are net rates ultimately due to a combination of both abiotic and biotic production and consumption reactions.

From April 1985 to June 1985, sedimentary (selenite+selenate) (Figure 4.4) formed at a rate of $0.0030 \mu\text{g Se/cm}^2\text{day}$, while from June 1985 to December 1985 sedimentary (selenite+selenate) decreased at a rate of $0.0006 \mu\text{g Se/cm}^2\text{day}$ (Figure 4.4). As a result of the slightly higher sedimentary (selenite+selenate) concentrations in the upper section of the March 1986 core (Figure 4.4), the calculated

rate of sedimentary (selenite+selenate) production was 0.0007 ug Se/cm²day between December 1985 and March 1986. From March 1986 to June 1986 sedimentary (selenite+selenate) increased at a rate similar to that calculated with previous winter-spring data (0.0028 ug Se/cm²day).

Concurrent with the changes in sedimentary (selenite+selenate) are changes in pore water selenium (see Tables 4.2 and 4.5, Figures 4.2 and 4.4). It is possible that when the upper 15 cm of the sediment is aerated by the S. alterniflora in the spring, elemental and/or organic selenium are oxidized to sedimentary (selenite+selenate) with a concurrent partial remobilization of selenium to the pore waters. The changes in the chemical forms of selenium might allow a repartition between the solid phases of selenium and the pore waters. For example, the formation of sedimentary (selenite+selenate) might concurrently release selenite and selenate into the pore waters as well as organic selenium. Selenium speciation data for the pore waters indicate that both inorganic and organic selenium are present (see above). The above data indicate a dynamic redox cycle for sedimentary selenium with a close coupling between the solid phase and pore water phase of selenium in the sediment.

Export of Selenium from the Marsh Sediments

The profiles of total selenium for all periods, show a loss with depth (Figure 4.3). Two methods were used to

quantify this loss. The first and simplest approach is to take the arithmetic average of the surface sections and bottom sections (≥ 34 cm) of each core and calculate the difference. The change between top and bottom is averaged for all cores and converted to a mass loss rate using the equation:

$$\text{Loss rate (ug Se/cm}^2\text{yr)} = \Delta C w p (1-\phi) \quad (2)$$

where ΔC is the average change of total selenium (0.22 ± 0.12 ug Se/g) between 0 and 34 cm, w is the sedimentation rate (0.47 cm/yr, Church et al., 1981), p is the dry sediment density (1.8 g/cm³, Church, personal communication), and ϕ is the average porosity (0.85, Lord and Church, 1983). This method yields a yearly average loss rate for total selenium of 0.028 ug Se/cm²yr.

A second approach to calculating a depth integrated loss of total sedimentary selenium is to use a simple first-order decay model. This method is similar to that which has been used to model organic carbon decomposition in marine sediments (Berner, 1980; Martens and Klump, 1984), and assumes that the rate of selenium loss is first order with respect to sedimentary selenium:

$$d\text{Se}/dt = -k [\text{Se}] \quad (3)$$

where k is a pseudo-first order rate constant.

The distribution of selenium in sediments has not been extensively studied in the past (see Chapter 1), so there are no data and models with which to compare. However, due to the relationship of selenium and organic carbon (see

above), it was postulated that the distribution of selenium might be fitted to a first order diagenetic model. The use of a first order decay model does not imply a specific mechanism to explain the decrease in total selenium with depth, but is used as an approach to determine the loss rate of total selenium and to compare this result to other models (i.e., mass balance approach). Also, the known cycle of selenium in seawater is biologically mediated (see Chapter 1), further indicating that this type of model is appropriate. Notably, a first order decay model has been used for other elements in which reactions are biologically mediated (Lord and Church, 1983; Klinkhammer et al., 1982; Burdige and Gieskes, 1983) Therefore, the distribution of total selenium in the marsh sediment was modeled using a steady state diagenetic equation which employs first order decrease of selenium with depth (Berner, 1980):

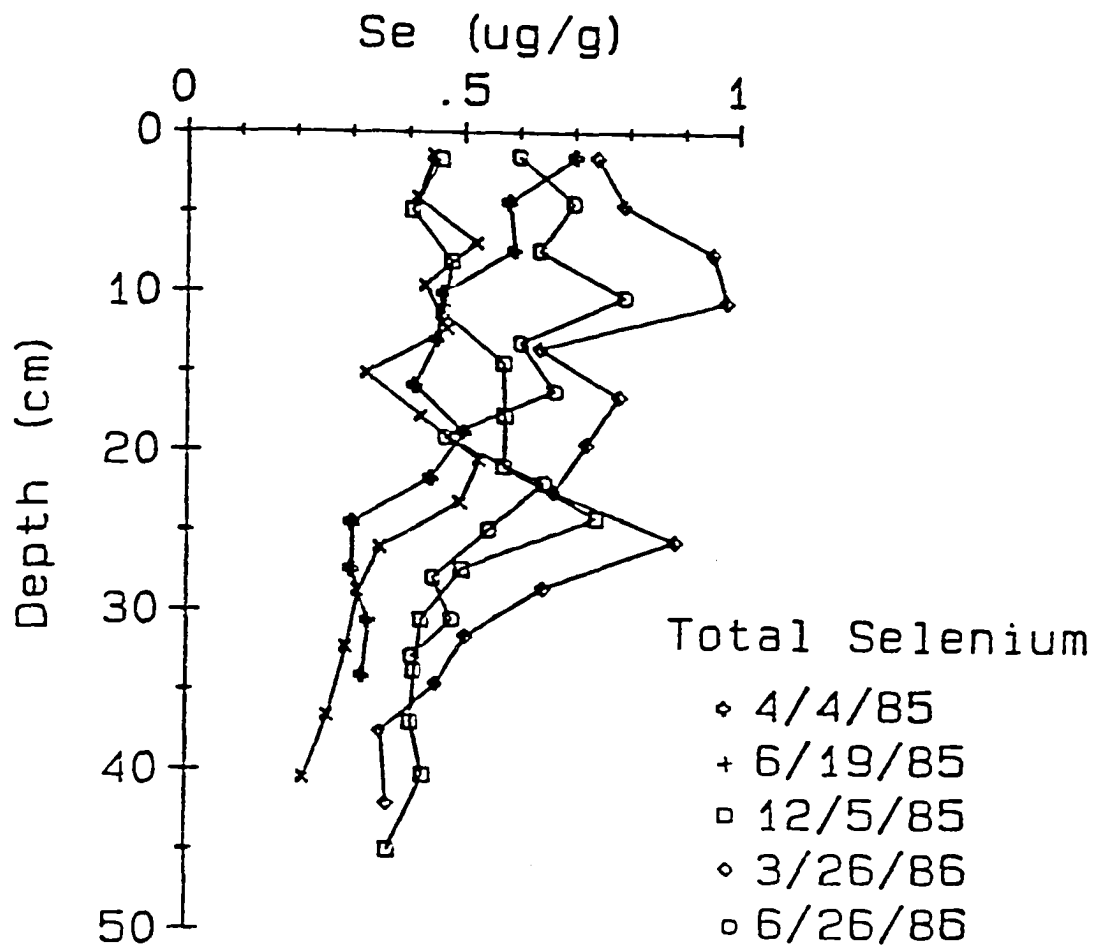
$$-w \frac{dSe}{dz} - k[Se] = 0. \quad (4)$$

This model assumes that porosity is constant with depth and neglects any bioturbation in the sediments. With the boundary condition $Se = Se_0$ at $z = 0$. The general solution is:

$$Se_z = Se_0 e^{(-k/w)z}. \quad (5)$$

From the composite profile (Figure 4.8) it appears that total selenium does not decrease to zero as depths $\rightarrow \infty$, as equation (5) would predict this. A more complex model was therefore employed to fit the data (Martens and Klump,

Figure 4.8. Composite depth distribution of total sedimentary selenium in the Great Marsh. Sediments were sectioned at 2.6 to 3.0 cm intervals, and the data are plotted versus the mean depth of each section.



1984). In this approach, total selenium (Se) was broken into two classes, an easily removable fraction (Se_r) and a "refractory" fraction (Se_{oo}). Equations (4) and (5) now apply only to Se_r with Se_o replaced by $Se_{ro}(= Se_o - Se_{oo})$. Equation (5) is then rewritten as:

$$Se = (Se_o - Se_{oo}) e^{(-k/w)z} + Se_{oo} \quad (6)$$

In order to obtain values for Se_{ro} (where $Se_{ro} = Se_o - Se_{oo}$) and k/w , the data for total selenium was fitted by an error minimization computer program. The program produces best fit Se_o , k/w , and Se_{oo} values which can be used to calculate Se_{ro} . The best fit parameters are listed in Table 4.7.

The depth integrated removal rate of easily removable total selenium (Se_{ro}) can be obtained by substitution of equation (5) (after substituting Se_{ro} for Se_o), into equation (3) and integrating over 34 cm:

$$dSe_{ro}/dt = -kFSe_{ro} \int_0^{34} e^{(-k/w)z} dz \quad (7)$$

which upon integration yields the loss rate of easily removable selenium:

$$= wFSe_r (1 - e^{(-k/w)z}), \quad (8)$$

where z is the depth interval (0 to 34 cm) and F is a concentration to mass conversion factor (Berner, 1980) equal to:

$$p (1 - \phi). \quad (9)$$

Substitution of the values in Table 4.7 into equation

Table 4.7

Diagenetic Model Results

Total Sedimentary Selenium

$$B = 0.021 \text{ cm}^{-1}$$

$$Se_o = 0.65 \text{ ug Se/g}$$

$$Se_{oo} = 0.25 \text{ ug Se/g}$$

$$k = 0.010 \text{ yr}^{-1}$$

Elemental Selenium

$$B = 0.046 \text{ cm}^{-1}$$

$$Se_o = 0.39 \text{ ug Se/g}$$

$$Se_{oo} = 0.10 \text{ ug Se/g}$$

$$k = 0.021 \text{ yr}^{-1}$$

(8) gives a depth integrated loss of total selenium of 0.026 ug Se/cm²yr. This value is virtually identical to the one calculated by the difference approach (0.028 ug Se/cm²yr).

The question arises as to what chemical form or forms of selenium are controlling the loss in total selenium within the sediments. From the results listed in Table 4.5 and shown in Figures 4.3 to 4.7, it appears that the only form of selenium that decreases in fashion similar to total sedimentary selenium is elemental selenium. To check if elemental selenium could account for the loss of total selenium, models similar to those used above were applied to the elemental selenium data.

Using the surface to 34 cm difference calculation, the loss rate of elemental selenium is 0.027 ug Se/cm²yr, while diagenetic modeling (e.g., equation (8)) yields a rate of 0.029 ug Se/cm²yr (see Table 4.7 for model results). These calculated rates account for essentially 100% of the total selenium loss and indicate that the loss of total selenium in these sediments appears to be controlled by the loss of elemental selenium.

Although the loss of total selenium in these sediments can be accounted for by elemental selenium, other mobile selenium intermediates must also be involved in this process. Elemental selenium is incorporated in the sediments as an insoluble solid and must therefore be removed through either gaseous or water intermediates that can flux out of the sediment.

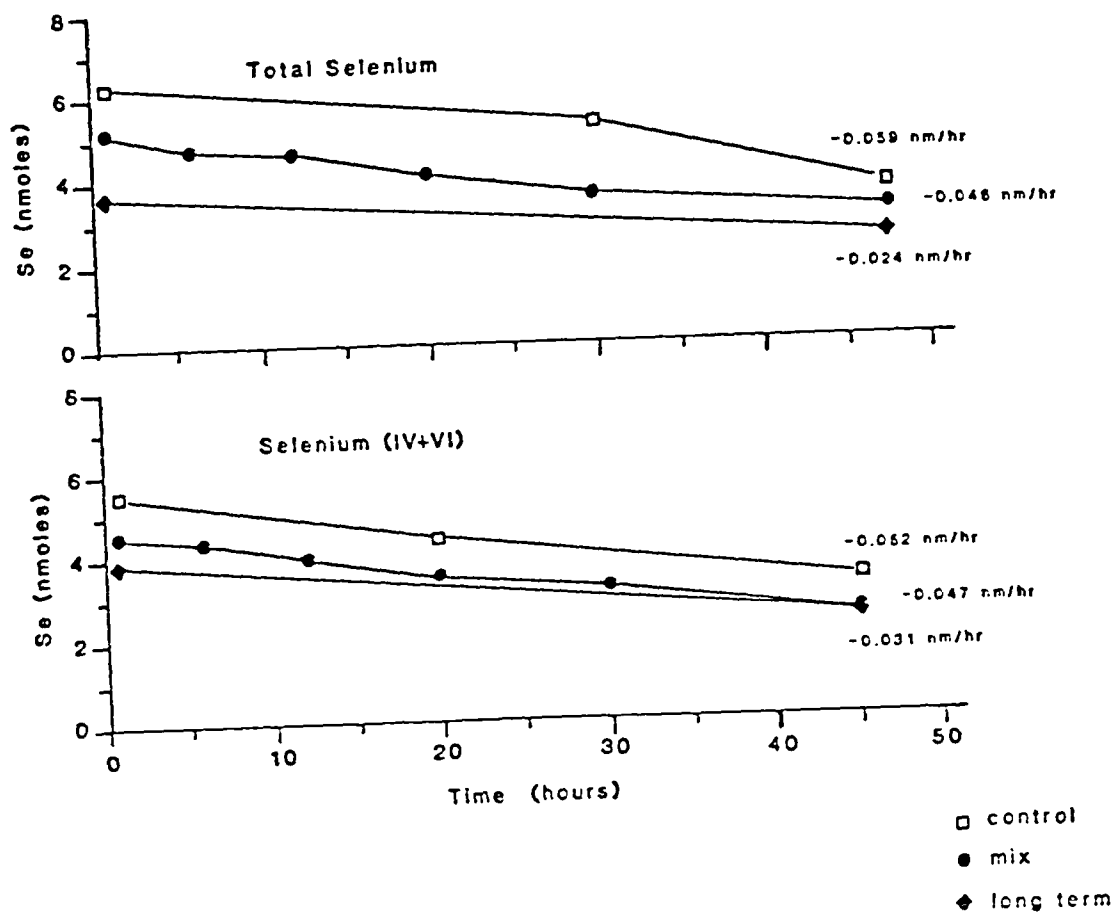
One mechanism that could remove elemental selenium from the marsh involves the conversion of elemental selenium to soluble forms and subsequent diffusion and/or advection of dissolved selenium species across the sediment-water interface. The pore water and sedimentary (selenite+selenate) profiles (Figures 4.2 and 4.4) suggest that the interconversion of selenium species is occurring. As described above, when the upper 20 cm of the marsh becomes oxidizing, sedimentary (selenite+selenate) increases in concentrations, as does pore water selenium. The source of the sedimentary (selenite+selenate) is either organic selenium or elemental selenium. The organic selenium data (Table 4.5) indicate that this fraction is relatively constant over time, while the data for elemental selenium (Table 4.5 and Figure 4.5) do show a slight deficit in the upper 15 to 20 cm in both June 1985 and 1986. It is possible that during oxidizing periods in the marsh, a small, but important fraction, of the elemental selenium is oxidized to sedimentary (selenite+selenate), and concurrently a fraction of this is released into the pore waters. For pore water export of selenium to be significant, the selenium concentration in pore water must be greater than that in the surrounding creek water. Examining Tables 4.3 and 4.4 and Figure 4.2 it is apparent that this is not the case. To confirm this hypothesis and directly observe selenium input/output from marsh sediment, a flux chamber experiment was conducted during the June 1986 sampling period.

To further confirm that the diffusion of pore water selenium is not significant, a flux chamber experiment was performed during the June 1986 sampling period. The profile of pore water selenium from this sampling date indicates that a small flux of selenium could be occurring (Figure 4.2). This experiment used five individual cores (ca. 45 cm long) taken at the same time and location. Cores were held at room temperature (22°C) and filled with filtered creek water of known selenium concentration. Water was sampled from each core at specific time intervals (0, 1, 6, 12, 20, 30, and 45 hours), and the five individual water samples combined for each sampling period (i.e., so there was sufficient volume for selenium analysis). A sixth core was incubated for 45 hours and sampled only at time 0 and at 45 hours. Concurrent with these six cores, an experimental control consisting of a core barrel filled with the creek water was sampled at time 0, 30 and 45 hours. All chambers were kept in the dark during incubation and bubbled with filtered laboratory air to enhance mixing and keep the overlying water aerobic. The collected water samples were passed through a 0.4 μ m Nuclepore filter and stored in borosilicate glass bottles (at pH 1.5 using HCl) until analyses (within two weeks). Samples were analyzed for total dissolved selenium and selenite+selenate using the procedures given in Chapter 2.

From the data in Figure 4.9, it appears that selenium is removed from the control tube at about the same rate as

Figure 4.9. Selenium as a function of time during the flux chamber incubation experiment; mix - combined water samples from five separate core incubations, long term - one core incubated for 45 hours, control - core barrel filled with filtered creek water.

Flux Chamber Experiment
Great Marsh, DE
6-26-86



in the sample tubes (both mix and long term). The June 1986 pore water data (Figure 4.2) would have predicted a flux into the overlying water from the sediment (i.e., pore water concentrations > creek water concentrations). The most likely mechanism which could inhibit the diffusive flux of selenium across the sediment-water interface is the reaction of dissolved selenium with surface iron oxides (see Chapter 1). The flux chamber experiment actually suggests a selenium input into the marsh sediment, but because the slope of the control and sample experiment are close, it appears that the walls of the core barrel are removing selenium from the water. Therefore, the results from this experiment confirm that the pore water flux of selenium by diffusion is small and most likely cannot account for the loss of total sedimentary selenium. Thus, another loss mechanism must be invoked. Two possible pathways for selenium loss are conversion to volatile selenium species (gaseous emissions) and export via detritus, more than likely S. alterniflora litter.

Export of Selenium via Spartina Detritus

To estimate the export of selenium from the marsh via S. alterniflora litter or detritus, the areal flux of plant detritus from the marsh to the creek/estuarine waters and the concentration of selenium in the detrital material is needed. This approach has been used to estimate the flux of trace metals (Cu, Zn, and Fe) from the Great Marsh (Pellenbarg, 1985) to surrounding waters and has been shown

to be an important aspect of the biogeochemistry of marsh systems (Windom, 1975; Pellenbarg, 1984). Unfortunately, no direct measurements of this flux have been made for selenium. Therefore, to estimate the export of selenium via plant detritus the flux of particulate organic carbon from the marsh and the Se/C ratio of the top 2.5 cm of the marsh sediment were used.

The flux of particulate organic carbon (POC) from the Great Marsh is taken from Lotrich et al. (1979). Their POC flux of $62 \text{ g C/m}^2\text{yr}$ is within the range of other POC fluxes from various East and Gulf coast marshes (see Nixon, 1979). Using a Se/C ratio (atomic) of $1.1 \pm 0.2 \times 10^{-6}$ ($n=5$), a selenium flux of $0.045 \text{ ug Se/cm}^2\text{yr}$ via plant litter is obtained. This estimate is 1.5X greater than the loss of total sedimentary selenium calculated from the diagenetic model.

This method of calculating a selenium export via plant detritus is based on many complicated factors. For instance, it is unclear if the source of POC is exclusively Spartina detritus or a combination of many sources within the marsh (e.g., sediment scouring, algal and bacterial production). Also, this mechanism must account for the continual loss of total selenium with depth (i.e., total selenium decreases well below the root zone). Therefore, a process must be invoked which transports sedimentary selenium, at depths greater than 15 cm, to the root zone. Presumably dissolved selenium could be taken up by the plants in the root zone

and subsequently transported from the sediment via Spartina litter. Pore water profiles do not reflect such a transport to the root zone (Figure 4.2), although diffusive gradients could be smaller than those detected by the procedures used here. Also this estimate, does not take into account the possible rapid recycling and/or preferential remineralization of selenium versus carbon prior to the material leaving the marsh system. Overall, these considerations would suggest that this export estimate of selenium via Spartina litter is a maximum.

Gaseous Emission of Selenium

The biogenic emission of volatile selenium compounds is another mechanism that could account for the loss of selenium from the marsh. Such a pathway would include the conversion of sedimentary selenium to methylated selenium compounds (e.g., dimethylselenide, DMSe, and dimethyl diselenide, DMDS_e) via microbial processes. The volatile selenium compounds could then degases out of the sediment. In a recent study of the Kesterson Reservoir, Cooke and Bruland (1987, submitted) observed significant amounts of dimethylselenide in the waters of Kesterson Reservoir. They estimated that approximately 30% of the selenium introduced to this system may be lost by the production of dimethylselenide and subsequent evasion to the atmosphere. Though it has been demonstrated that microbial processes produce volatile selenium compounds in sediments and waters

(Lewis et al., 1974; Chau et al., 1976; Reamer and Zoller, 1980; Shamberger, 1983; Cooke and Bruland, 1987, submitted), no data on the flux of these compounds from marsh or other sediments exist.

The total sedimentary selenium data and the lack of apparent pore water selenium loss indicate the gaseous flux must be approximately $0.03 \text{ ug Se/cm}^2\text{yr}$. As an attempt to independently calculate the flux of volatile selenium compounds from the marsh, the correlation between total selenium and sulfur in these sediments and an estimate of the gaseous sulfur flux from the marsh surface. Selenium fluxes are estimated using sulfur data because the metabolic pathways which volatilize selenium and sulfur are similar (Shamberger, 1983; Ross, 1985). The selenium to sulfur ratio (atomic) for all cores are listed in Table 4.8. Ratios range from 8.3 to 54.5×10^{-6} with an average value of 20.0×10^{-6} (n=67). The significance of the distribution of the selenium to sulfur ratio will be more fully discussed in Chapter 5. For the purpose of this calculation a ratio of 20.0×10^{-6} will be used.

The sulfur flux from S. alterniflora marshes has been measured by a number of researchers (Aneja et al., 1981; Adams et al., 1981; Goldberg et al., 1981; Carroll, 1983; Steudler and Peterson, 1985; Cooper et al., 1987; de Mello et al., 1987). Only East Coast salt marshes and those studies in which most or all of the dominant sulfur gases (H_2S , DMS, COS, DMDS, CS_2 , and CH_3SH) were measured are

TABLE 4.8

Solid Phase Selenium/Sulfur Data

Depth (cm)	Se/S X 10 ⁻⁶ (atomic)	Depth (cm)	Se/S X 10 ⁻⁶ (atomic)
Sampling date: 4/4/85		Sampling date: 6/19/85	
0-2.9	43.4	0-2.7	34.2
2.9-5.8	24.3	2.7-5.5	13.8
5.8-8.6	23.6	5.5-8.2	29.2
8.6-11.5	15.8	8.2-10.9	10.1
11.5-14.4	13.9	10.9-13.7	21.5
14.4-17.3	10.8	13.7-16.4	11.4
17.3-20.2	19.2	16.4-19.1	10.4
20.2-23.0	20.3	19.1-21.8	23.3
23.0-25.9	11.4	21.8-24.6	17.3
25.9-28.8	10.9	24.6-27.3	9.91
28.8-32.3	10.1	27.3-30.0	9.58
32.3-35.7	8.70	30.0-34.4	8.32
		34.4-38.8	14.0
		38.8-42.0	9.53
Sampling date: 12/5/85		Sampling date: 3/26/86	
0-3.2	15.1	0-3.0	54.5
3.2-6.4	14.3	3.0-6.0	52.8
6.4-9.6	9.95	6.0-9.0	22.6
9.6-12.8	17.0	9.0-12.0	32.8
12.8-16.1	24.3	12.0-15.0	27.2
16.1-19.3	16.3	15.0-18.0	20.0
19.3-22.5	14.2	18.0-21.0	19.5
22.5-25.7	25.6	21.0-24.0	42.0
25.7-28.9	25.4	24.0-27.0	26.5
28.9-32.1	24.2	27.0-30.0	23.5
32.1-35.3	11.7	30.0-33.0	10.3
35.3-38.6	12.7	33.0-36.0	10.7
38.6-41.7	14.1	36.0-39.0	11.7
41.7-48.1	13.9	39.0-45.0	13.2
48.1-54.5	8.76		
Sampling date: 6/26/86			
0-2.9	31.4		
2.9-5.9	32.8		
5.9-8.8	26.4		
8.8-11.7	34.9		
11.7-14.7	24.6		
14.7-17.6	17.5		
17.6-20.5	23.5		
20.5-23.4	40.3		
23.4-26.4	24.1		
26.4-29.3	10.3		
29.3-31.6	12.1		
31.6-34.0	14.3		

considered for this calculation. The average annual total sulfur flux and location are listed in Table 4.9. Most studies indicate that DMS and H₂S are the dominant sulfur species emitted from marsh sediments, with the remaining sulfur species up to an order of magnitude lower. The flux of dimethylsulfide is usually higher in vegetated locations, while H₂S is the major compound from mudflats (Cooper et al., 1987; de Mello et al., 1987). Spatial and temporal (diel and seasonal) variability is observed for all species of gaseous sulfur (Stuedler and Peterson, 1985; de Mello et al., 1987). The values reported in Table 4.9 are yearly integrated averages which cover vegetated and unvegetated areas. The Great Marsh site is a vegetated location (see Chapter 1). Using the selenium to sulfur ratio stated above and a range of sulfur emissions from Table 4.9 of 51.7 to 580.4 ug S/cm²yr, a selenium flux of 0.003 to 0.03 ug Se/cm²yr is calculated.

The procedure of calculating the volatile flux of selenium from the Great Marsh is complicated by several factors. Chau et al. (1976) found no direct correlation between concentrations of sedimentary selenium and volatile emissions. Moreover, volatilization rates are dependent upon types of microorganisms present within the sediment and the oxidation state of the available selenium. Reamer and Zoller (1980) and Doran and Alexander (1977) show that selenite is incorporated and volatilized faster than elemental selenium. Moreover, it is assumed that organisms take up and

Table 4.9

Sulfur Gas Fluxes From Various Salt Marshes

Location	Flux Rate (ug S/cm ² yr)	Reference
Cedar, NC	69.0	Aneja et al. (1981)
Lewes, DE	65.9	Adams et al. (1981)
Great Sippewissett, MA	580.4	Steudler and Peterson (1985)
Wallops Island, VA	353.9	Adams et al. (1981)
Florida Marsh, FL	51.7	Cooper et al. (1987)

Total Sulfur Flux Range: 51.7 - 580.4 ug S/cm² yr

volatilize selenium and sulfur in the same ratio as that found in these sediments.

In spite of these difficulties, this flux calculation indicates that volatile selenium emissions from marsh sediments are of the same order of magnitude as the loss of total selenium from the marsh. In fact, the flux of gaseous selenium from the marsh can account for up to 100% of this removal. The importance of this mechanism can only be fully understood when direct flux measurements are obtained.

SUMMARY AND CONCLUSIONS

The geochemical cycle of selenium in a coastal marsh is presented in Figure 4.1 and the results of the various models are given in Table 4.10. This cycle depicts the external inputs/outputs of selenium as well as internal changes between the different oxidation states of selenium.

Overall, depth profiles of the different chemical forms of sedimentary selenium along with profiles of pore water selenium have revealed the following information:

- 1) The dominant forms of selenium in marsh sediments are elemental selenium and organic selenium, their distribution in the sediments shows no strong seasonal variability. Concentrations of sedimentary (selenite+selenate) account for at most 30% of the total selenium and shows strong seasonal variations. Chromium reducible selenium is a minor fraction of the total selenium and shows no coherent trend with depth or season.

Table 4.10
Summary of Model Results^a

INPUTS

- (1) Creek waters = 57.7 ng Se/cm²yr (76%)
- (2) Atmospheric = 17.7 ng Se/cm²yr (24%)
- Total Input = 74.9 ng Se/cm²yr

INTERNAL REACTIONS WITHIN THE SEDIMENT

- (3) Loss of total selenium = 0.026-0.028 ug Se/cm²yr
Loss of elemental selenium = 0.027-0.029 ug Se/cm²yr
- (4) Net change of sedimentary (selenite+selenate) =
+0.001 ug Se/cm²day

EXPORTS

- (5) Plant litter = 0.045 ug Se/cm²yr
- (6) Gaseous selenium flux = 0.003 to 0.03 ug Se/cm²yr

a - see Figure 4.1.

2) Pore water selenium reflects the diagenetic cycling of sedimentary (selenite+selenate) and suggests that a partial remobilization of sedimentary selenium occurs when the upper sediments become oxidizing.

3) The sources of selenium to the marsh are dominated by creek water inputs and to a lesser extent atmospheric deposition. Once the selenium is "fixed" into the marsh sediment, a gradual decrease in total sedimentary selenium occurs. This decrease is mainly controlled by the decrease in elemental selenium.

4) Mass balance calculations in conjunction with diagenetic modeling indicate that the loss of total selenium is related to the decrease in elemental selenium. Major outputs of selenium from this marsh are estimated to be gaseous emissions from the marsh surface, or possibly by the export of particulate selenium via Spartina alterniflora litter.

5) Calculations indicate that biological uptake of selenium can be an important process in the cycling of selenium in the marsh. The majority of the selenium taken up by the marsh grass is not incorporated into plant biomass and sediment. Selenium is rapidly cycled through the marsh grass with an average residence time of 10 days.

Chapter 5

Comparative Geochemistries of Selenium and Sulfur

INTRODUCTION

In Chapters 3 and 4 sulfur and selenium data for the Great Marsh were presented. These data were qualitatively described and quantitatively modeled to highlight their respective geochemistries. It might be expected that selenium should behave similarly to sulfur during the early diagenesis of marine sediments due to the proximity of selenium and sulfur on the periodic table (Group VI). Other investigators have examined the comparative geochemistry of element pairs such as Ge/Si (Froelich et al., 1985; Bernstein, 1985) and As/P (Neal et al., 1979; Morris et al., 1984). The objective of this chapter is to compare the geochemistries of sulfur and selenium during early diagenesis in a salt marsh.

DISCUSSION

Comparative Chemistries of Selenium and Sulfur

Thermodynamics

Group VI elements (oxygen, sulfur, selenium, tellurium, and polonium) show a gradual transition from non-metallic to more metallic character with increasing atomic number. All of the VI elements form covalent compounds of the type H_2X ($X = O, S, Se, Te, \text{ and } Po$). The electron configurations for sulfur and selenium are given in Table 5.1. For both

Table 5.1

Some Physical and Chemical Properties of Selenium and Sulfur^a

	Selenium (Se)	Sulfur (S)
Atomic Weight	78.96	32.06
Covalent Radii, A	1.17	1.04
Ionic Radii, A		
(-2)	1.98	1.84
(+6)	0.28	0.12
Electronegativity (Pauling's)	2.55	2.58
Oxidation States	6,4,0,-2	6,4,3,2,0,-2
Electron structure	[Ar] 3d ¹⁰ 4s ² 4p ⁴	[Ne] 3s ² 3p ⁴

^a Data taken from Henderson (1982). Ionic radii (tetrahedral) as revised by Shannon (1976), covalent radii are from Heslop and Robinson (1960).

selenium and sulfur, d hybridization can occur yielding complexes in which the atom can exhibit the +4 and +6 oxidation states (Whitten and Gailey, 1981).

In general, differences in the physical properties of sulfur and selenium are related to their atomic structures. Some physical and chemical properties of sulfur and selenium are given in Table 5.1. Of these properties, the ionic and covalent radii of an element are important to its ability to substitute for other ions (i.e., isomorphous substitution, Shcherbina, 1969). Goldschmidt (1958) states that when the ionic radii of two elements are within 15% of each other, substitution is possible. Such is the case for selenium and sulfur, as both their ionic and covalent radii differ by 7% and 11%, respectively (Table 5.1). Other factors which may influence isomorphous substitution, such as coordination number and ionization potential are also similar for these two elements (Henderson, 1982). Therefore, on the basis of crystal chemistry, substitution of sulfide by selenide may occur.

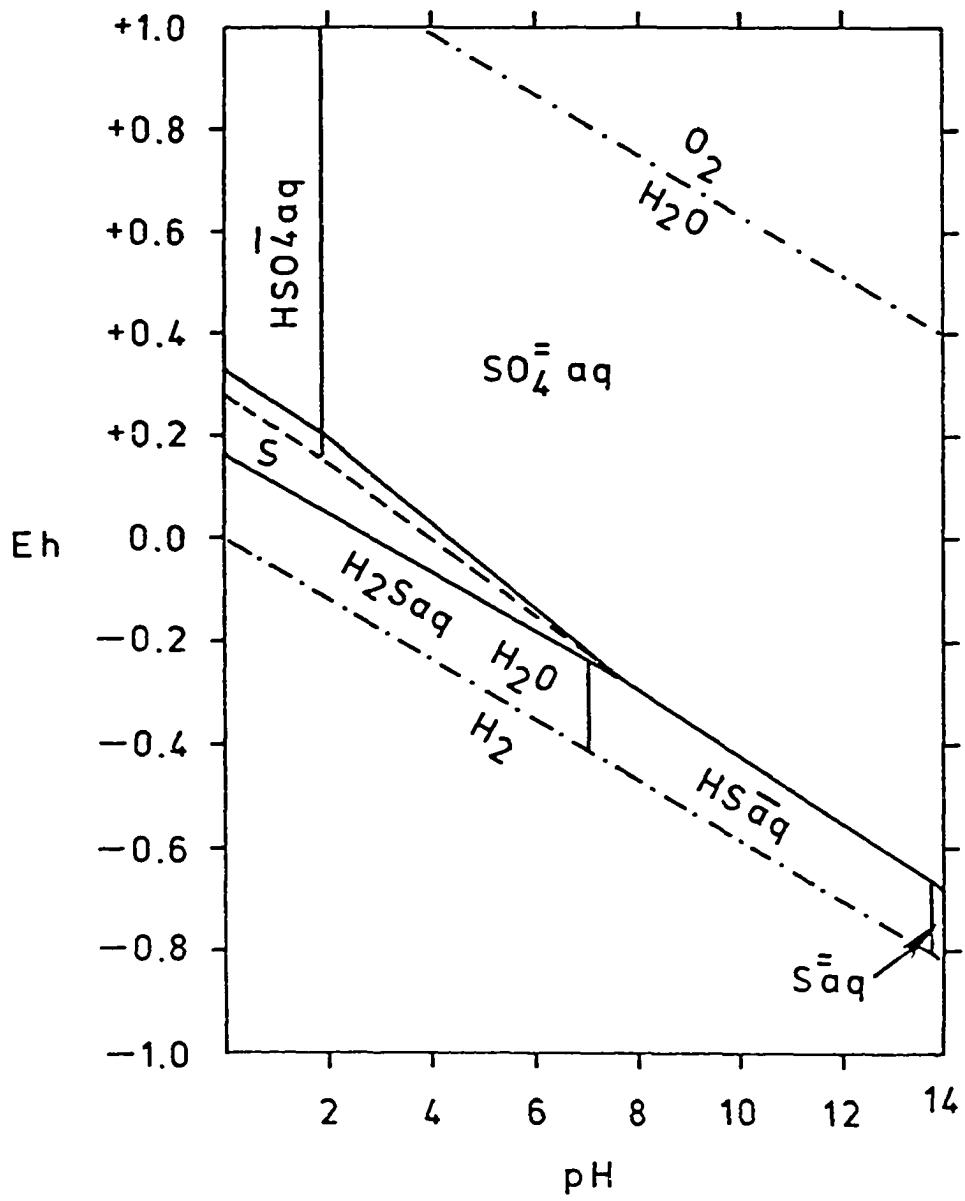
The differences between the reduction potentials of equivalent selenium and sulfur compounds might cause the behavior of these elements to diverge and physically separate during early diagenesis. Reduction potentials for several selenium and sulfur reactions are presented in Table 1.2b. Although the chemical forms of selenium and sulfur given in Table 1.2b are not exactly those present in the environment (e.g., selenite is $\text{HSeO}_3^- + \text{SeO}_3^{=}$ at pH = 8),

the data indicate a distinct trend among similar compounds of selenium and sulfur. Hydrogen selenide is more readily oxidized to elemental selenium than hydrogen sulfide is to elemental sulfur. Selenite and selenate are both stronger oxidants than the equivalent sulfur compounds, sulfite and sulfate. Overall, the difference in reduction potentials of similar selenium and sulfur compounds should cause the geochemical behavior of selenium and sulfur to diverge.

Differences in the thermodynamic properties of selenium and sulfur can be further illustrated by use of E_H/pH diagrams (Figures 5.1 and 1.2). These diagrams are useful for predicting the dominant oxidation states and forms of an element under equilibrium conditions. However, they do not take into account reaction rates and biological mediation of certain redox reactions (Stumm and Morgan, 1981). Specifically, some redox reactions may take long periods of time to reach equilibrium, thereby allowing thermodynamically unstable species to persist (Stumm and Morgan, 1981). This process is termed "kinetic stabilization" and has been shown to be important in the oceanic biogeochemistry of selenium (Cutter and Bruland, 1984). Biological processes have also been shown to affect the redox chemistry of selenium and sulfur (Goldhaber and Kaplan, 1974; Cutter and Bruland, 1984).

In Figure 5.1, the E_H/pH diagram for the $SO_4^{2-} - S^0 - H_2S$ system is presented. This diagram does not include sulfur species such as polysulfides (e.g., S_5^{-2}) and

Figure 5.1. Equilibrium distribution of sulfur species in water at 25°C and 1 atm for an activity of total sulfur = 0.1M (from Garrels and Christ, 1965).



thiosulfate ($\text{S}_2\text{O}_3^{2-}$). Under oxic conditions ($E_{\text{H}} = 0.7$, pH = 6 to 8), sulfate is the dominant sulfur species, while at an E_{H} below approximately zero, hydrogen sulfide should be the predominant species. Elemental sulfur occupies a very narrow stability region (Figure 5.1).

The E_{H} /pH diagram of various selenium species is shown in Figure 1.2. In comparison to sulfur, elemental selenium occupies the largest stability regime. Selenate should predominate in oxic conditions ($E_{\text{H}} = 0.7$, pH = 6 to 8), while selenite can be found in suboxic environments. The stability region for hydrogen selenide is very small and exists in conditions more reducing (below a E_{H} of -0.5) than the $\text{H}_2\text{O}/\text{H}_2$ couple.

Mobility of Sulfur and Selenium

Many factors may cause a physical separation of isomorphous elements (Goldschmidt, 1958). Shcherbina (1969) states that a change in the ionic or covalent radius is one of the most important factors in determining if isomorphous substitution between two elements can occur. Changes in the ionic or covalent radius may be caused by a change in the oxidation state (Henderson, 1982). Selenium, as selenide, can enter into sulfide minerals because the ionic and atomic radii are similar (Table 5.1). However, the ionic radii of Se(VI) is about 40% larger than that of S(VI) (Table 5.1), and separation of these elements would occur upon oxidation of sulfide and selenide to sulfate and selenate,

respectively. These differences are demonstrated by the enrichment of selenium in pyrite versus sulfate minerals such as anhydrites (Badalov et al., 1969). The Se/S ratio (atomic) in sulfide minerals (pyrite, chalcopyrite, and enargite) is 56×10^{-6} , while in sulfate minerals (anhydrite) the ratio is lower (2×10^{-6} , Badalov et al., 1969). Therefore, the change in size of one of the elements during redox processes appears to be an important mechanism in the separation of selenium and sulfur.

As stated above, it is possible that selenium as selenide could be incorporated into various sulfide minerals (Table 1.6) such as pyrite (i.e., FeS₂) based on its ionic radius, or form minerals like ferroselite (FeSe₂) and achavalite (FeSe) (Howard, 1977). Upon oxidation, the sulfur present in pyrite can be converted to dissolved species such as sulfite, thiosulfate, sulfate, and polysulfides, and solid phase elemental sulfur (Luther et al., 1986). Concurrently, selenide would be oxidized to elemental selenium, selenite or selenate. Both elemental selenium and selenite are relatively immobile, elemental selenium being a solid and selenite being very particle reactive (Hingston et al., 1968; Howard, 1977). Thus a physical separation of selenium from sulfur could occur based on the greater mobility of dissolved sulfur species compared to either elemental selenium or selenite. However, if selenium is oxidized to selenate, it would be expected to follow sulfate (i.e., selenates are very soluble, Faust and Aly, 1981).

Reaction Rates

The thermodynamic calculations discussed above are useful in predicting the most important species of selenium and sulfur at equilibrium. However, in dynamic natural systems departures from equilibrium often occur. Unfortunately, there are few studies in which the kinetics of the oxidation-reduction reactions of selenium are actually quantified.

The interconversion of selenite and selenate via oxidation/reduction processes is "slow" (Geering et al., 1968), whereas the rate of selenite reduction to elemental selenium is "rapid" (Geering et al., 1968). Cutter and Bruland (1984) show that the rate of selenite oxidation to selenate is slow with a psuedo first order rate constant on the order of 10^{-3}yr^{-1} . Similarly, the abiotic oxidation of elemental selenium to selenite is "slow" (Geering et al., 1968; Howard, 1977; Sarathchandra and Watkinson, 1981). The oxidation/reduction processes discussed above have been shown to be biologically mediated (Sarathchandra and Watkinson, 1981; Cutter, 1982; Foda et al., 1983; and others). Biological mediation of certain redox reaction can increase reaction rates and allow certain "unstable" species to form (Stumm and Morgan, 1981).

Much more is known about the rates of transformation of sulfur, especially sulfide oxidation (Stumm and Morgan, 1981; see review by Millero, 1986). The oxidation of sulfide is fast, with half-times of a few hours to days (Millero,

1986). The chemical oxidation of sulfide produces sulfate, thiosulfate, sulfite and elemental sulfur. The relative distribution of these products is dependent on pH, the concentration of reactants, and the presence of catalysts (Millero, 1986). Boulegue and Michard (1979) state that the oxidation of elemental sulfur is a "slow" process and probably biologically controlled (Stumm and Morgan, 1981; Faust and Aly, 1981). The next oxidation step is the "rapid" oxidation (half life of less than one minute) of sulfite to sulfate and thiosulfate (Avrahami and Golding, 1968; Chen and Morris, 1972; Clarke and Radojevic, 1983).

In general, the mechanisms of oxidation and reduction of various selenium and sulfur compounds are complex. It appears that kinetic differences, either biologically or non-biologically related, could lead to differences in the geochemical distribution of these two elements.

Geochemical Behavior of Selenium and Sulfur in Marsh Sediments

In this section, I will discuss geochemical evidence for the geochemical separation of selenium and sulfur based on data generated in this research and from literature studies. Chapters 3 and 4 should be consulted for the specific selenium and sulfur data and profiles mentioned below.

The selenium concentrations found in a variety of marine and freshwater sediments are given in Table 5.2. Also

TABLE 5.2

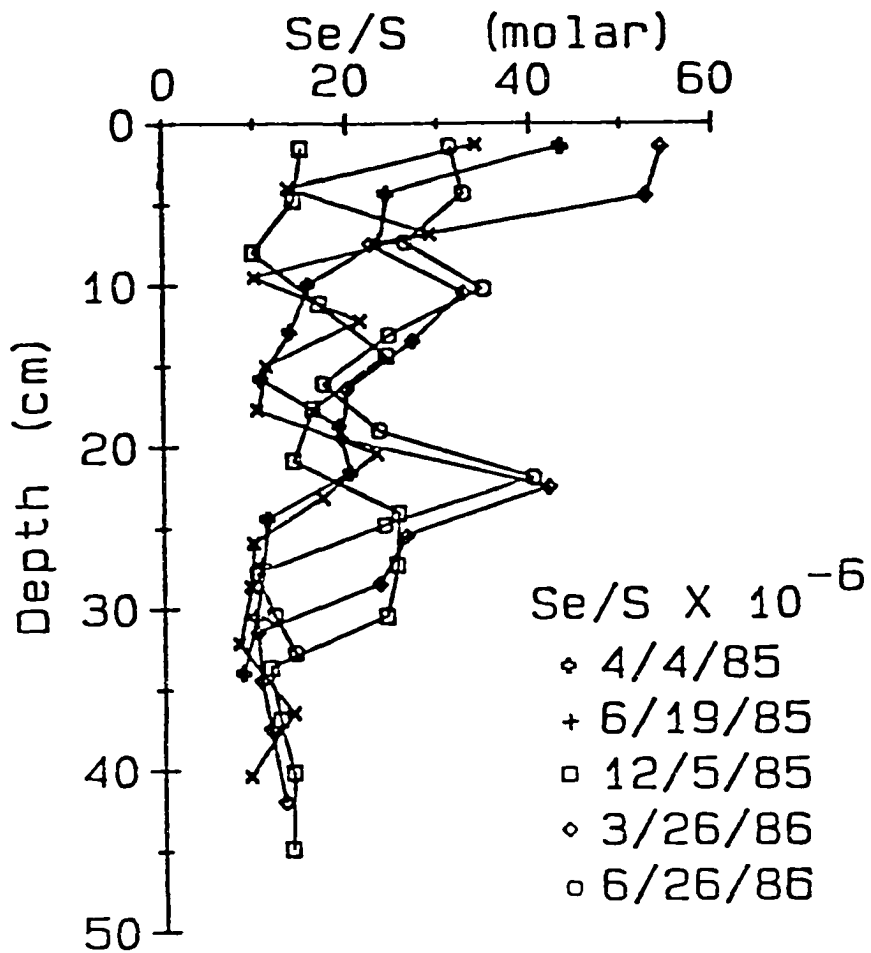
Total Sedimentary Selenium Concentrations from Different Environments.

Total Selenium (ug Se/g)	Location	References
0.1 - 1.7	N.W. Pacific	Sokolova and Pilphuck (1973)
1.0 - 3.0	Wisconsin Lakes	Wiersma and Lee (1971)
0.5 - 250	Sundbury, Ontario	Nriagu and Wong (1983)
0.2 - 9.0	England, streams	Webb et. al. (1966)
0.07 - 3.2	N. Pacific, Japan	Tamari (1978)
0.05	Crustal Rock	Turekian and Wedepohl (1961)
0.21 - 0.97	Great Marsh, DE	This Study

listed in Table 5.2 is the range of total selenium concentrations in the sediments of the Great Marsh (see Table 4.5). The concentrations of total sedimentary selenium from the Great Marsh are in good agreement with other non-polluted locations and are up to two orders of magnitude lower than polluted sediments (Nriagu and Wong, 1983). Total sulfur concentrations in Great Marsh sediments are typical of organic rich marine sediments (Goldhaber and Kaplan, 1974; Howarth, 1984) and are approximately four orders of magnitude greater than total selenium concentrations (see Tables 3.1 and 4.5). While total sulfur accumulates in the sediments of the Great Marsh as indicated by a general increase with depth (especially from 0 to 10 cm, Figure 3.2), total selenium decreases with depth, and is this removed from these sediments (Figure 4.3). Evidently, biogeochemical processes affect the overall distribution of selenium and sulfur quite differently (see Chapters 3 and 4).

Another way to examine the differences between total sedimentary selenium and sulfur with depth is by calculating a selenium to sulfur ratio (molar); Figure 5.2 presents the selenium to sulfur ratios for all cores. Overall, selenium to sulfur ratios (Figure 5.2, see Table 4.10) vary from 8.3 to 54.5×10^{-6} and generally decrease with depth. The distribution of the Se/S ratios with depth reflects the changes in the individual forms of selenium and sulfur, and therefore interpretation of the data is difficult. Overall,

Figure 5.2. Composite depth distribution of selenium:sulfur ratio (molar) in the Great Marsh. Sediments were sectioned at 2.6 to 3.0 cm intervals, and the data are plotted versus the mean depth of each section.



the decrease in the Se/S ratio with depth is ultimately related to the sulfur accumulation and selenium removal with depth.

The mechanisms of selenium and sulfur incorporation into the sediments of the marsh appear to be different. The processes that incorporate sulfur into marine sediments are well established and are related to the in-situ production of sulfide and organic sulfur compounds via dissimilatory and assimilatory sulfate reduction (Goldhaber and Kaplan, 1974; Jannasch, 1983). Sulfide produced by sulfate reduction can be incorporated into the sediment by reactions with certain trace metals (e.g., Fe, Berner, 1967; 1970; Aller, 1980). The sources of selenium to the marsh sediment were estimated in Chapter 4. These inputs include both creek water and atmospheric deposition. Possible processes leading to selenium incorporation in marsh sediments include: biological uptake of dissolved selenite by plants and bacteria, adsorption of dissolved selenium onto iron oxides, precipitation of elemental and metal selenides, or deposition of detrital selenium (see Chapter 4).

The loss mechanism of selenium from the sediments is a combination of gaseous emissions and possibly the flux plant detritus from the marsh (see Chapter 4), while a certain fraction of the sedimentary sulfur appears to be lost from the marsh by different mechanisms. Steudeler and Peterson (1985) estimate that gaseous sulfur fluxes are small when compared to the total amount of sulfur reduced by sulfate

reduction (i.e., less than 0.1% of the sulfide produced via sulfate reduction is emitted from a marsh). The oxidation of sulfide minerals can be an important mechanism for the removal of sulfur from marsh sediment (Howarth, 1984; Luther and Church, submitted). Howarth (1984) calculates that less than 1% of the sulfate reduced by sulfate reduction is ultimately buried in salt marsh sediments (as pyrite). The remaining sulfur is transported out of the sediments (Howarth et al., 1983) or reoxidized to sulfate and other dissolved sulfur species within the sediments (Howarth and Teal, 1979; Howarth et al., 1983; Luther et al., 1986; Luther and Church, submitted). In summary, a difference between selenium and sulfur diagenesis is that a small fraction of the sulfide, produced via dissimilatory sulfate reduction, is permanently buried in the marsh sediments (as pyrite), while selenium is continually lost from the marsh (i.e., there is no concurrent formation and deposition of a mineral phase of selenium).

The distribution of the different solid phases of selenium and sulfur within marsh sediments (see Chapters 3 and 4) further highlights the diagenetic differences between these elements. The dominant forms of selenium in Great Marsh sediments are organic and elemental (see Table 4.5), whereas the major forms of sulfur are divided between the organic, pyrite and elemental fractions (see Figures 3.5 and 3.6). In the surface layers of the marsh, organic and elemental sulfur are the dominant sulfur phases, while with

depth pyrite becomes the major sulfur phase. In contrast, elemental and organic selenium are the main chemical forms of selenium in both surface and deep layers. In contrast to elemental selenium, elemental sulfur displays large seasonal changes in concentration and depth distribution (see Figure 3.5). These data verify thermodynamic predictions that elemental selenium is relatively stable compared to elemental sulfur (Goldhaber and Kaplan, 1974; Howard, 1977). As stated above, a difference between sulfur and selenium diagenesis in marsh sediment is the formation of a stable sulfur mineral phase (i.e., pyrite) with depth and little or no formation of a corresponding selenium phase (i.e., chromium reducible selenium). Chromium reducible selenium (see Table 4.6) is only a minor phase of selenium throughout the sediment column (i.e., substitution of selenium for sulfur does not occur to any appreciable extent).

Further differences between selenium and sulfur are apparent during the seasonal redox cycle within the marsh sediment. In the surface layer (0 to 15 cm), the marsh is seasonally oxic (Table 4.1). At this time, selenite and selenate forms (either from elemental selenium and/or from organic selenium) and are primarily bound to the sediments (Figure 4.4). Concurrent with these changes, increases are seen the excess sulfate within the pore waters (Table 4.2). The increase in dissolved sulfur species (e.g., sulfate, thiosulfate, sulfite) is related to the oxidation of pyrite (Luther and Church, submitted) and is in part controlled by

plant production, evapotranspiration and/or water uptake by roots (Dacey and Howes, 1984). Other seasonal changes are more evident for sulfur phases than for selenium phases. At the beginning of the growing season (March/April) large increases are seen in elemental sulfur (see Figure 3.5). Similar seasonal changes in elemental selenium are not noticed (see above).

Howard (1977) suggests that FeSe (achavalite) could form during the alkaline oxidation of FeS-Se° or FeS-HSe^{-} . The FeSe (acid volatile selenide) fraction would be chemically similar to acid volatile sulfide (Berner, 1967; Goldhaber and Kaplan, 1974). While there is no detectable acid volatile selenide from sediments of the Great Marsh (see Chapter 4), there is appreciable concentrations of acid volatile sulfide (Figure 3.3). The presence of acid volatile sulfide and undetectable concentrations of acid volatile selenide indicate that this phase of selenium is not stable compared to acid volatile sulfide in these sediments. Another possibility is that acid volatile selenide is not stable during storage. These conclusions are in agreement with the calculations by Howard (1977). He shows that FeSe occupies a very narrow stability field (Figure 1.5) and that FeSe should be unstable, especially in an environment with more sulfur present than selenium.

CONCLUSIONS

Based on the above discussion, three chemical and

geochemical differences between selenium and sulfur can be noted:

1) On the basis of crystal chemistry data it is possible that selenide can substitute for sulfide, although this is not evident from the geochemical data generated from this research.

2) The dominant forms of selenium in the marsh are organic and elemental selenium while the majority of the sulfur is in organic, pyrite and elemental phases. Sulfur diagenesis ultimately forms pyrite with depth and this sulfur mineral phase is stable over long time periods. In contrast, selenium does not form a similar mineral phase with depth. Further, selenium does not appear to substitute for sulfur during pyritization.

4) Selenium is physically separated from sulfur during oxic periods in the surface (0 to 15cm) layers of the marsh. While selenium is oxidized to selenite and selenate which are mostly bound to the sediments, the majority of the reduced sulfur is oxidized to dissolved sulfur species which are mobile in the pore waters.

Overall, selenium and sulfur appear to follow distinctly different pathways in the sediments of the salt marsh during early diagenesis. The contrasting geochemical behavior between selenium and sulfur are related to their respective thermodynamic properties in conjunction with

kinetic considerations and biological processes. Use of selenium as a stable analogue of sulfur is therefore not feasible

Chapter 6

SUMMARY AND CONCLUSIONS:

The Geochemistry of Selenium and Sulfur in a Coastal Salt Marsh

The development of new analytical techniques has enabled the elucidation of the sedimentary geochemistry of selenium and sulfur in coastal marsh sediments. These techniques include the determination of elemental selenium, chromium reducible selenium, greigite, and elemental sulfur along with other more established methods which include: total sedimentary selenium, sedimentary (selenite+ selenate), dissolved selenium speciation, pyrite, and acid volatile sulfur (see Chapter 2). Using these techniques to analyze sediments from the Great Marsh over a one year period, along with diagenetic and mass balance modeling, yields the following conclusions concerning the sedimentary cycle of selenium and sulfur:

1) Sulfur is present in various mineral phases such as acid volatile sulfide, elemental sulfur, greigite, pyrite, and organic sulfur. The dominant forms of sulfur are organic sulfur and pyrite. Iron monosulfides and elemental sulfur both display large seasonal changes in concentration and distribution with depth, indicating a coupling with redox conditions. Greigite is a meta-stable intermediate in the slow formation of pyrite at depth (ca. 15-30cm). Pyrite

formation was also shown to be rapid in the seasonally anoxic upper depths (ca. 0-15cm) of the marsh.

2) The dominant forms of selenium in the sediments of the marsh are elemental and organic selenium. These forms of selenium are stable on short time scales (months). However, elemental selenium is either converted to other selenium forms and/or removed from the marsh on time scales that are longer (years). Changing redox conditions enable reduced forms of selenium, either elemental or organic, to be converted to sedimentary (selenite+selenite). The cycling of selenium through sedimentary (selenite+ selenate) also remobilizes selenium into the pore waters of the marsh.

3) Atmospheric deposition and creek water inputs are the two dominant sources of selenium to the marsh surface. Wet and dry fallout account for 24% of the selenium input, while dissolved and particulate selenium from creek waters account for the remaining 76% of the selenium input to the marsh surface.

4) Diagenetic modeling of the total and elemental selenium data indicate that the loss of total selenium is related to the decrease in elemental selenium.

5) Gaseous fluxes of selenium, presumably dimethylselenide, and/or export of selenium via plant detritus can account for the majority of the loss of total selenium from the marsh.

6) A distinct geochemical/separation of selenium and sulfur occurs during early diagenesis in marsh sediments. Total sulfur accumulates while total selenium is lost from the marsh. Elemental and organic selenium are dominant phases of selenium while pyrite and organic sulfur are the dominant phases of sulfur. While selenium and sulfur both respond to the seasonal redox conditions in the marsh, they ultimately follow different pathways during diagenesis.

While the diagenesis of sulfur has received much attention in past years (see Chapter 3), the data generated from this study yield evidence for the importance of greigite in the slow formation of pyrite. However, the processes controlling pyrite formation are still not fully described or understood. Future field and laboratory work should include studies of both the reactants and products of pyrite formation in sediments. Studies should be performed using contrasting depositional environments (i.e., sulfur limited to iron limited). It should be emphasized that both solid phase and pore water sulfur and iron species should be determined. These studies should further help elucidate the different processes controlling the formation of pyrite in marine sediments.

The geochemical cycle of selenium is shown in Figure 4.1 and the results of the various models are given in Table 4.10. This picture is by no means complete, since more

research is needed to better qualify and quantify the various parts of this cycle. As examples; lowering the detection limits for the chromium reducible and acid volatile selenium methods are needed; the characterization of the organic fraction needs further study; a more thorough study of the pore water distribution and speciation; and the in-situ determination of the gaseous flux of selenium from the marsh surface is needed. These studies would help determine the importance of organic selenium compounds in the selenium cycle and if chromium reducible selenium is affected by the ambient redox environment. Also, a more rigorous study of the pore waters and gaseous forms of selenium would help determined the mechanisms for the loss of total selenium. A thorough study is needed of the export of selenium via plant detritus. This export process could be important in the geochemical cycle of selenium in the marsh. Overall, this study shows that a rigorous examination of the speciation of selenium and sulfur allow actual mechanisms to be observed (not inferred). It is hope that this dissertation laid the groundwork and opened up new ideas for future studies pertaining to the geochemistry of selenium and sulfur in sediments.

REFERENCES

- Adams, D.F., S.O. Farwell, M.R. Pack, and E. Robinson 1981. Biogenic sulfur emissions from soils in eastern and south eastern United States. *J. Air Pollut. Control Ass.* 31: 1035-1140.
- Agemiam, H. and A.S.Y. Chau 1976. Evaluation of extraction techniques for the determination of metals in aquatic sediments. *Analyst* 101: 761-767.
- Aller, R.C. 1980. Diagenetic processes near the sediment water interface of Long Island Sound. II. Fe and Mn. In: *Estuarine Physics and Chemistry: Studies in Long Island Sound*, B. Saltzman [ed.] *Advances in Geophysics*, Volume 22, Academic Press, N.Y..
- Aneja, V.P., J.H. Overton, L.T. Cupitt, J.L. Durham, and W. Wilson 1979. Direct measurements of some atmospheric biogenic sulfur compounds. *Tellus* 31: 174-178.
- Avrahami, M. and R.M. Golding 1968. The oxidation of the sulphide ion at very low concentrations in aqueous solutions. *J. Chem. Soc. (A)*: 647-651.
- Badalov, S.T., T.L. Belopol'skaya, P.L. Prikhid'ko, and A. Turesebekov 1969. Geochemistry of selenium in sulfate-sulfide mineral parageneses. *Geokhimiya* 8: 1007-1010.
- Ben-Yaakov, S. 1973. pH Buffering of pore water of recent anoxic marine sediments. *Limnol. Oceanogr.* 18: 86-94.
- Berner, R.A. 1967. Thermodynamic stability of sedimentary iron sulfides. *Am. Jour. Sci.* 265: 773-785.
- Berner, R.A. 1970. Sedimentary pyrite formation. *Am. Jour. Sci.* 268: 1-23.
- Berner, R.A. 1974. Kinetic models for the early diagenesis of nitrogen, sulfur, phosphorus, and silicon in anoxic marine sediments. In: E. Goldberg [ed.], *The Sea*, Vol 5, Wiley, 427-449.
- Berner, R.A. 1980. *Early Diagenesis - A Theoretical Approach*. Princeton Series in Geochemistry, Princeton Press, N.J..
- Berner, R.A. and R. Raiswell 1983. Burial of organic carbon and pyrite sulfur in sediments over Phanerozoic time: a new theory. *Geochim. Cosmochim. Acta*, 47: 855-862.

- Bernstein, L.R. 1985. Germanium geochemistry and mineralogy. *Geochim. Cosmochim. Acta* 49: 2409-2422.
- Bollinger, M.S. and W.S. Moore 1984. Radium fluxes from a salt marsh. *Nature* 309: 444-446.
- Boulegue, J. and G. Michard 1979. Sulfur speciation and redox processes in reducing environments. In: *Chemical Modeling in Aqueous Systems*. E. Jenne [ed.] ACS Symp. Series 93, Washington D.C..
- Boulegue, J., C.J. Lord III, and T.M. Church 1982. Sulfur speciation and associated trace metals (Fe,Cu) in the pore waters of Great Marsh, Delaware. *Geochim. Cosmochim. Acta*. 46: 453-464.
- Breteler, R.J., J.M. Teal, and I. Valiela 1981. Retention and fate of experimentally added mercury in a Massachusetts salt marsh treated with sewage sludge. *Mar. Environ. Res.* 5: 211-225.
- Burdige, D.J. and J.M. Gieskes 1983. A pore water/solid phase diagenetic model for manganese in marine sediments. *Am. Jour. Sci.* 283: 29-47.
- Carlo Erba, 1985. *Instruction Manual: Nitrogen Analyzer*. Carlo Erba Instrumentazione, Milan, Italy.
- Carroll, M.A. 1983. An experimental study of the fluxes of reduced sulfur gases from a salt water marsh. Ph.D Dissertation, Mass. Inst. Tech., Cambridge, MA..
- Chanton, J.P. 1985. Sulfur Mass Balance and Isotopic Fractionation in an Anoxic Marine Sediment. Ph.D Dissertation, Univ. of North Carolina, Chapel Hill, N.C..
- Chau, Y.K., P.T.S. Wong, B.A. Silverberg, P.L. Luxon, and G.A. Bengert 1976. Methylation of selenium in the aquatic environment. *Science* 192: 1130-1131.
- Chen, K.Y. and J.C. Morris 1972. Kinetics of oxidation of aqueous sulfide by oxygen. *Environ. Sci. Tec.* 6: 529-537.
- Chester, R. and J.M. Hughes 1967. A chemical technique for the separation of ferromanganese minerals, carbonate minerals and adsorbed trace elements from pelagic sediments. *Chem. Geol.* 2: 249-262.
- Church, T.M., C.J. Lord III, and B.L.K. Somayajulu 1981. Uranium, thorium, and lead nuclides in a Delaware salt marsh sediments. *Estuar. Coast. Shelf Sci.* 13: 267-275.

- Church, T.M., J.R. Scudlark, J.M. Tramontano, and C.J. Lord III 1983. Comparative estimates of trace element fluxes from sediments of the Delaware Estuary. *Trans. Amer. Geophys. Union* 64: 250. (Abstract).
- Clarke, A.G. and M. Radojevic 1983. Chloride ion effects on the aqueous oxidation of SO₂. *Atmos. Environ.* 17: 617-624.
- Coleman, R.G. and M. Delevaux 1957. Occurrence of selenium in sulfides from some sedimentary rocks of the western United States. *Econ. Geol.* 52: 499-527.
- Cooke, T.D. and K.W. Bruland 1987. Aquatic speciation of selenium: Evidence of biomethylation. *Environ. Sci. Tec.*, in press.
- Cooper, D.J., W.Z. de Mello, W.J. Cooper, R.G. Zika, E.S. Saltzman, J.M. Pospero, and D.L. Savoie 1987. Short term variability in biogenic emissions from a Florida Spartina alterniflora marsh. *Atmos. Environ.* 21: 7-12.
- Cutter, G.A. 1978. Species determination of selenium in natural waters. *Anal. Chim. Acta* 98: 59-66.
- Cutter, G.A. 1982. Selenium in reducing waters. *Science* 217: 829-831.
- Cutter, G.A. 1983. Elimination of nitrite interference in the determination of selenium by hydride generation. *Anal. Chim. Acta.* 149: 391-394.
- Cutter, G.A. and K.W. Bruland 1984. The marine biogeochemistry of selenium: A re-evaluation. *Limnol. Oceanogr.* 29: 1179-1192.
- Cutter, G.A. 1985. Determination of selenium speciation in biogenic particles and sediments. *Anal. Chem.* 57: 2951-2955.
- Cutter, G.A. and T.M. Church 1986. Selenium in western Atlantic precipitation. *Nature* 322: 720-722.
- Cutter, G.A. and T.J. Oatts 1987. Determination of dissolved sulfide and sedimentary sulfur speciation using gas chromatography - photoionization detection. *Anal. Chem.* 59: 717-721.
- Dacey, J.W.H. and B.L. Howes 1984. Water uptake by roots controls water table movement and sediment oxidation in short Spartina marsh. *Science* 224: 487-489.

- Davison, W., J.P. Lishman, and J. Hilton 1985. Formation of pyrite in freshwater sediments: Implications for C/S ratios. *Geochim. Cosmochim. Acta* 49: 1615-1620.
- de Mello, W.Z., D.J. Cooper, W.J. Cooper, E.S. Saltzman, R.G. Zika, D.L. Savoie, and J.M. Prospero. 1987. Spatial and diel variability in the emissions of some biogenic sulfur compounds from a Florida Spartina alterniflora coastal zone. *Atmos. Environ.* 21: 987-990.
- deSouza, T.L.C., D.C. Lane, and S.P. Bhatia 1975. Analysis of sulfur-containing gases by gas-solid chromatography on a specially treated porapak QS column packing. *Anal. Chem.* 45: 543-545.
- Doran, J.W. and M. Alexander 1977. Microbial transformations of selenium. *Appl. Environ. Microbiol.* 33: 31-37.
- Elderfield, H., P.J. McCaffrey, N. Luedtke, M. Bender and V.W. Truesdale 1981. Chemical diagenesis in Narragansett Bay sediments. *Am. J. Sci.* 281: 1021-1055.
- Faust, S.D. and O.M. Aly 1981. *Chemistry of Natural Waters.* Ann Arbor Press, MI..
- Foda, A., J.H. Vandermeulen, and J.J. Wrench 1983. Uptake and conversion of selenium by a marine bacterium. *Can. J. Fish. Aq. Sci.* 40: 215-220.
- Froelich, P.N., G.P. Klinkhammer, M.L. Bender, N.A. Luedtke, G.R. Heath, D. Cullen, P. Dauphin, D. Hammond, B. Hartman, and V. Maynard 1979. Early oxidation of organic matter in pelagic sediments of the eastern equatorial Atlantic: suboxic diagenesis. *Geochim. Cosmochim. Acta* 43: 1075-1090.
- Froelich, P.N., G.A. Hambrick, M.O. Andreae, and R.A. Mortlock 1985. The geochemistry of inorganic germanium in natural waters. *J. Geophys. Res.* 90(C1): 1133-1141.
- Gattow, G. and G. Heinrich 1964. Thermochemistry of selenium: II Conversions of crystalline selenium modifications. III Conversion of amorphous selenium modifications. *Z. Allgem. Anorg. Chem.* 331: 256-260.
- Garrels, R.M. and C.L. Christ 1965. *Solutions, Minerals and Equilibria.* Freeman, Cooper and Co., San Francisco, CA.
- Geering, H.R., E.E. Cary, L.H.P. Jones, and W.H. Allaway 1968. Solubility and redox criteria for the possible forms of selenium in soils. *Soil Sci. Am. Proceed.* 32: 35-40.

- Giblin, A.E., I. Valiela, and J.M. Teal 1983. The fate of metals introduced into a New England salt marsh. *Water Air Soil Pollution* 20: 81-98.
- Giblin, A.E. and R.W. Howarth 1984. Porewater evidence for dynamic sedimentary iron cycle in salt marshes. *Limnol Oceanogr.* 29: 47-63.
- Gjessing, E. 1976. *Physical and Chemical Characteristics of Aquatic Humus*. Ann Arbor Science, MI.
- Goldberg, A.B., P.J. Maroulis, L.A. Wilner, and A.R. Bandy 1981. Study of H₂S emissions from a salt water marsh. *Atmos. Environ.* 15: 11-18.
- Goldhaber, M.B. and I.R. Kaplan 1974. The sulfur cycle. In: E. Goldberg [ed.], *The Sea, Vol 5.*, Wiley Interscience, N.Y..
- Goldschmidt, V.M. 1958. *Geochemistry*. Oxford Press, U.K.
- Good, R.E., N.F. Good, and B.R. Frasco 1982. A review of primary production and decomposition dynamics of the belowground marsh component. In: V. Kennedy [ed.], *Estuarine Comparisons*, Academic Press, Inc., England.
- Granger, H.C. 1966. Ferroselite in a roll-type uranium deposit, Powder Ridge Basin, Wyoming. *U.S. Geol. Surv. Prof. Paper* 550-C: 133-137.
- Granger, H.C. and C.G. Warren 1969. Unstable sulfur compounds and the origin of roll-type uranium deposits. *Econ. Geol.* 64: 160-171.
- Grob, R.L. 1977. Theory of gas chromatography. In: R.L. Grob [ed.], *Modern Practice of Gas Chromatography*, Wiley Interscience, N.Y.
- Hardisky, M.A., F.C. Daiber, C.T. Roman, and V. Klemas 1984. Remote sensing of biomass and annual net aerial productivity of a salt marsh. *Remote Sen. Environ.* 16: 91-106.
- Henderson, P. 1982. *Inorganic Geochemistry*. Pergamon Press, N.Y..
- Heslop, R.B. and P.L. Robinson 1960. *Inorganic Chemistry: A Guide to Advanced Study*. Elsevier Publishing Co., N.Y..
- Hingston, F.J., A.M. Posner, and J.P. Quirk 1968. Adsorption of selenite by goethite. In: W. Webber and E. Matijevic [eds.], *Adsorption from Aqueous Solution. Advances in Chemistry Series 79*, ACS, Washington D.C.

- Howard III, J.H. 1977. Geochemistry of selenium: formation of ferroselite and selenium behavior in the vicinity of oxidizing sulfide and uranium deposits. *Geochim. Cosmochim. Acta* 41: 1665-1678.
- Howarth, R.W. and J.M. Teal 1979. Sulfate reduction in a New England salt marsh. *Limnol. Oceanogr.* 24: 999-1013.
- Howarth, R.W. and J.M. Teal 1980. Energy flow in salt marsh ecosystem: The role of reduced inorganic sulfur compounds. *Am. Nat.* 116: 862-872.
- Howarth, R.W. and A.E. Giblin 1983. Sulfate reduction in salt marshes at Sapelo Island, Georgia. *Limnol. Oceanogr.* 28: 70-82.
- Howarth, R.W., A. Giblin, J. Gale, B.J. Peterson, and G.W. Luther 1983. Reduced sulfur compounds in the pore waters of a New England salt marsh. In: R.O. Hallberg [ed.], *Environmental Biogeochemistry, Ecological Bulletin (Stockholm)* 35: 135-152.
- Howarth, R.W. 1984. The ecological significance of sulfur in the energy dynamics of salt marsh and coastal marine sediments. *Biogeochem.* 1: 5-27.
- Howes, B.L., J.W.H. Dacey, and G.M. King 1984. Carbon flow through oxygen and sulfate reduction pathways in salt marsh sediments. *Limnol. Oceanogr.* 29: 1037-1051.
- Jannasch, H.W. 1983. Interactions between carbon and sulphur cycles in the marine environment. In: B. Bolin and R.B. Cook [eds.], *The Major Biogeochemical Cycles and Their Interactions*. SCOPE.
- Jorgensen, B.B., H. Fossing, and S. Thode-Anderson 1984. Radio-tracer studies of pyrite and elemental sulfur formation in coastal sediments. *Trans. Am. Geophys. Union* 65: 906. (Abstract).
- Jorgensen, B.B. 1983. Processes at the sediment-water interface. In: B. Bolin and R.B. Cook [eds.] *The Major Biogeochemical Cycles and Their Interactions*. SCOPE.
- Jorgensen, B.B. 1977. The sulfur cycle of a coastal marine sediment (Limfjorden, Denmark). *Limnol. Oceanogr.* 22: 814-832.
- King, G.M., M.J. Klug, R.G. Wiegert, and A.G. Chalmers 1982. Relation of soil water movement and sulfide concentration to *Spartina alterniflora* production in a Georgia salt marsh. *Science* 218: 61-63.

- King, G.M., B.L. Howes, and J.W.H. Dacey 1985. Short-term endproducts of sulfate reduction in a salt marsh: Formation of acid volatile sulfides, elemental sulfur, and pyrite. *Geochim. Cosmochim. Acta* 49: 1561-1566.
- Klinkhammer, G., D.T. Heggie, and D.W. Graham 1982. Metal diagenesis in oxic marine sediments. *Earth Planet. Sci. Letters* 6: 211-219.
- Koval'skii, V.V. and V.V. Ermakov 1970. The Biological Importance of Selenium. Translated by S. Wilson, Ed. R. Powell, National Lending Library for Science and Technology, Yorkshire, U.K..
- Lakin, H.W. 1973. Selenium in our environment. In: E. Kothny [ed.], *Trace Elements in the Environment*. Adv. Chem. Series 123, ACS, Wash. D.C..
- Latimer, W.M. 1952. *The Oxidation States of the Elements and their Potentials in Aqueous Solutions*. 2nd edition, Prentice Hall, N.J..
- Leutwein, F. 1972. Selenium (B-O). In: *Handbook of Geochemistry*. K. Wedepohl [ed.], Vol. II/3, Springer Verlag, N.Y..
- Levine, V. 1925. The reducing properties of microorganisms with special reference to selenium compounds. *J. Bacteriol.* 10: 217-225.
- Lewis, B.G., C.M. Johnson, and T.C. Broyer 1974. Volatile selenium in higher plants. The production of dimethyl-selenide in cabbage leaves by enzymatic cleavage of Se-methyl-selenomethionine selenonium salt. *Pl. Soil* 40: 107-118.
- Loder, T.C., W.B. Lyons, S. Murray, and H.D. McGuinness 1978. Silicate in anoxic pore waters and oxidation effects during sampling. *Nature* 273: 373-374.
- Lord III, C.J. 1980. The chemistry and cycling of iron, manganese, and sulfur in salt marsh sediments. Ph.D dissertation. Univ. of Delaware, Lewes, DE.
- Lord III, C.J. and T.M. Church 1983. The geochemistry of salt marshes: Sedimentary ion diffusion, sulfate reduction, and pyritization. *Geochim. Cosmochim. Acta* 47: 1381-1391.

- Lotrich, V.A., W.H. Meredith, S.B. Weisberg, L.E. Hurd, and F.C. Daiber 1979. Dissolved and particulate nutrient fluxes via tidal exchange between salt marsh and lower Delaware Bay. The Fifth Biennial International Estuarine Research Conference Abstracts, Jekyll Island, GA, Oct. 7-12.
- Luther III, G.W., A.L. Meyerson, J.J. Krajewski, and R. Hires 1980. Metal sulfides in estuarine sediments. *J. Sed. Pet.* 50: 1117- 1120.
- Luther III, G.W., A.E. Giblin, R.W. Howarth, and R.A. Ryans 1982. Pyrite and oxidized iron mineral phases formed from pyrite oxidation in salt marsh and estuarine sediments. *Geochim. Cosmochim. Acta* 46: 2671-2676.
- Luther III, G.W., A.E. Giblin, and R. Varsolona 1985. Polarographic analysis of sulfur species in marine porewaters. *Limnol. Oceanogr.* 30: 727-736.
- Luther III, G.W., T.M. Church, J.R. Scudlark, and M. Cosman 1986. Inorganic and organic sulfur cycling in salt marsh pore waters. *Science* 232: 746-749.
- Luther III, G.W. and T.M. Church 1987. Seasonal cycling of sulfur and iron in porewaters of a Delaware salt marsh. *Mar. Chem.* (submitted).
- Martens, C.S., R.A. Berner, and J.K. Rosenfeld 1978. Interstitial water chemistry of anoxic Long Island Sound sediments. 2. Nutrient regeneration and phosphate removal. *Limnol. Oceanogr.* 23: 605-617.
- Martens, C.S. and J.V. Klump 1984. Biogeochemical cycling in an organic rich coastal marine basin 4. An organic carbon budget for sediments dominated by sulfate reduction and methanogenesis. *Geochim. Cosmochim. Acta* 48: 1987-2004.
- Measures, C.I. and J.D. Burton 1978. Behavior and speciation of dissolved selenium in estuarine waters. *Nature* 273: 293-295.
- Measures, C.I., B.C. Grant, B.J. Mangum, and J.M. Edmonds 1983. The relationship of the distribution of dissolved selenium IV and VI in the three oceans to physical and biological processes. In: *Trace Metals in Seawater*. C. Wong, E. Boyle, K. Bruland, J. Burton, and E. Goldberg [eds.], Plenum Press, N.Y.
- Measures, C.I., B.C. Grant, M. Khadem, D.S. Lee, and J.M. Edmond 1984. Distribution of Be, Al, Se, and Bi in the surface waters of the western North Atlantic and Caribbean. *Earth Planet. Sci. Lett.* 71: 1-12.

- Millero, F.J. 1986. The thermodynamics and kinetics of the hydrogen sulfide system in natural waters. *Mar. Chem.* 18: 121-147.
- Morris, R.J., M.J. McCartney, A.G. Howard, M.H. Arbab-Zavar, and J.S. Davis 1984. The ability of a field population of diatoms to discriminate between phosphate and arsenate. *Mar. Chem.* 14: 259-265.
- Nixon, S.W. 1979. Between coastal marshes and coastal waters- A review. In: *Estuarine and Wetlands Processes.*, P. Hamilton and K. Macdonald [eds.] Plenum Press, N.Y.
- Neal, C., H. Elderfield, and R. Chester 1979. Arsenic in sediments of the north Atlantic Ocean and the eastern Mediterranean Sea. *Mar. Chem.* 7: 207-219.
- Nriagu, J.O. and H.K. Wong 1983. Selenium pollution of lakes near the smelters at Sudbury, Ontario. *Nature* 301: 55-57.
- Nriagu, J.O. and Y. Soon 1985. Distribution and isotopic composition of sulfur in lake sediments of northern Ontario. *Geochim. Cosmochim. Acta* 49: 823- 834.
- Pellenbarg, R.E. 1984. On Spartina alterniflora litter and trace metal biogeochemistry of a salt marsh. *Estuar. Coast. Shelf Sci.* 18: 331-346.
- Pellenbarg, R.E. 1985. Spartina alterniflora litter in salt marsh geochemistry. In: *Marine and Estuarine Geochemistry.* A.C. Sigleo and A. Hattori [eds.], Lewis Publishers, Inc., MI.
- Peterson, P.J. and G.W. Butler 1962. The uptake and assimilation of selenite by higher plants. *Austral. J. Biol. Sci.* 15: 126-146.
- Pierce, F.D. and H.R. Brown 1977. Comparison of inorganic interferences in atomic absorption spectrometric determination of arsenic and selenium. *Anal. Chem.* 49: 1417-1422.
- Presley, B.J. and J.H. Trefry 1980. Sediment-water interactions and the geochemistry of interstitial waters. In: *Chemistry and Biogeochemistry of Estuaries* . E. Olausson and I. Cato [eds.], Wiley Interscience, N.Y.
- Reamer, D.C. and W.H. Zoller 1980. Selenium biomethylation products from soil and sewage sludge. *Science* 208: 500-502.
- Reeburgh, W.S. 1967. An improved interstitial water sampler. *Limnol. Oceanogr.* 12: 223-234.

- Reeburgh, W.S. 1983. Rates of biogeochemical processes in anoxic sediments. *Ann. Rev. Earth Planet. Sci.* 11: 269-298.
- Richards, F.A., J.D. Cline, W.W. Broenkow, and L.P. Atkinson 1965. Some consequences of the decomposition of organic matter in Lake Nitinat, an anoxic fjord. *Limnol Oceanogr.* 10: R185-201 (suppl.).
- Richards, F.A. 1965. Anoxic basins and fjords. In: *Chemical Oceanography, Vol 1.*, J. Riley and G. Skirrow [eds.], Academic Press, N.Y..
- Rickard, D.T. 1969. The chemistry of iron sulfide formation at low temperatures. *Stockholm. Contr. Geology* 20: 67-95.
- Rickard, D.T. 1975. Kinetics and mechanism of pyrite formation at low temperatures. *Am. Jour. Sci.* 275: 636-652.
- Roden, D.R. and D.E. Tallman 1982. Determination of inorganic selenium species in groundwaters containing organic interferences by ion chromatography and hydride generation/atomic absorption spectrometry. *Anal. Chem.* 54: 307-309.
- Roman, C.T. and F.C. Daiber 1984. Aboveground and belowground primary production dynamics of two Delaware Bay tidal marshes. *Bul. Tor. Bot. Club* 111: 334-41.
- Rosenfeld, I. and O.A. Beath 1964. *Selenium*. Academic Press, N.Y..
- Ross, H.B. 1985. An atmospheric selenium budget for the region 30°N to 90°N. *Tellus* 37B: 78-90.
- Salomons, W. and U. Forstner 1984. *Metals in the Hydrocycle*. Springer-Verlag, N.Y..
- Sarathchandra, S.U. and J.H. Watkinson 1981. Oxidation of elemental selenium to selenite by Bacillus megaterium. *Science* 211: 600-601.
- Schulek, E. and E. Koros 1960. Contributions to the chemistry of selenium and selenium compounds-V. The hydrolysis of selenium. *J. Inorg. Nucl. Chem.* 13: 58-63.
- Shamberger, R.J. 1983. *Biochemistry of Selenium*. Plenum Press, N.Y..

- Shannon, R.D. 1976. Revised effective ionic radii and systematic studies of interatomic distances in halides and chalcogenides. *Acta Cryst. A*, 32: 751-767.
- Shcherbina, V.V. 1969. Separation of isomorphous elements. In: *Problems of Geochemistry*. N. Khitarov [ed.], Nat. Acad. Sci. USSR, Translated from Russian by Israel Program for Scientific Translations.
- Sholkovitz, E.R. 1973. Interstitial water chemistry of Santa Barbara Basin sediments. *Geochim. Cosmochim. Acta* 37: 2043-2073.
- Sillen, L.G. 1961. The physical chemistry of seawater. In: *Oceanography*. M. Sears [ed.], Am. Assoc. Adv. Sci., N.Y..
- Sindeeva, N.D. 1964. *Mineralogy and Types of Deposits of Selenium and Tellurium*. Wiley Interscience, N.Y..
- Sokolova, Y.G. and M.F. Pilipchuk. 1973. Geochemistry of selenium in sediments in the N.W. part of the Pacific Ocean. *Geokhimiya* 10: 1537-1546.
- Stadtman, T.C. 1974. Selenium biochemistry. *Science* 183: 915-922.
- Stone, A.T. and J.J. Morgan 1987. Reductive dissolution of metal oxides. In: *Aquatic Surface Chemistry: Chemical Processes at the Particle-Water Interface*, W. Stumm [ed.], Wiley and Sons, N.Y..
- Strom, R.N. and R.B. Biggs 1972. Trace metals in cores from the Great Marsh. Univ. of Del. Sea Grant, DEL-SG-12-72, p. 35.
- Stumm, W. and J.J. Morgan 1981. *Aquatic Chemistry*. Wiley Interscience, N.Y..
- Stuedler, P.A. and B.J. Peterson 1985. Annual cycle of gaseous sulfur emissions from a New England Spartina alterniflora marsh. *Atmos. Environ.* 19: 1411-1416.
- Suess, E. 1979. Mineral phases formed in anoxic sediments by microbial decomposition of organic matter. *Geochim. Cosmochim. Acta* 43: 339-352.
- Swain, F.M. 1971. Biogeochemistry of sediment samples from Broadkill Marsh, Delaware. *J. Sed. Pet.* 41: 549-556.
- Sweeney, R.E. and Kaplan, I.R., 1973. Pyrite framboid formation: laboratory synthesis and marine sediments. *Econ. Geol.* 68: 618-634.

- Takayanagi, K. and G.T.F. Wong 1983. Fluorimetric determination of selenium (IV) and total selenium in natural waters. *Anal. Chem. Acta* 148: 263-269.
- Takayanagi, K.K. and G.T.F. Wong 1984a. Total selenium and selenium (IV) in the James River Estuary and southern Chesapeake Bay. *Estuar. Coast. Shelf Sci.* 18: 113-114.
- Takayanagi, K.K. and G.T.F. Wong 1984b. Organic and colloidal selenium in southern Chesapeake Bay and adjacent waters. *Mar. Chem.* 14: 141-148.
- Takayangai, K.K. and G.T.F. Wong 1985. Dissolved inorganic and organic selenium in the Orca Basin. *Geochim. Cosmochim. Acta* 49: 539-546.
- Takayangai, K.K. and D. Cossa 1985. Speciation of dissolved selenium in the upper St. Lawrence estuary. In: *Marine and Estuarine Geochemistry*. A.C. Sigleo and A. Hattori [eds.], Lewis Publishers, Inc., MI.
- Tamari, Y. 1978. Studies on the state analysis of selenium in sediments. Ph.D dissertation, Kinki University, p. 51.
- Terada, K., T. Ooba, and T. Kiba 1975. Separation and determination of selenium in rocks, marine sediments and plankton by direct evolution with the bromide-condensed phosphoric acid reagent. *Talanta* 22: 41-49.
- Tessier, A., P.G.C. Campbell, and M. Bisson 1979. Sequential extraction procedure for the speciation of particulate trace metals. *Anal. Chem.* 51: 844-850.
- Tourtelot, H.A. 1964. Minor-element composition and organic carbon content of marine and nonmarine shales of Late Cretaceous age in the western interior of the United States. *Geochim. Cosmochim. Acta* 28: 1579-1604.
- Tramontano, J.M., S. Murray, and T.M. Church 1985. Trace metal biogeochemistry and flux through the Delaware Estuary. *Trans Amer. Geophys. Union* 66: 278 (Abstract).
- Troelsen, H. and B.B. Jorgensen 1982. Seasonal dynamics of elemental sulfur in two coastal sediments. *Estuar. Coast. Shelf Sci.* 15: 255-266.
- Troup, B.N., O.P. Bricker, and J.T. Bray 1974. Oxidation effect on the analysis of iron in the interstitial waters of recent anoxic sediments. *Nature* 249: 237-239.
- Turekian, K.K. and K.H. Wedepohl 1961. Distribution of the elements in some major units of the earth's crust. *Geol. Soc. Amer. Bull.* 72: 175.

- Valiela, I., J.M. Teal, and N.Y. Persson 1976. Production and dynamics of experimentally enriched salt marsh vegetation: below ground biomass. *Limnol. Oceanogr.* 21: 245-252.
- Vine, J.D. and H.A. Tourtelot 1970. Geochemistry of black shales deposits- a summary report. *Econ. Geol.* 65: 253-272.
- Warren, C.G. 1968. The synthesis of ferroselite from an aqueous solution at low temperature. *Econ. Geol.* 63: 418-419.
- Webb, J.S., I. Thornton, and K. Fletcher 1966. Seleniferous soils in parts of England and Wales. *Nature* 207: 327.
- Wedepohl, K.H. 1972. *Handbook of Geochemistry Vol. II/3.*, Springer-Verlag, N.Y..
- Wiess, H.V., M. Koide, and E.D. Goldberg 1971. Selenium and sulfur in a Greenland ice sheet: Relation to fossil fuel combustion. *Science* 172: 261-263.
- Whitten, K.W. and K.D. Gailey 1981. *General Chemistry.* Saunders College Publishing, Phila..
- Wiersma, J.H. and G.F. Lee 1971. Selenium in lake sediments- Analytical procedure and preliminary results. *Environ. Sci. Tec.* 5: 1203-1206.
- Windom, H.L. 1975. Heavy metal fluxes through salt-marsh estuaries. In: *Estuarine Research, Volume I*, L. Cronin [ed.], Academic Press, Orlando, FL..
- Wrench, J.J. 1978. Selenium metabolism in the marine phytoplankters Tetraselmis tetrathele and Dunaliella minuta. *Mar. Biol.* 49: 231-236.
- Wrench, J.J. and C.I. Measures 1982. Temporal variations in dissolved selenium in a coastal ecosystem. *Nature* 299: 431-433.
- Zhabina, N.N. and I.I. Volkov 1978. A method of determination of various sulfur compounds in sea sediments and rocks. In: W. Krumbein [ed.], *Environmental Biogeochemistry and Geomicrobiology Vol 3.* Ann Arbor Science, MI..

David Jay Velinsky

Place of Birth: Plainfield, New Jersey
Date of Birth : May 21, 1955

Education

1977 B.S. in Oceanography, minor in Chemistry
Florida Institute of Technology (Melbourne, FL)

Publications

- Velinsky, D.J., T.L. Wade and G.T.F. Wong 1986.
Atmospheric deposition of organic carbon to Chesapeake Bay. Atmospheric Environment 20(5): 941-947.
- Cutter, G.A. and D.J. Velinsky 1987. Temporal variations of sedimentary sulfur in a Delaware salt marsh. in press (Marine Chemistry).
- Velinsky, D.J. and R.C. Harriss 1987. Chloride budget for the United States: The dominant role of pollution sources. In preparation.

Abstracts and Presentations

- Velinsky, D.J. and G.A. Cutter 1987. Sulfur diagenesis in a coastal salt marsh. EOS 68(16), 458.
- Velinsky, D.J. and G.A. Cutter 1987. Seasonal redox diagenesis of selenium in a coastal salt marsh. Presented at the 193rd American Chemical Society National Meeting, Division of Geochemistry, Denver, CO.
- Cutter, G.A., D.J. Velinsky, C.H. Culberson and T.M. Church 1985. The redox environment of the Chesapeake Bay. EOS 66(51), 1319.
- Velinsky, D.J. and T.L. Wade 1985. The atmospheric deposition of organic carbon from stations surrounding Chesapeake Bay. Virginia Jour. Sci. 36(2).
- Velinsky, D.J. and G.A. Cutter 1985. Selenium diagenesis in a coastal salt marsh. EOS 66(51), 1329.
- Velinsky, D.J. and T.L. Wade 1982. Distribution of fatty acids and hydrocarbons during estuarine mixing. Virginia Jour. Sci. 33(3).

Velinsky, D.J., T.L. Wade and G. Oertel 1981. Enrichment of organic carbon and chlorophyll a in the surface microlayer of coastal frontal zones. Virginia Jour. Sci. 32(3).

Oertel, G., D.J. Velinsky, and T.L. Wade 1981. Influence of frontal mechanics on the variability of hydrocarbons concentrations in the entrance to the Chesapeake Bay. Virginia Jour. Sci. 32(3).

Scholarships and Awards

Old Dominion University Summer Scholarship (1984)
Outstanding Doctoral Student, Dept. of Ocean. (1987)

Memberships

American Geophysical Union
American Chemical Society
Phi Kappa Phi